Earth-Science Reviews 217 (2021) 103581

Contents lists available at ScienceDirect

Earth-Science Reviews

journal homepage: www.elsevier.com/locate/earscirev

Invited Review

Arctic ocean mega project: Paper 2 – Arctic stratigraphy and regional tectonic structure

Anatoly M. Nikishin [a,*], Eugene I. Petrov [b], Sierd Cloetingh [c], Nikolay A. Malyshev [d], Andrey F. Morozov [b], Henry W. Posamentier [e], Vladimir E. Verzhbitsky [d], Sergey I. Freiman [a], Elizaveta A. Rodina [a], Ksenia F. Startseva [a], Nikolay N. Zhukov [a]

[a] Geological Faculty, Moscow State University, Moscow, Russia
[b] The Federal Subsoil Resources Management Agency, Moscow, Russia
[c] Utrecht University, Utrecht, the Netherlands
[d] Rosneft, Moscow, Russia
[e] Consultant, 25 Topside Row Drive, The Woodlands, TX 77380, USA

ARTICLE INFO

Keywords:
Arctic
seismic stratigraphy
Lomonosov Ridge
Amundsen Basin
Nansen Basin
Podvodnikov Basin
North Chukchi Basin
Mendeleev Rise
Laptev Sea Basin
East Siberian Sea Basin
Gakkel Ridge
climate change
SDR

ABSTRACT

A seismic stratigraphic framework and basin fill geohistory for Arctic Ocean basins is presented based on data collected by several Russian Government organized expeditions to the Arctic Ocean. This analysis tied together seismic stratigraphic interpretations for the shelf and the deep-water part of the ocean. The stratigraphic framework is based on age data derived from linear magnetic anomalies in the Eurasia Basin, borehole data for the Lomonosov Ridge and Alaska Shelf, and correlations with various regional geological events. Six seismic boundaries were identified and traced regionally over large areas. We present as a hypothesis that the Arctic Ocean probably was formed during four phases with different kinematics: 133-125 Ma – Canada Basin opening, 125-80 Ma – superplume-related tectonics and magmatism in the Alpha-Mendeleev Rise area and adjacent basins, 80-56 Ma - strike-slip fault tectonics, and 56-0 Ma – Eurasia Basin opening. The time interval of 45-20 Ma appears to be a period of large-scale vertical intraplate movements and normal faulting. Climatic events are recorded in the sedimentary cover of the Arctic Ocean.

The analyses were based on a comprehensive dataset that included more than 23,000 km of 2D seismic lines, which were acquired in the deep-water part of the ocean, supplemented by a large number of federal and commercial seismic lines, which were acquired for the Russian shelves during the past 10-15 years. In addition, special multiple Russian expeditions collected samples on scarps of the Mendeleev Rise that served as ground truth for the seismic interpretation.

1. Introduction

The Arctic Ocean has been actively studied in recent years. In this paper we discuss the geological structure of the Arctic Ocean as well as associated aspects of paleoenvironment and paleoclimate. The tectonic structure of the Arctic Ocean has been discussed recently in a series of reviews (e.g., Vernikovsky et al., 2013; Gaina et al., 2014; Pease et al., 2014; Nikishin et al., 2014; Lobkovsky, 2016; Coakley et al., 2016). Various versions of the stratigraphy of the ocean's sedimentary cover have been presented (Embry and Dixon, 1994; Backman et al., 2008; Bruvoll et al., 2010; Grantz et al., 2011; Houseknecht and Bird, 2011; Mosher et al., 2012; Rekant and Gusev, 2012; Døssing et al., 2013; Franke, 2013; Brumley, 2014; Weigelt et al., 2014; Jokat and Ickrath, 2015; Nikishin et al., 2014, 2017, 2018, 2019; Rekant et al., 2015; Thórarinsson et al., 2015; Evangelatos and Mosher, 2016; Hutchinson et al., 2017; Petrov, 2017; Ilhan and Coakley, 2018; Miller et al., 2018a, 2018b; Homza and Bergman, 2019; Piskarev et al., 2019). Paleoenvironmental and paleoclimatic investigations of the Arctic Ocean during the Cenozoic were based primarily on results of drilling on the Lomonosov Ridge within the framework of the ACEX Project (Brinkhuis et al., 2006; Moran et al., 2006; Jakobsson et al., 2007; Backman et al., 2008; Backman and Moran, 2009; O'Regan et al., 2010; Ehlers and Jokat, 2013; Stein et al., 2015). Prior to the current study reported here, the limited data available, which included information from a single well as

* Corresponding author.
E-mail address: nikishin@geol.msu.ru (A.M. Nikishin).

https://doi.org/10.1016/j.earscirev.2021.103581
Received 12 March 2019; Received in revised form 26 February 2021; Accepted 27 February 2021
Available online 20 March 2021

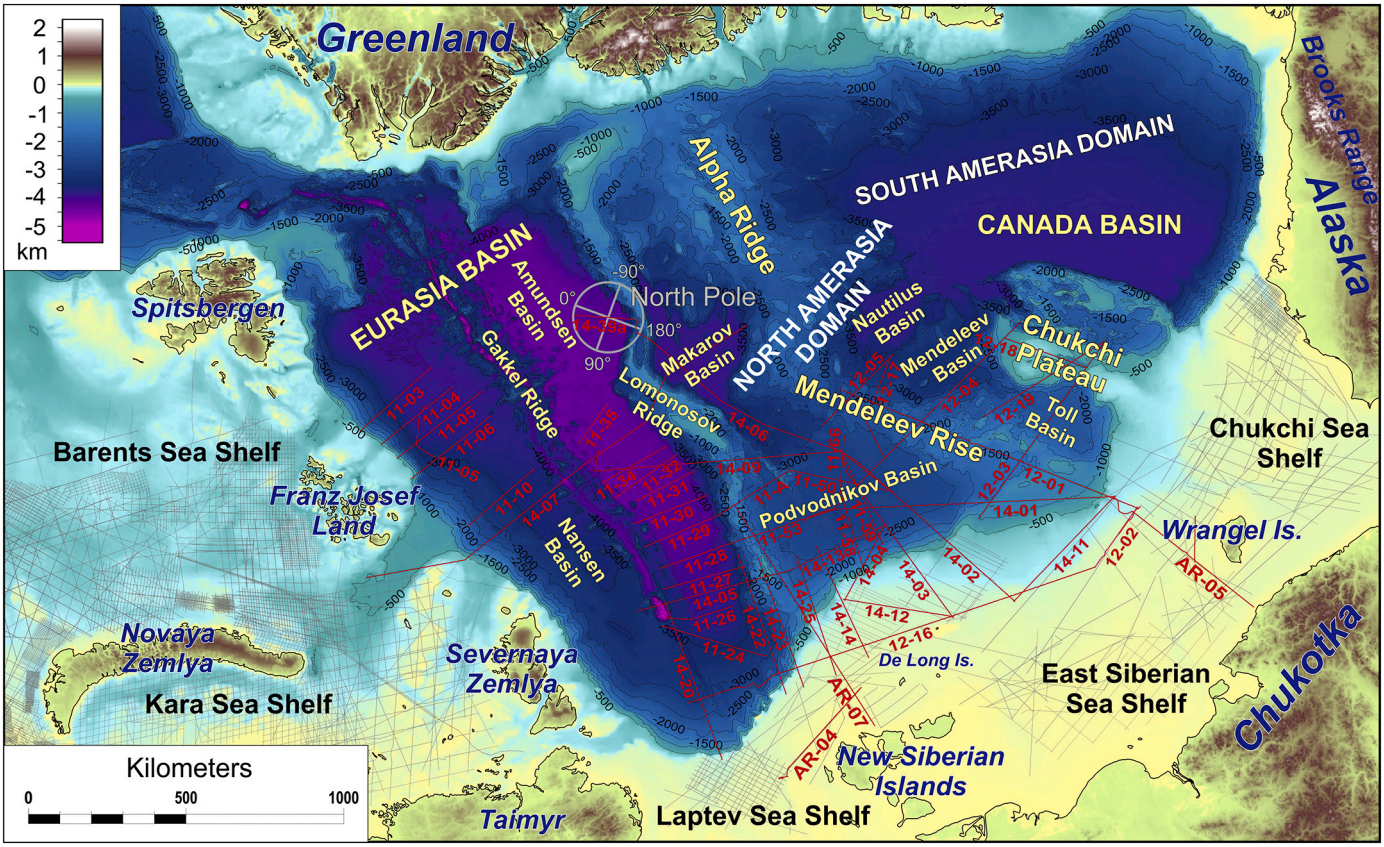

Fig. 1. Location and names of new Russian and other seismic profiles used for the seismic stratigraphic interpretation. The background map illustrates the topography and bathymetry of the Arctic region (Jakobsson et al., 2012, 2020). Red lines indicate seismic data acquired during the Russian Federal projects Arktika-2011, Arktika-2012, and Arktika-2014. Black lines in the shelf areas are federal and commercial profiles used for the regional seismic stratigraphy.

well as several seismic lines (note that the well was not tied to the seismic data), did not allow for compiling a reliable stratigraphic framework of the Arctic Ocean that could lead to a reasonable understanding of its paleogeography and paleotectonics.

In recent years, the Russian Government organized several expeditions to the Arctic Ocean. In this paper we mainly use findings of the projects Arktika-2011, Arktika-2012 and Arktika-2014, which collected more than 23,000 km of 2D seismic lines in the deep-water part of the ocean (see Paper-1, Nikishin et al., 2021a) (Fig. 1). In addition to these data, numerous federal and commercial seismic lines acquired for the Barents, Kara, Laptev, East Siberian and Chukchi shelves during the past 10-15 years (e.g., Drachev et al., 2010; Kumar et al., 2011; Nikishin et al., 2014, 2017, 2018, 2019; Ilhan and Coakley, 2018) also were available. For ground truth, rock samples were taken on sea floor scarps along the Lomonosov Ridge and Mendeleev Rise (Morozov et al., 2013; Petrov et al., 2016; Skolotnev et al., 2017, 2019; Knudsen et al., 2018; Rekant et al., 2019). In this paper we tie together seismic stratigraphic interpretations from the shelf to the deep-water parts of the ocean. Based on this new stratigraphic framework, we will discuss the tectonic structure and formation history of the Arctic Ocean. The improved understanding of Arctic Ocean paleogeography enables further examination of the relationship between the paleoenvironment and global climatic changes of this region.

2. Geological setting and study area

The Arctic Ocean comprises a deep-water basin with complex structure surrounded by multiple shelf seas (Fig. 2, Supplementary Fig. 1). The deep-water basin can be subdivided into two parts, the Eurasia and Amerasia basins, separated by the Lomonosov Ridge. The Eurasia Basin is a continuation of the North Atlantic Ocean with the ultra-slow spreading Gakkel Mid-Oceanic Ridge running along its axis (Dick et al., 2003). The Lomonosov Ridge, which separates the Eurasia and Amerasia basins, comprises a terrane associated with a continental crust. Based on plate reconstructions, the crust of the Lomonosov Ridge is formed by Paleozoic orogens (a continuation of the Caledonian, Timanian and Taimyr orogens) (Ziegler, 1988; Nikishin et al., 2021a; Knudsen et al., 2018; Miller et al., 2018b; Miller et al., 2018a; Rekant et al., 2019).

In the Amerasia Basin, two domains can be identified: the North Amerasia and the South Amerasia domains (Nikishin et al., 2014). The South Amerasia Domain is represented by the Canada Basin, which is characterized by three principal crustal types. In the central zone, gravity and magnetic anomaly maps clearly indicate the presence of an axial rift zone. It is commonly assumed that typical oceanic crust is present there, whereas continental crust strongly extended by rifting is identified along the basin margins (Mosher et al., 2012; Chian et al., 2016; Hutchinson et al., 2017). In some marginal zones of the basin, the crust has been suggested to be composed of serpentinized mantle (Mosher et al., 2012; Chian et al., 2016). The timing of Canada Basin formation has been the subject of debate with estimates ranging from Early Jurassic to Late Cretaceous (e.g., Embry and Dixon, 1994; Embry, 1990; Grantz et al., 2011; Helwig et al., 2011; Coakley et al., 2016; Hutchinson et al., 2017; Miller et al., 2018b, Miller et al., 2018a; Homza and Bergman, 2019;). The North Amerasia Domain is represented by the Alpha-Mendeleev Rise (we will use this name to collectively refer to the Alpha Ridge and Mendeleev Rise) and the associated conjugate deep basins. Two basins are present between the Alpha-Mendeleev Rise and

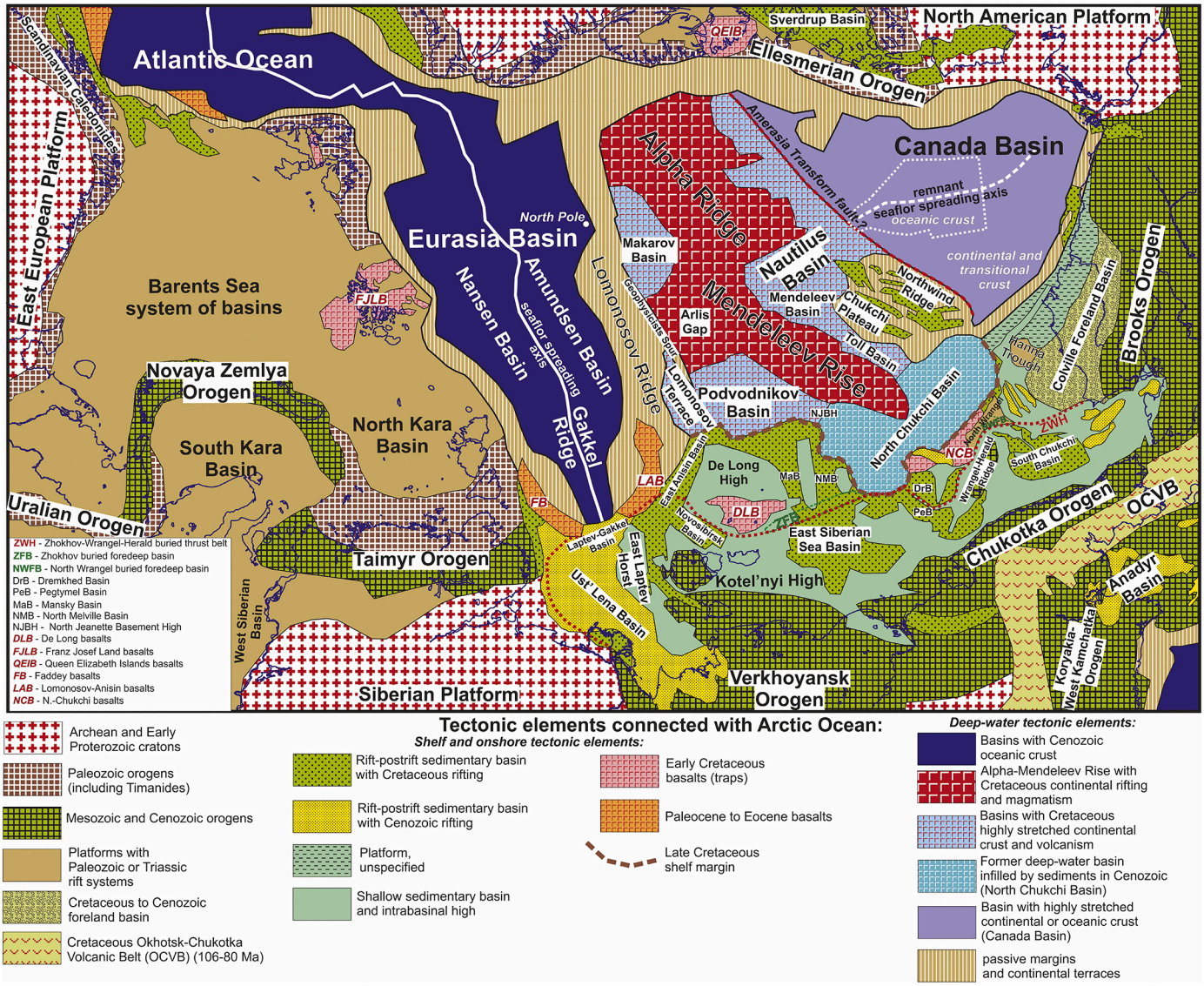

Fig. 2. Tectonic scheme of the Arctic Ocean region. New version, based on Nikishin et al. (2014, 2017, 2018) and new data. The Canada Basin structure has been resolved using data from Mosher et al. (2012) and Chian et al. (2016). For details and geography see Supplementary Fig. 1. Geographic base map is the Geological map of the Arctic (Harrison et al., 2011).

the Lomonosov Ridge: the Podvodnikov and the Makarov basins. In the area between the Alpha-Mendeleev Rise and the Canada Basin, the Nautilus, Mendeleev and the Chukchi Abyssal Plain basins (or Toll Basin) (Nikishin et al., 2017; Nikishin et al., 2014) are observed.

The Alpha-Mendeleev Rise crosses the Amerasia Basin and is located between the Russian East Siberian-Chukchi Sea shelves and the shelf associated with the islands of the Canadian Archipelago. The Alpha-Mendeleev Rise comprises a relative bathymetric high area with a relatively thickened crust up to 20-30 km thick (Alvey et al., 2008; Gaina et al., 2014; Jokat and Ickrath, 2015; Petrov et al., 2016; Lebedeva-Ivanova et al., 2019; Piskarev et al., 2019). Two main hypotheses concerning the crustal structure of this uplift exist (e.g., Gaina et al., 2014; Pease et al., 2014). Some authors propose that the uplifted zone comprises a Cretaceous oceanic plateau with a basaltic crust formed above a mantle plume (Jokat, 2003; Dove et al., 2010; Funck et al., 2011; Grantz et al., 2011; Bruvoll et al., 2012; Jokat and Ickrath, 2015). Other researchers suggest that this uplifted domain consists of a continental crust strongly thinned by rifting and within which Cretaceous plume volcanism manifested itself (Døssing et al., 2013; Miller and Verzhbitsky, 2009; Nikishin et al., 2017; Nikishin et al., 2014; Oakey and Saltus, 2016; Petrov et al., 2016; Vernikovsky et al., 2014). The uplifted area is characterized by complex structure and associated significant seabed relief, and in general is expressed as an alternation of basins and ranges.

The crustal structure of the Makarov-Podvodnikov basin system has been a matter of debate (e.g., Evangelatos et al., 2017; Lebedeva-Ivanova et al., 2019). Some authors assume that this basin has an oceanic crust of an age that is not precisely known (Alvey et al., 2008; Grantz et al., 2011). Other authors believe that the basin has a continental crust thinned by rifting (Langinen et al., 2009; Glebovsky et al., 2013; Kashubin et al., 2013; Laverov et al., 2013; Jokat and Ickrath, 2015; Nikishin et al., 2014, 2017; Petrov et al., 2016; Piskarev et al., 2019).

The Nautilus-Mendeleev-Toll basin system is situated between the Chukchi Plateau and the Mendeleev Rise. The structure of its crust is subject to debate. Some authors suggest that the basin's crust is oceanic (Grantz et al., 2011; Hegewald and Jokat, 2013). However, seismic data and gravity modeling suggest that the crust is likely characterized by continental crust strongly extended by rifting (Brumley, 2014; Nikishin et al., 2014, 2019).

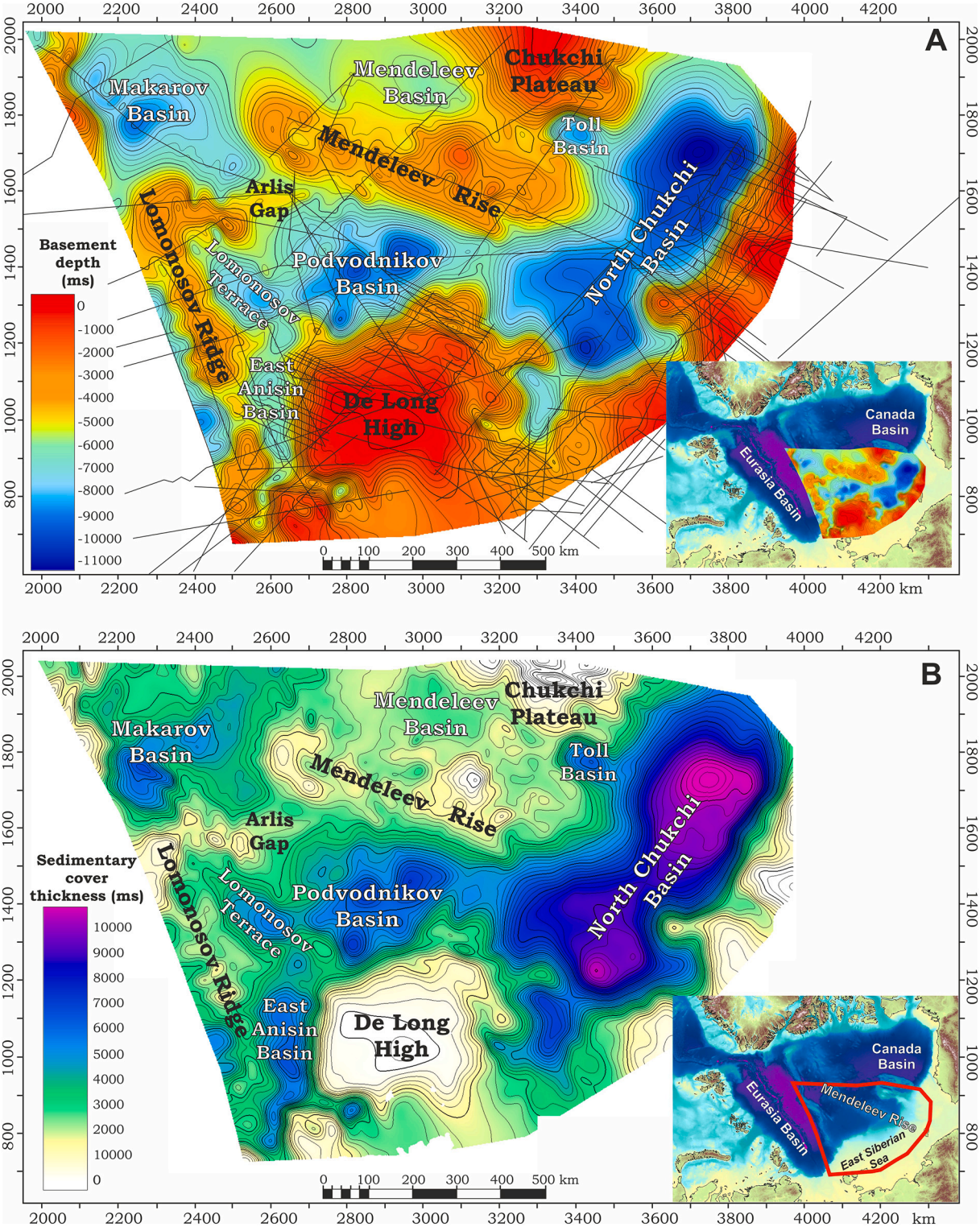

Fig. 3. A. Basement time depth map compiled using interpretation of 2D seismic lines (demonstrated as black solid lines). B. Sedimentary cover time thickness map (in msec) (for the southern margin of the North Chukchi Basin and to the south of the De Long High the maps were constructed using the base of Aptian sediments). The maps are for the Mendeleev Rise and North Chukchi Basin region (see map for location). The maps were compiled using Petrel software.

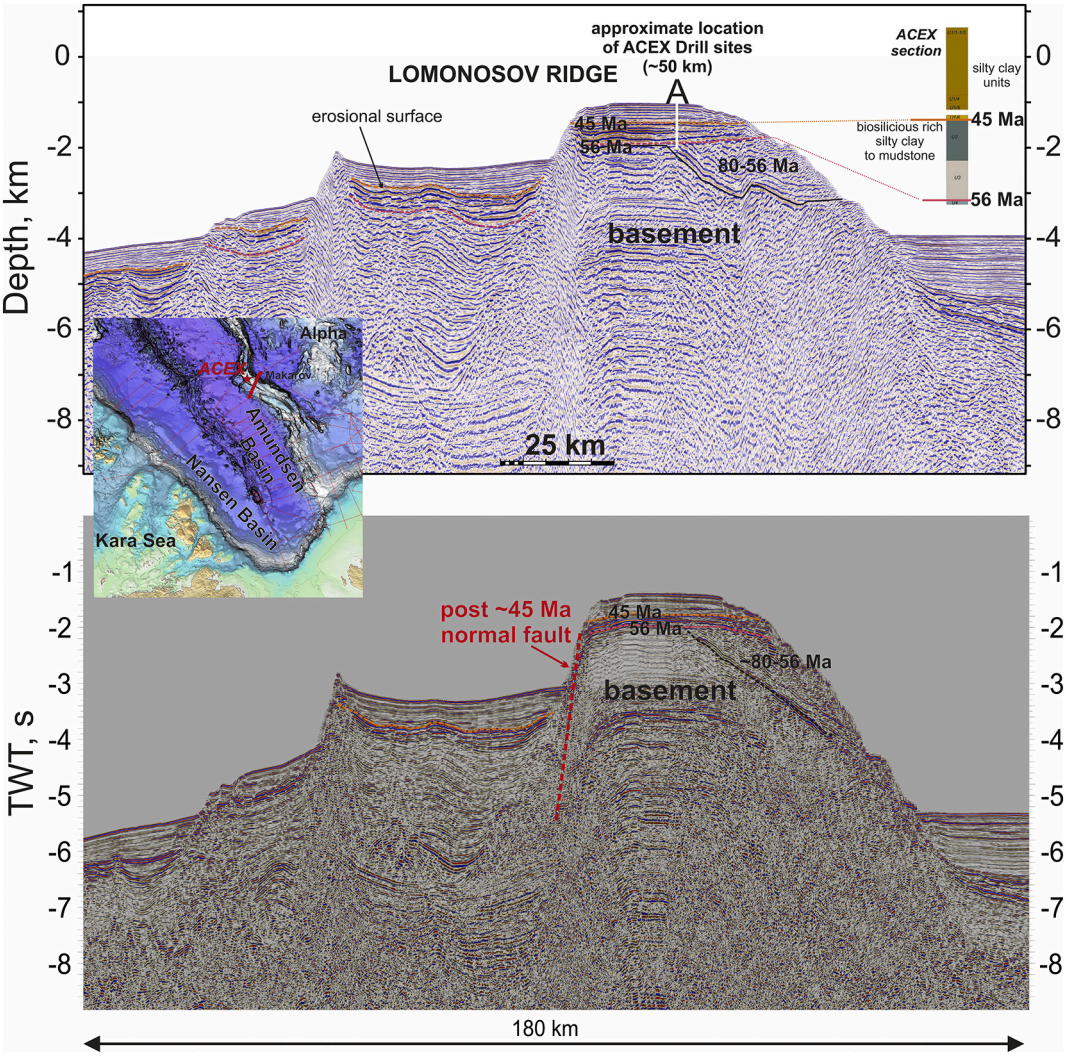

Fig. 4. Interpretation of a fragment of seismic profile ARC 14-07 for the Lomonosov Ridge area. The profile is located nearly 50 km from the ACEX drill sites. The profile is in time and depth scales. Depth-conversion methodology was discussed by Kashubin et al. (2018) and Nikishin et al. (2021a). Location of the profile is shown on the map. 56 Ma, 45 Ma are seismic horizons and their ages. Data for ACEX from Bruvoll et al. (2010).

The Chukchi Plateau is a zone of relatively shallow bathymetry associated with continental crust (Alvey et al., 2008; Kashubin et al., 2013; Gaina et al., 2014; Coakley et al., 2016; Ilhan and Coakley, 2018). Within the central part of the Chukchi Plateau, dredging revealed the presence of igneous rocks with an age of ca. 428 Ma, providing evidence of Early Paleozoic orogeny in this area of the plateau (Brumley et al., 2015). Consequently, it is likely that a crust of Early Paleozoic and older age exists there (Brumley et al., 2015).

The shelf seas of the Arctic Ocean display a broad range of geological structures. The Barents and Kara shelves and the shelf north of the Canadian Arctic Islands and Greenland are underlain by Paleozoic and Neoproterozoic basement. These shelves are characteristic of sedimentary basins with Paleozoic rifts (e.g., Nikishin et al., 2014; Pease et al., 2014). Jurassic and Cretaceous rifts are known for the area of the Sverdrup Basin (Harrison and Brent, 2005; Embry and Beauchamp, 2008; Hadlari et al., 2016).

The Alaskan Shelf is narrow with the Mesozoic and Cenozoic Brooks Orogen situated close to the shelf. On the Laptev, East Siberian and Chukchi shelves, numerous Cretaceous and Cenozoic rifts have been identified recently (Drachev et al., 2010, 2018; Franke, 2013; Nikishin et al., 2014, 2017, 2018, 2019; Ilhan and Coakley, 2018; Savin, 2020). These rifts extend to the continental margin of the deep-water Arctic Basin, suggesting that the rifts and basins were formed within a single geodynamic environment. This issue is a prime focus in the present study, with an emphasis on the part of the Arctic Basin adjacent to Russia's territory.

3. Data and methods

In this paper, we will use data collected primarily by the Arktika-2011, Arktika-2012, and Arktika-2014 Projects. Characteristics of the seismic and other data are presented in Paper-1 (Nikishin et al., 2021a). In the present paper we use mainly 2D seismic data. We incorporated results of seismic sonobuoys published in some technical reports and papers (e.g., Poselov et al., 2012, 2019; Petrov, 2017; Butsenko et al., 2019), however we will not further discuss these data here as they will be fully reported in a separate paper.

For the Russian and American shelves, we utilized seismic lines acquired by the companies MAGE (Murmansk, Russia), DMNG (Yuzhno-Sakhalinsk, Russia), SMNG (Murmansk, Russia), ION-GXT (USA), and others. In addition, for the Russian part of the shelf we utilized all seismic lines available to the Ministry of Natural Resources and Environment of the Russian Federation. These data together formed the basis for the seismic stratigraphic framework presented here.

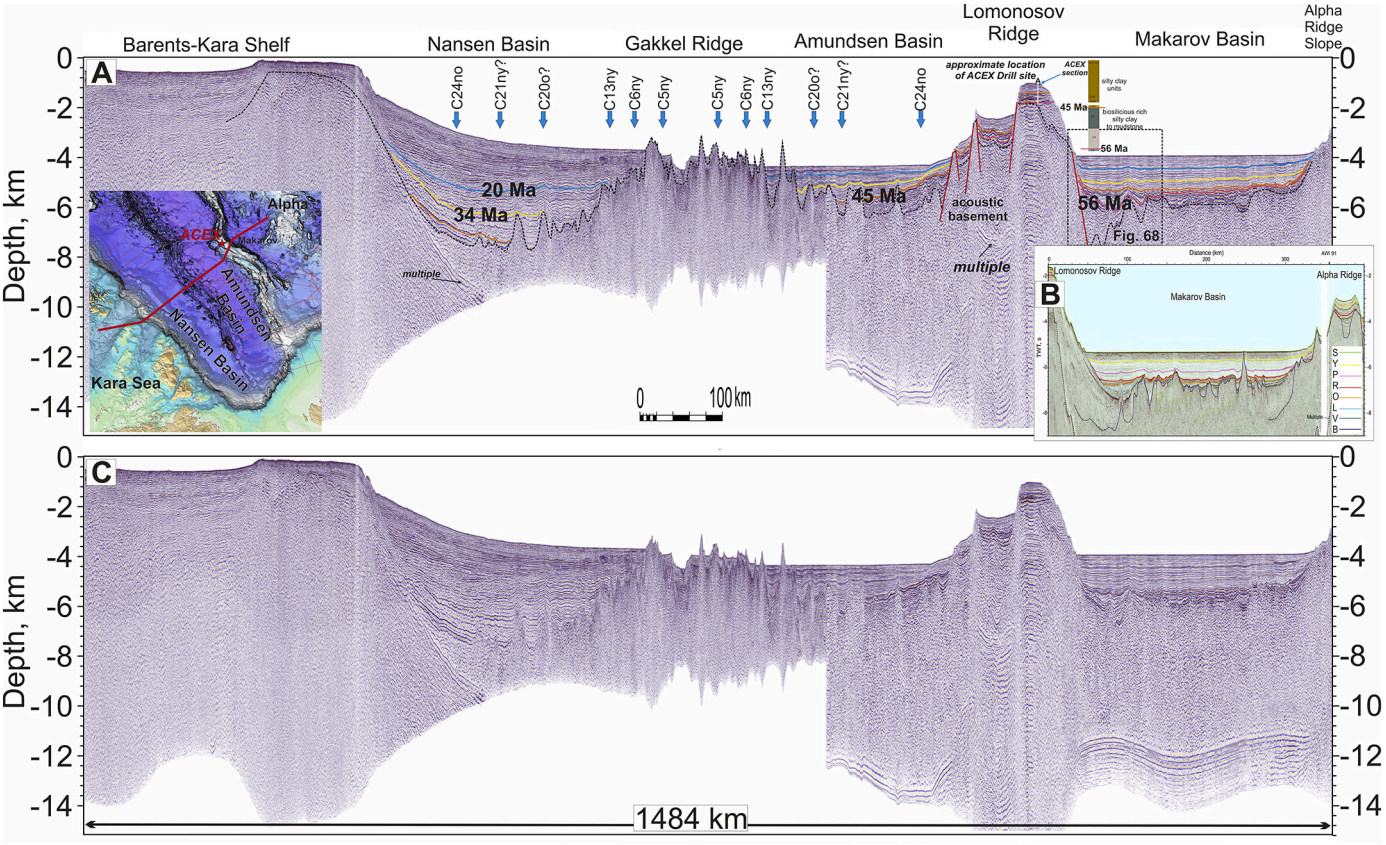

Fig. 5. A. Interpretation of regional seismic profile ARC 14-07. Location of the profile is shown on the map. 56 Ma, 45 Ma, 34 Ma, and 20 Ma are seismic horizons and their ages. Position of linear magnetic anomalies (C5ny and others) modified after Gaina et al. (2011). Data for ACEX from Bruvoll et al. (2010). B. Seismic profile and its interpretation for the Makarov Basin from Evangelatos and Mosher (2016). This line is nearly parallel to our line. C. Seismic profile without interpretation. See also supplementary data, Fig. 5 (seismic profile without interpretation at high resolution). Depth-conversion methodology was discussed by Kashubin et al. (2018) and Nikishin et al. (2021a).

We used published and unpublished basement depth maps and structural maps for all Russian shelf basins based on all available data from the Ministry of Natural Resources and Environment of the Russian Federation as well as industry organizations. An example of our data is illustrated in Fig. 3.

4. Observations and interpretations of the stratigraphy of the Arctic Ocean area

The following data formed the basis for establishing the chronostratigraphic framework of the Arctic Ocean: (1) drilling data from the Lomonosov Ridge acquired within the ACEX Project (Moran et al., 2006; Backman et al., 2008), (2) age data of linear magnetic anomalies of the Eurasia Basin (Glebovsky et al., 2006; Gaina et al., 2011), (3) age data of the sedimentary cover of the Chukchi Sea Shelf based on well ties (Kumar et al., 2011; Hegewald and Jokat, 2013; Houseknecht and Wartes, 2013; Nikishin et al., 2014, 2017, 2019; Aleksandrova, 2016; Craddock and Houseknecht, 2016; Houseknecht et al., 2016; Ilhan and Coakley, 2018; Popova et al., 2018; Homza and Bergman, 2019; Houseknecht, 2019b; Houseknecht, 2019a; Skaryatin et al., 2020), (4) data on formation history of Mesozoic orogens on islands in the East Siberian and Chukchi Seas, (5) data on ages of De Long and Alpha-Mendeleev Rise basalts, which are a part of the Alpha-Mendeleev LIP or HALIP (Drachev and Saunders, 2006; Grantz et al., 2011; Morozov et al., 2013; Brumley, 2014; Coakley et al., 2016; Mukasa et al., 2020), (6) data on climate stratigraphy (Backman and Moran, 2009; Stein et al., 2015), and (7) other miscellaneous data.

4.1. Drilling data from the Lomonosov Ridge – the ACEX Project

Wells from the ACEX Project across the Lomonosov Ridge have been tied with seismic lines, which together formed the basis for the stratigraphic interpretation of that area (Jokat, 2005; Moran et al., 2006; Backman et al., 2008; Backman and Moran, 2009; Langinen et al., 2009; Bruvoll et al., 2010; Poselov et al., 2012; Rekant and Gusev, 2012; Jokat et al., 2013; Weigelt et al., 2020). Two principal stratigraphic units with minimal structural dip are identified within the sedimentary cover: Miocene-Quaternary deposits (18.2-0 Ma) are separated from underlying Eocene deposits with an age of over 44.4 Ma, by an erosional surface. Within the Eocene deposits, a significant lithological boundary at 45.4 Ma lies between two stratigraphic units, U1/6 and U/2 (Backman et al., 2008; Bruvoll et al., 2012). Below this boundary, mud-bearing biosiliceous ooze is present, whereas above the boundary clays are dominant. This boundary corresponds to a climate transition from “green house” to “ice house” (Backman et al., 2008; Moran et al., 2006). In general, transparent seismic facies are observed above this boundary, whereas below this boundary a package with bright reflections is observed (Backman et al., 2008; Bruvoll et al., 2010; Weigelt et al., 2014). According to ACEX Project drilling data, this boundary is characterized by a sharp change in rock density (Jakobsson et al., 2007). This surface corresponds precisely to the boundary which we date it as 45 Ma (Nikishin et al., 2014, 2017, 2018) and represents a regional stratigraphic boundary that is associated with a major change in the character of sedimentation and paleoclimate. In previous studies (Bruvoll et al., 2010; Weigelt et al., 2014), this seismic boundary was tied to an erosional hiatus and was dated as a much younger intra-Early Miocene

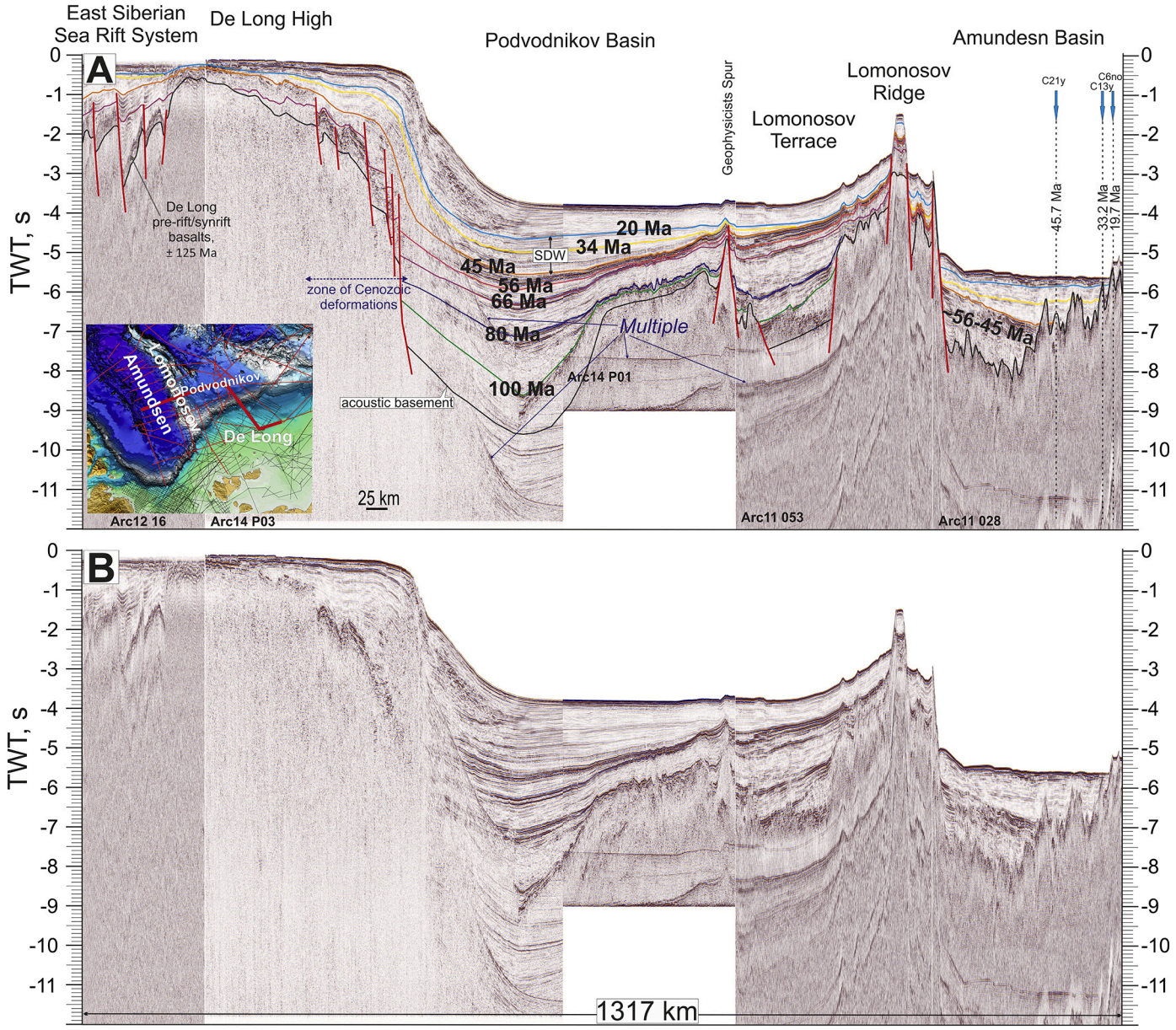

Fig. 6. A. Interpretation of composite seismic profile (lines ARC 12-06, ARC 14-03, ARC 11-53, and ARC 11-28) for the region from the East Siberian Shelf to Amundsen Basin and Gakkel Ridge. Location of the profile is shown on the map. Magnetic anomalies and their ages are after Gaina et al. (2011). Different color lines are seismic horizons and their ages. SDW – syntectonic depositional wedge. B. Seismic profile without interpretation. See also supplementary data, Fig. 6 (seismic profile without interpretation at high resolution).

surface.

Below the Eocene deposits, sediments in tilted fault blocks are observed, and are probably of Cretaceous age (the presence of Campanian deposits has been documented in previous studies) (Backman et al., 2008; Bruvoll et al., 2010). The Pre-Eocene unconformity may correspond to the onset of oceanic crust spreading in the Eurasia Basin (a breakup unconformity caused by the onset of oceanic crust spreading) (Backman et al., 2008; Bruvoll et al., 2010; Rekant and Gusev, 2012, Weigelt et al., 2014, 2020, Nikishin et al., 2014). We date this boundary on seismic lines as 56 Ma (Nikishin et al., 2018; Nikishin et al., 2017; Nikishin et al., 2014). The Russian seismic line Arktika 14-07 is located close the ACEX wells (Fig. 4), which allows correlation between borehole and seismic data and consequent inclusion of borehole data in the regional interpretation of the seismic data.

4.2. *Magnetostratigraphy of the Eurasia Basin*

The stratigraphy of the Eurasia Basin's sedimentary cover is based on the correlation of linear magnetic anomalies with the age of the basement. Knowing the age of the basement, one can approximate the maximum age of the overlying sediments (Chernykh and Krylov, 2011; Rekant and Gusev, 2012). The linear magnetic anomalies are well known for the Eurasia Basin (Gaina et al., 2011; Glebovsky et al., 2006). We utilized these anomalies, each having its definite age, coupled with new seismic lines acquired in through the Arktika-2011 and Arktika-2014 Projects, as the basis for the chronostratigraphic framework. The least ambiguous pattern was observed on line ARC-028 (Nikishin et al., 2014, 2017, 2018). More regionally, analyses were carried out for the seismic line Arktika-2014-07, which crosses the entire Eurasia Basin (Fig. 5). The position of magnetic anomalies 21ny (45.7 Ma), 13ny

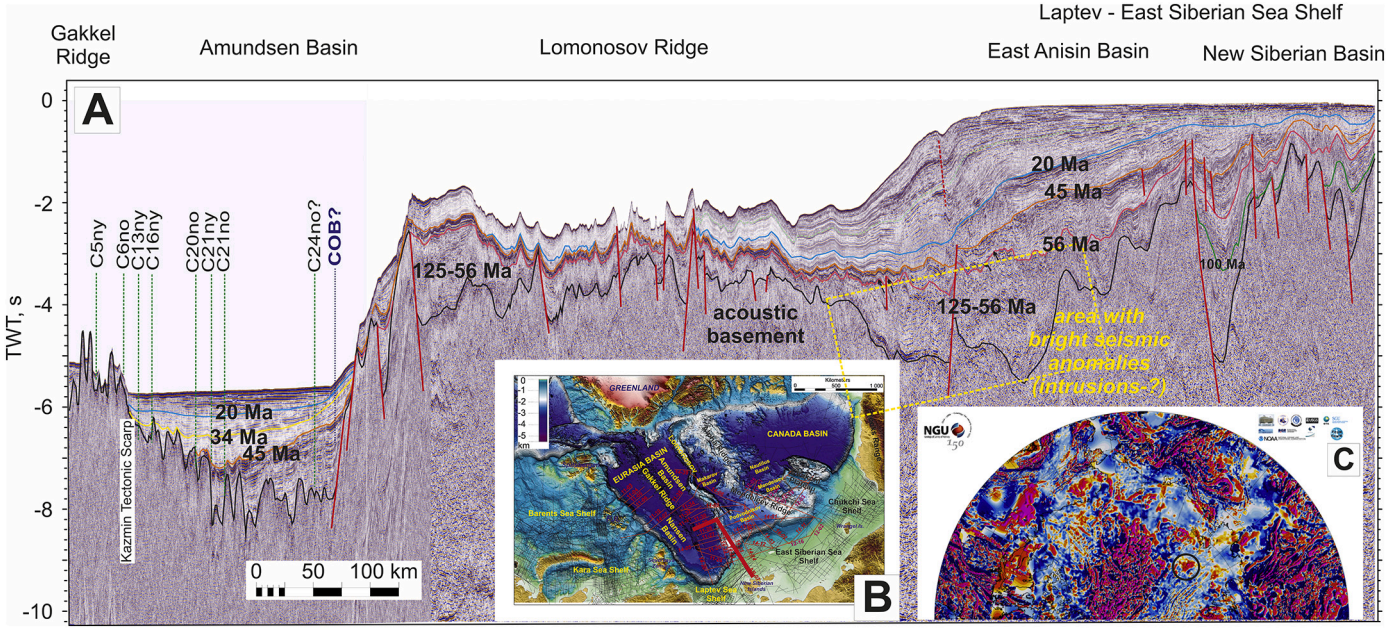

Fig. 7. A. Interpretation of composite seismic profile (lines ARC 11-A7 and ARC 11-29) for the region from the Laptev-East Siberian Sea Shelf and Lomonosov Ridge to Gakkel Ridge. Location of the profile is shown on the map (B). Magnetic anomalies and their ages are after Gaina et al. (2011). Different color lines are seismic horizons and their ages (Ma). C. Fragment of Arctic magnetic anomaly map (Gaina et al., 2011). Black circle shows a bright magnetic anomaly, which corresponds to a possible area with intrusions observed on the seismic profile. See also supplementary data, Fig. 7 (seismic profile without interpretation at high resolution).

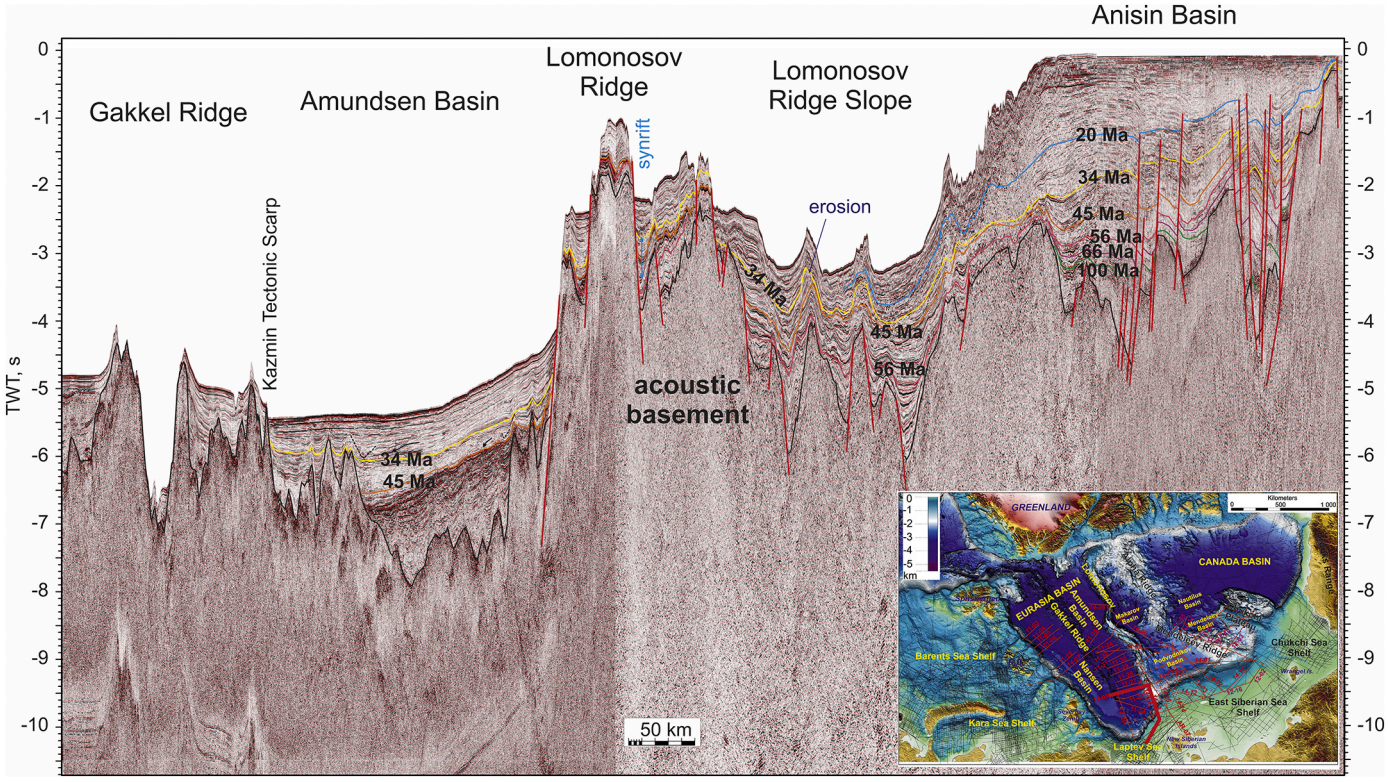

Fig. 8. Interpretation of composite seismic profile (lines ION11-4600, ARC 14-23, and ARC 14-05) for the region from the Laptev Sea Shelf and Lomonosov Ridge to Gakkel Ridge. Location of the profile is shown on the map. Different color lines are seismic horizons and corresponding ages (Ma). Kazmin Tectonic Scarp after Nikishin et al. (2018). See also supplementary data, Fig. 8 (seismic profile without interpretation at high resolution).

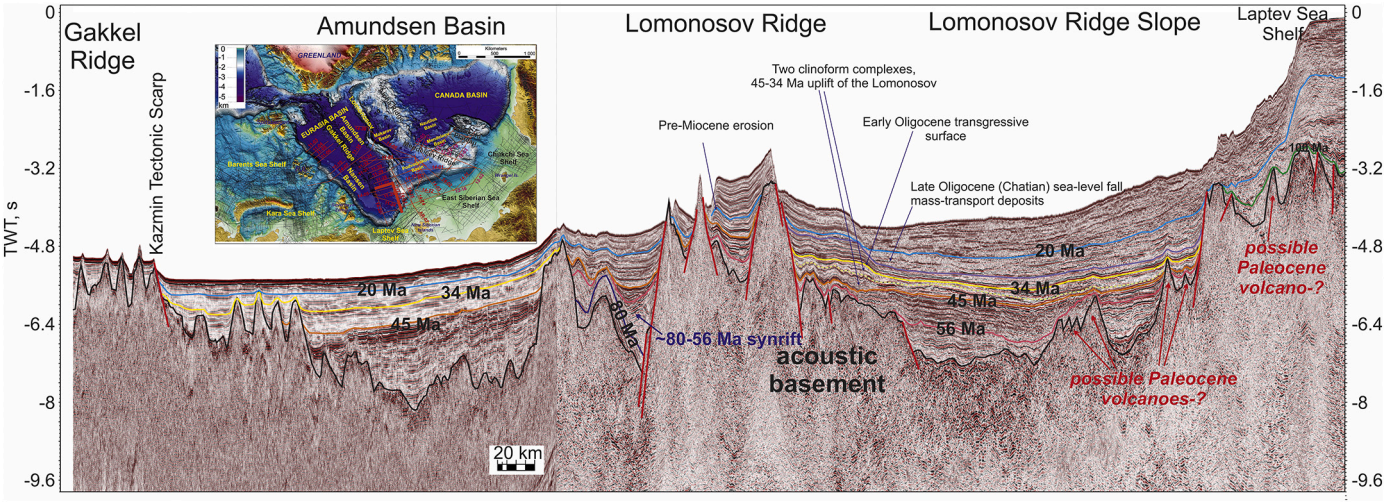

Fig. 9. Interpretation of composite seismic profile (lines ARC 14-22 and ARC 11-27) for the region from the Laptev Sea Shelf and along Lomonosov Ridge slope to Gakkel Ridge. Location of the profile is shown on the map. Different color lines are seismic horizons and corresponding ages (Ma). See also supplementary data, Fig. 9 (seismic profile without interpretation at high resolution).

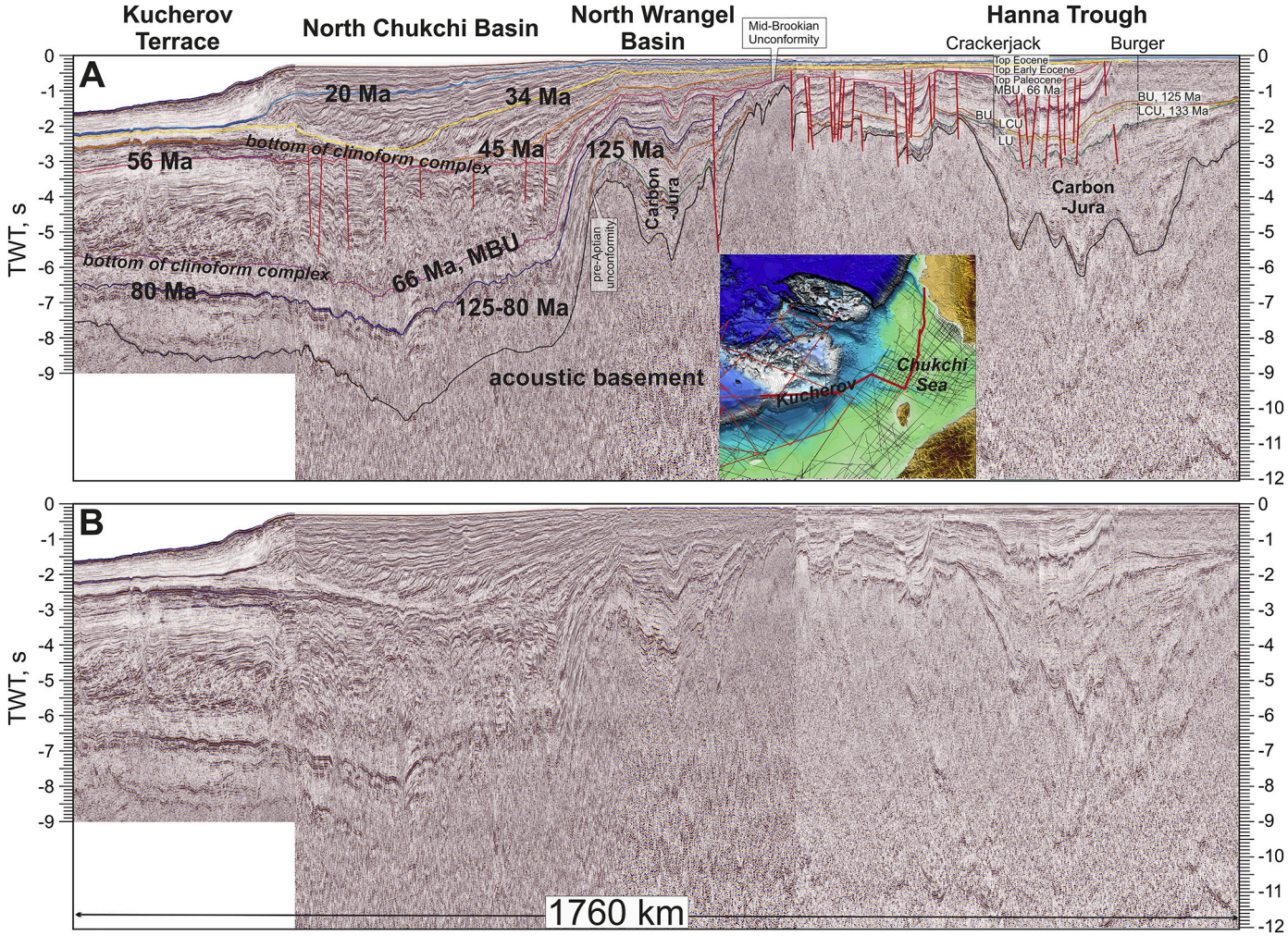

Fig. 10. A. Interpretation of composite seismic profile for the Chukchi Sea (fragments of lines ARC 14-01, ION 11-1400, ION 11-4200, ION 15-2000, CS1-11200, CS1-16100). Location of the profile is shown on the map. Location of boreholes is shown on the map and seismic profile in Fig. 11. Data are from Sherwood et al. (2002) and Kumar et al. (2011). Pre-Aptian (BU) and pre-Paleocene (MBU) unconformities can be traced from shelf areas toward the deep water Arctic Ocean. B. Seismic profile without interpretation. See also supplementary data, Fig. 10 (seismic profile without interpretation at high resolution).

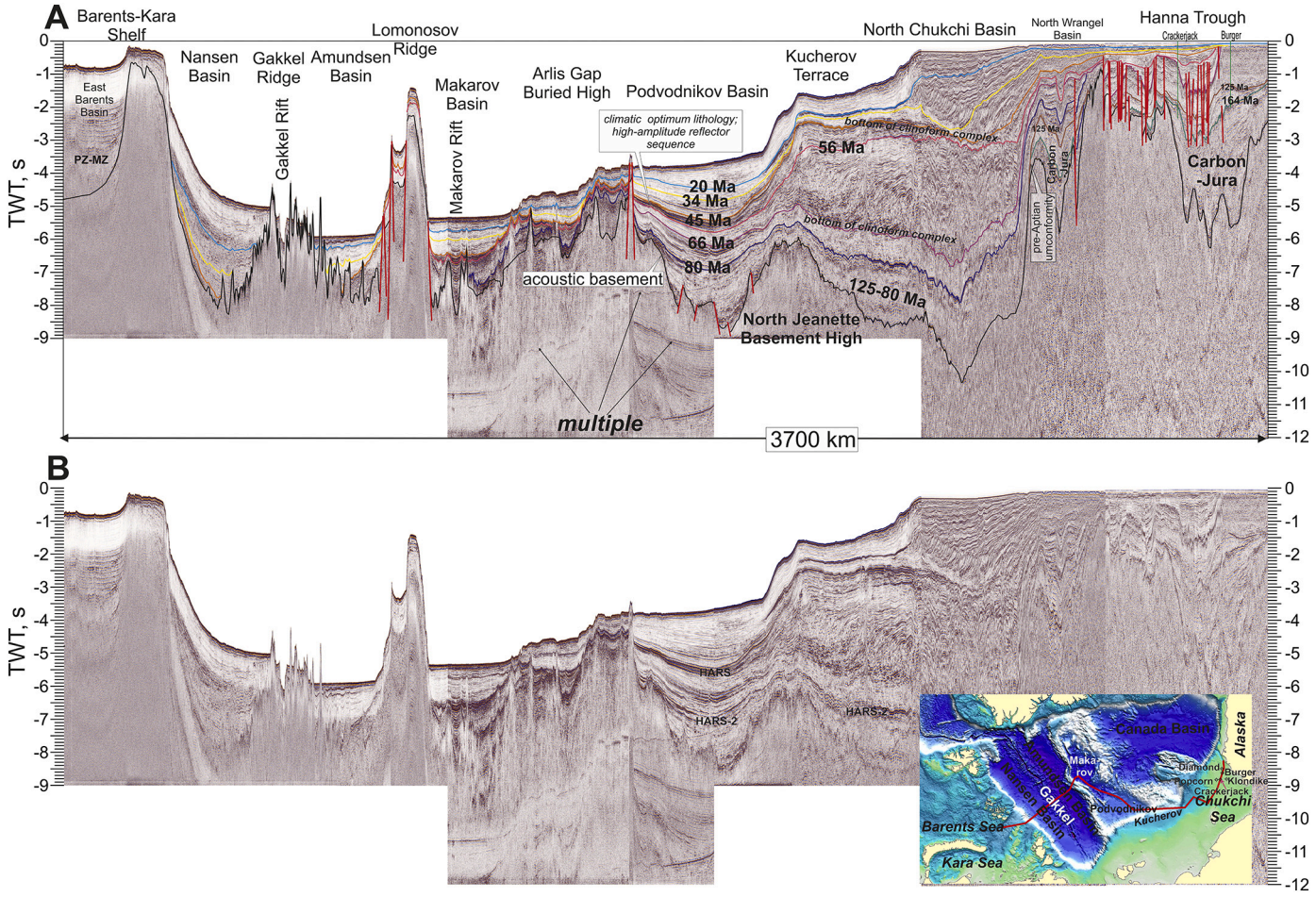

Fig. 11. A. Interpretation of composite seismic profile running from the Barents-Kara Seas shelf to Alaska Shelf (fragments of lines ARC 14-07, ARC 14-06, ARC 14-01, ION 11-1400, ION 11-1100, ION 11-1100, CS1-11200, CS1-16100). Location of the profile is shown on the map. The ages of seismic horizons were correlated with those of linear magnetic anomalies in the Eurasian Basin and data from Alaska Shelf boreholes. B. Seismic profile without interpretation. HARS - high-amplitude reflection sequence. See also supplementary data, Fig. 11 (seismic profile without interpretation at high resolution).

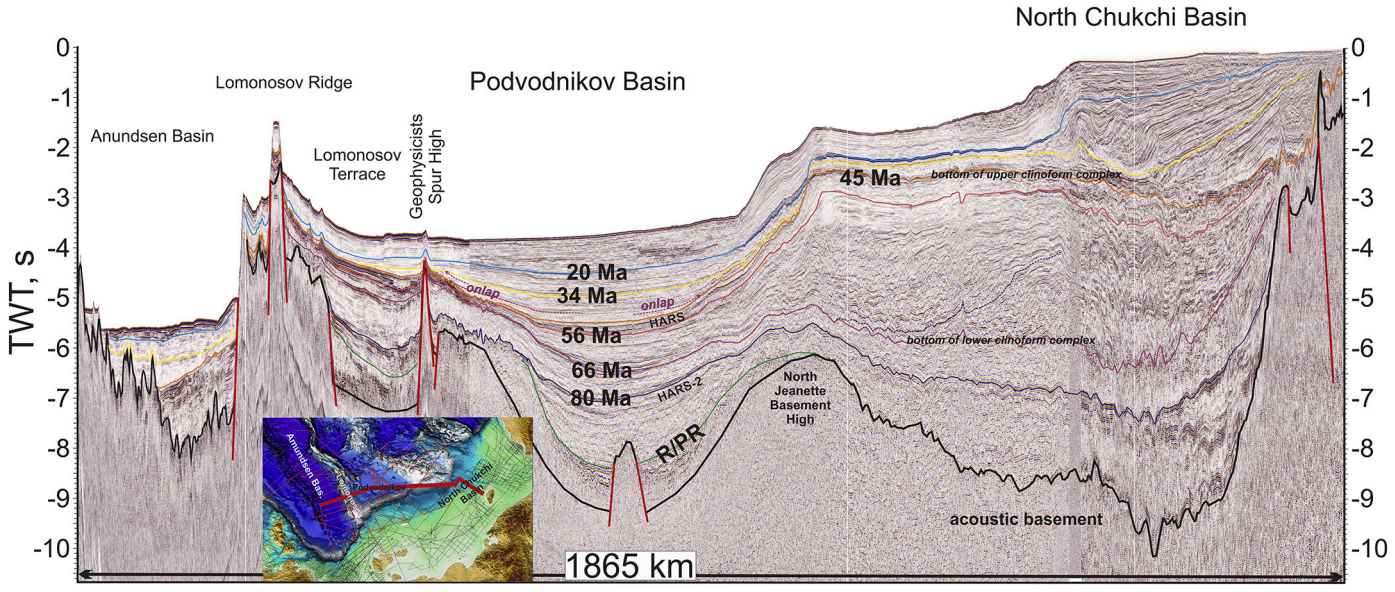

Fig. 12. Interpretation of composite seismic profile running from the Amundsen Basin to the North Chukchi Basin (fragments of lines ARC 11-28, ARC 14-01, ION 11-4300, and ION 11-1400). R/PR - rift/postrift boundary. Location of the profile is shown on the map. See also supplementary data, Fig. 12 (seismic profile without interpretation at high resolution).

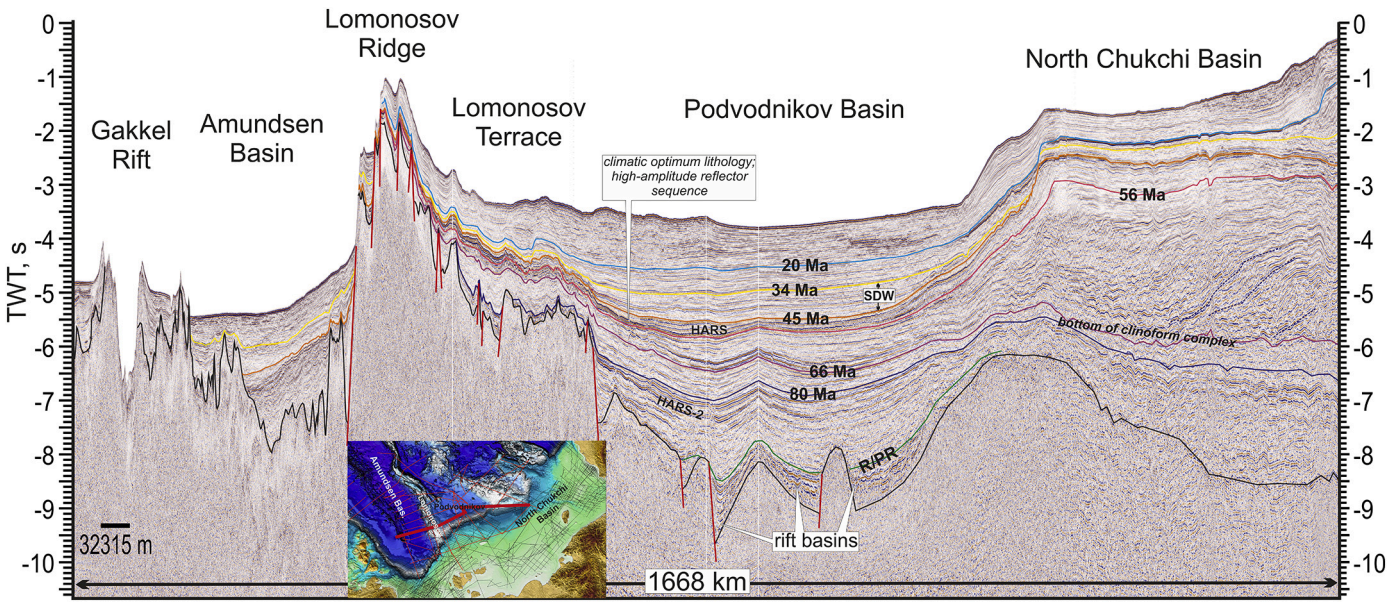

Fig. 13. Interpretation of composite seismic profile from the Gakkel Ridge to the North Chukchi Basin (fragments of lines ARC 14-05, ARC 14-13, ARC 14-03, and ARC 14-01). R/PR - rift/postrift boundary. Location of the profile is shown on the map. SDW – syntectonic depositional wedge. See also supplementary data, Fig. 13 (seismic profile without interpretation at high resolution).

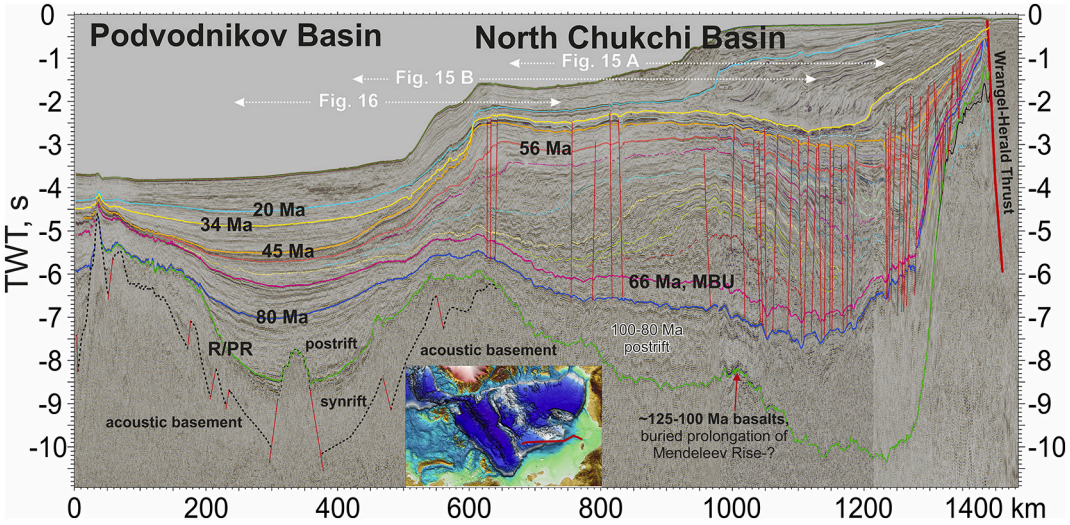

Fig. 14. Interpretation of composite seismic profile running from the Podvodnikov Basin to the North Chukchi Basin (fragments of lines ARC14_P01, ARS10F24, ION11_4200A). Location of the profile is shown on the map. See also supplementary data, Fig. 14 (seismic profile without interpretation at high resolution).

(33.16 Ma) and 6ny (19.7 Ma) is shown on the seismic profile. Sedimentary sequences with ages of 56-45.7 Ma, 45.7-33.16 Ma, 33.16-19.7 Ma and younger than 19.7 Ma, respectively, correspond to these magnetic anomalies ages.

The ages of magnetic anomalies do not coincide exactly with the ages of global sedimentary sequences (Gradstein et al., 2012). We also cannot exactly tie boundaries of seismically-identified sequences to ages of magnetic anomalies. Consequently, we assume that the boundary of sedimentary sequences with a magnetic age of 33.16 Ma likely correspond to the Eocene/Oligocene boundary (ca. 34 Ma). Similarly, the boundary with an age of 19.7 Ma may be close to the Oligocene/Miocene boundary (ca. 20 Ma) (Figs. 5, 6).

It should be noted that the 45.7 Ma boundary within the Eurasia Basin nearly coincides with the boundary of 45.4 Ma observed on the Lomonosov Ridge. The tops of the seismic sequences with these ages also have similar attributes. Therefore, we interpret the 45 Ma boundary across the Eurasia Basin, in the Podvodnokov Basin, and on the Lomonosov Ridge with some confidence (Figs. 4, 5, 6). We also trace the 34 Ma boundary (approximately base of the Oligocene) across the Eurasia Basin and with high probability also into the Podvodnikov Basin (Figs. 5, 6). As sediments in the Eurasia Basin cannot be older than the basement, the oldest sediments, which correspond to the base of the sedimentary section and hence the age of basin formation, are 56 Ma (bottom of the Eocene). The base of these sediments correlates with the base of sediments on the Lomonosov Ridge (these sediments are present above an angular unconformity and the rift/postrift boundary).

In the Eurasia Basin and in the Podvodnikov Basin, the 45 Ma boundary separates the lower seismic facies characterized by high-amplitude reflections from the upper more transparent seismic facies. This is probably a regional lithological boundary (Figs. 5, 6). Note that

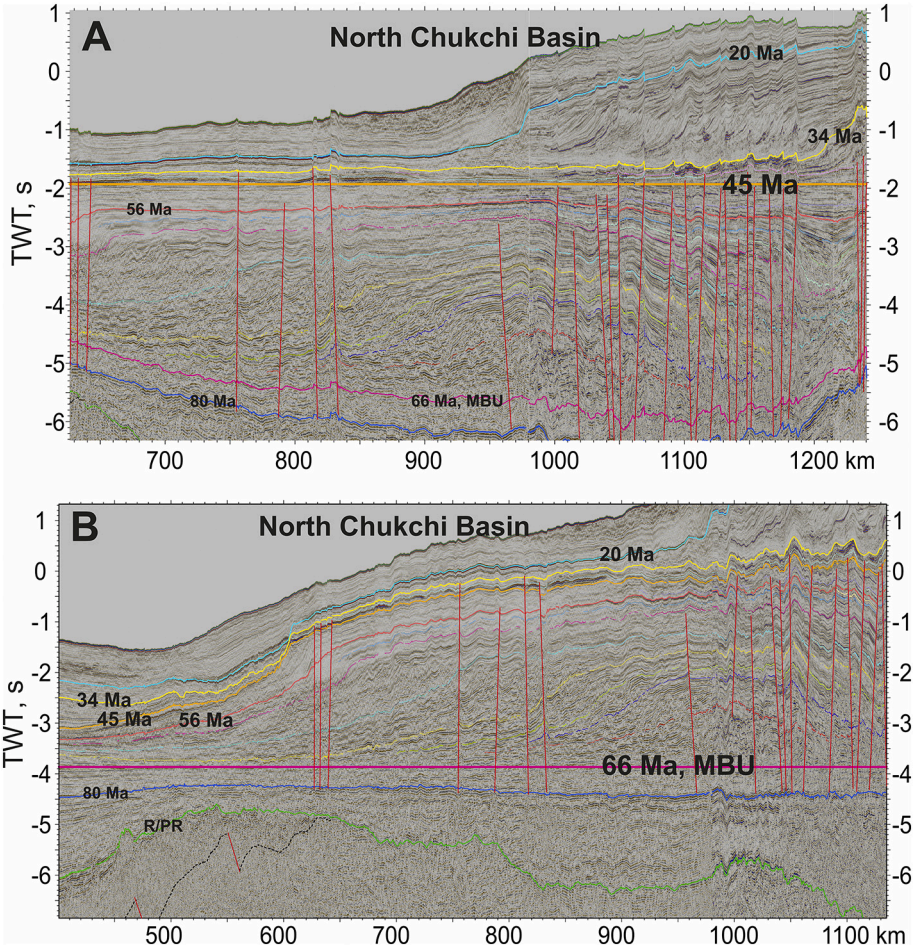

Fig. 15. Flattening on seismic horizons 45 Ma (A) and 66 Ma (B) for southern part of the seismic line shown in the Fig. 14. Large shelf clinoform complexes of the North Chukchi Basin with transition to deep-water deposits in the Podvodnikov Basin can be observed.

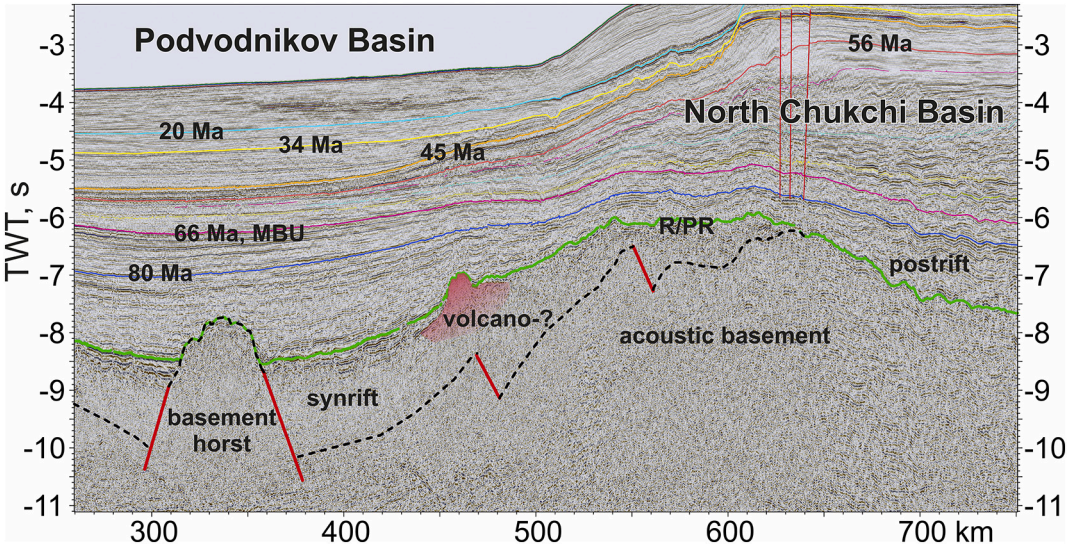

Fig. 16. Fragment of seismic profile presented on Fig. 14. Synrift and postrift complexes are observed in the Podvodnikov Basin. Rift/postrift (R/PR) boundary of the Podvodnikov Basin grades to a boundary between sedimentary cover and acoustic basement in the North Chukchi Basin. A volcano-like structure is observed on the top of synrift complex in the Podvodnikov Basin.

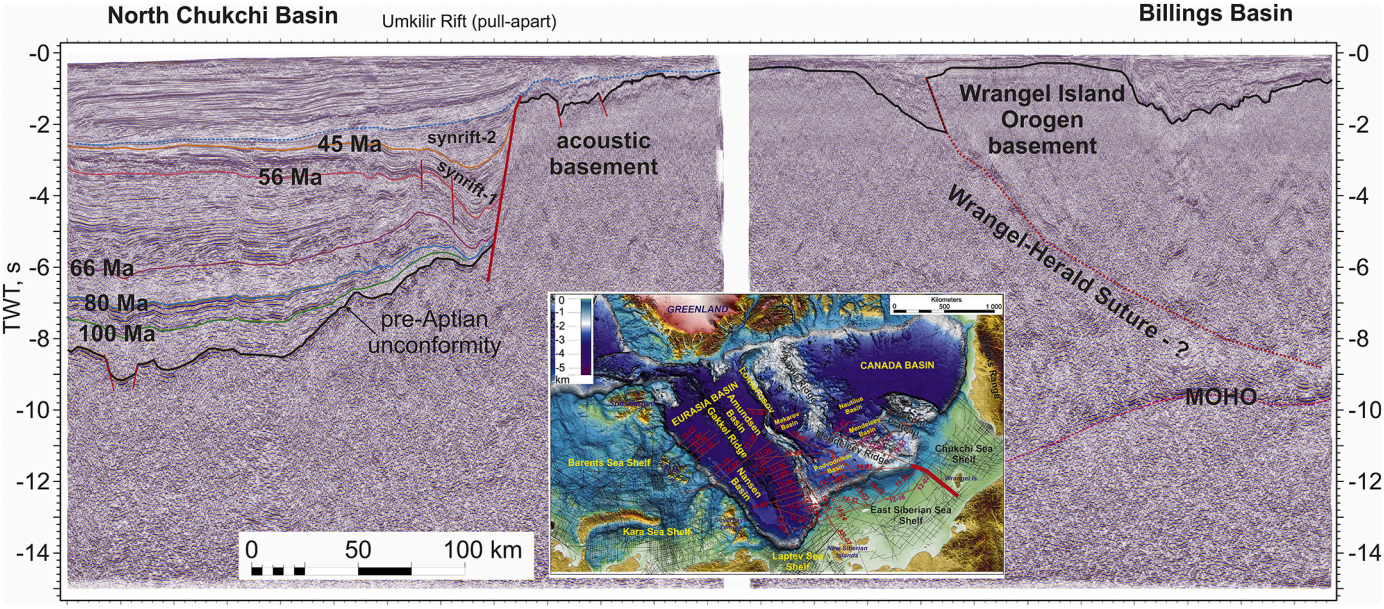

Fig. 17. Interpretation of regional seismic profile 5AR for the Chukchi Sea region. Location of the profile is shown on the map. Different color lines are seismic horizons and corresponding ages (Ma). See also supplementary data, Fig. 17 (seismic profile without interpretation at high resolution).

according to Moran et al. (2006) and Backman et al. (2008) ice-rafted sediments appear in Arctic deposits at ca. 44.8 Ma, as calibrated by the wells on the Lomonosov Ridge. Hence, a sharp climatic cooling likely started at approximately that time. Concurrently, this apparently was associated with a major change in the character of sedimentation. This boundary associated with linked lithological and climatic contrast has regional significance and can be mapped across the Arctic Ocean.

Examples of regional correlation of seismic stratigraphy between the Eurasia Basin, Lomonosov Ridge, and Laptev Sea Shelf are shown in Figs. 7, 8, 9. Our magnetostratigraphy of the Eurasia Basin (Nikishin et al., 2014, 2017, 2018) has been corroborated by new data presented by Weigelt et al. (2020). These authors recognize also seismic horizons 45 Ma, 34 Ma and 20 Ma in the Eurasia Basin.

4.3. Age data of the sedimentary cover of the Chukchi Sea Shelf

Several commercial wells (Popcorn, Crackerjack, Klondike, Burger, Diamond) have been drilled in the Arctic region in the American part of the Chukchi Sea (Sherwood et al., 2002; Kumar et al., 2011; Houseknecht and Wartes, 2013; Craddock and Houseknecht, 2016; Houseknecht et al., 2016; Ilhan and Coakley, 2018; Homza and Bergman, 2019). Based on data from these wells, a stratigraphic scheme has been developed for the Alaskan Shelf (Sherwood et al., 2002). We compiled composite seismic profiles linking the Russian seismic lines in the Arctic as well as some commercial seismic lines on the shelf and tied the stratigraphy to the Popcorn-1, Crackerjack-1, and Burger-1 wells. Figs. 10 and 11 show an example of this analysis. The Cretaceous/Paleogene boundary (the Mid-Brookian Unconformity, MBU) is traced rather robustly into the North Chukchi Basin and into the Amerasia Basin. On the Alaskan Shelf, this boundary commonly has an erosional character and an angular unconformity is observed (Sherwood et al., 2002; Kumar et al., 2011; Houseknecht et al., 2016; Ilhan and Coakley, 2018). In the North Chukchi Basin, the bottom of a thick clinoform sequence corresponds to this ca. 66 Ma boundary (Figs. 12–16). The Wrangel-Herald Ridge is located in the Russian part of the Chukchi Sea (e.g., Nikishin et al., 2015; Verzhbitsky et al., 2015, Verzhbitsky et al., 2012) (Figs. 17, 18). Analysis of seismic and AFT data shows that a phase of thrust faulting in this uplift zone near the Cretaceous/Paleogene boundary with considerable uplift during the Maastrichtian-Paleocene occurred (Verzhbitsky et al., 2012, 2015; Nikishin et al., 2014). This event widely manifested itself in Alaska in the Brooks Orogen as well (O'Sullivan et al., 1997; Peters et al., 2011).

The most complete Cenozoic section, which includes Eocene deposits, is penetrated by the Popcorn-1 well (Sherwood et al., 2002; Ilhan and Coakley, 2018; Homza and Bergman, 2019; Houseknecht, 2019a, 2019b). The Eocene section is divided into three units: the Lower Eocene, the Middle Eocene and the Upper Eocene. The 45 Ma boundary can be traced into the North Chukchi Basin and into the deep-water part of the Arctic Ocean (Figs. 5–15), and in general can be traced all over the Arctic Ocean. In the North Chukchi Basin, this stratigraphic level corresponds to the bottom of a thick upper clinoform complex. The Paleocene/Eocene boundary (ca. 56 Ma) is also penetrated by the Popcorn-1 well and has been seismically mapped across the Arctic Ocean (Figs. 10–14). The Popcorn-1 well also penetrated Mesozoic deposits, though unequivocal seismic correlation of these deposits across the Arctic Ocean was not possible because of lack of definitive data. In general, at this stratigraphic level, seismic correlations with the wells on the Alaskan Shelf remain ambiguous.

Late Paleozoic to Jurassic sections were penetrated by several wells drilled in the American part of the Chukchi Sea and Alaska. (e.g., Homza and Bergman, 2019; Houseknecht, 2019a, 2019b; Sherwood et al., 2002). A Late Paleozoic to Jurassic stratigraphic framework was proposed for the southern part of the North Chuchi Basin using these borehole data (e.g., Drachev et al., 2010; Nikishin et al., 2014) (Fig. 10). Geoscientists from Rosneft Oil Company have carried out stratigraphic analyses of seismic data tied to American wells in the North Chukchi Basin (Fig. 19). They proposed the presence of a Carboniferous to Jurassic section below the Cretaceous section of the North Chukchi Basin. The key element proving the presence of a Paleozoic section is the presence of salt diapirs, as the salt can have only a Late Paleozoic age.

In the Russian part of the Chukchi Sea, one well, on the Ayon Island near the Chukchi Peninsula, is available (Aleksandrova, 2016). The well

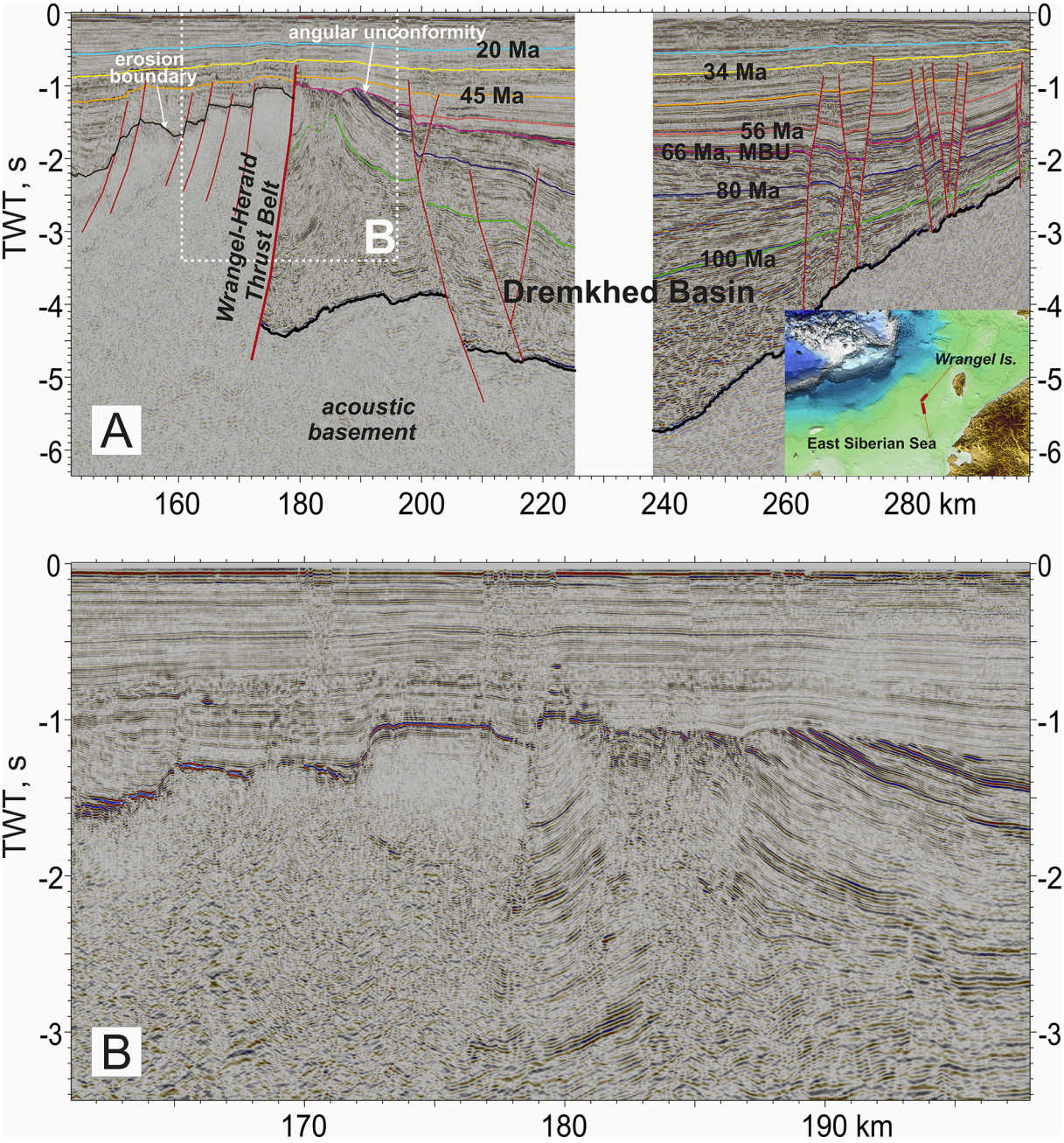

Fig. 18. A. Interpretation of composite seismic profile (DMNG_ES10Z05A, SC-90-20c). Location of the profile is shown on the map. Wrangel-Herald thrust belt is clearly observed. Thrusting started before 66 Ma. Orogenic collapse together with normal faulting took place before 45 Ma. B. Fragment of the seismic profile. Modified after Nikishin et al. (2019).

penetrated deposits from the Paleocene to the Quaternary (Supplementary Fig. 2) that are characterized by continental and shelf sediments. The principal hiatus is dated at 47-39 Ma, which generally coincides with the hiatus observed in the ACEX wells (44.4-18.2 Ma).

In Alaska two wells were drilled on the margin of the Hope Basin in the Chukchi Sea (Bird et al., 2017) and penetrate Neogene to Eocene deposits. Near the base of the well, Paleozoic carbonates are encountered. The Eocene sections contain volcanoclastic deposits and basalts. The basalts have isotopic ages of 42.3±10 Ma and 40.7±2 Ma. We use these data to calibrate the seismic stratigraphy of the Chukchi Sea.

4.4. Formation history of Mesozoic orogens on islands of the East Siberian and Chukchi Seas

An orogen of Mesozoic age is located in the Russian Far East in the area from the Verkhoyansk Range to the Chukchi Peninsula. The common name of this orogen is the Verkhoyansk-Chukotka Orogen (e.g., Puscharovsky, 1960) (Fig. 2). The main collisional event took place in the Early Cretaceous whereas the post-collision extension and intrusion of granites took place at ca. 118-100 Ma (Parfenov and Kuzmin, 2001; Sokolov et al., 2002; Miller et al., 2008, 2010, 2018a, 2018b;

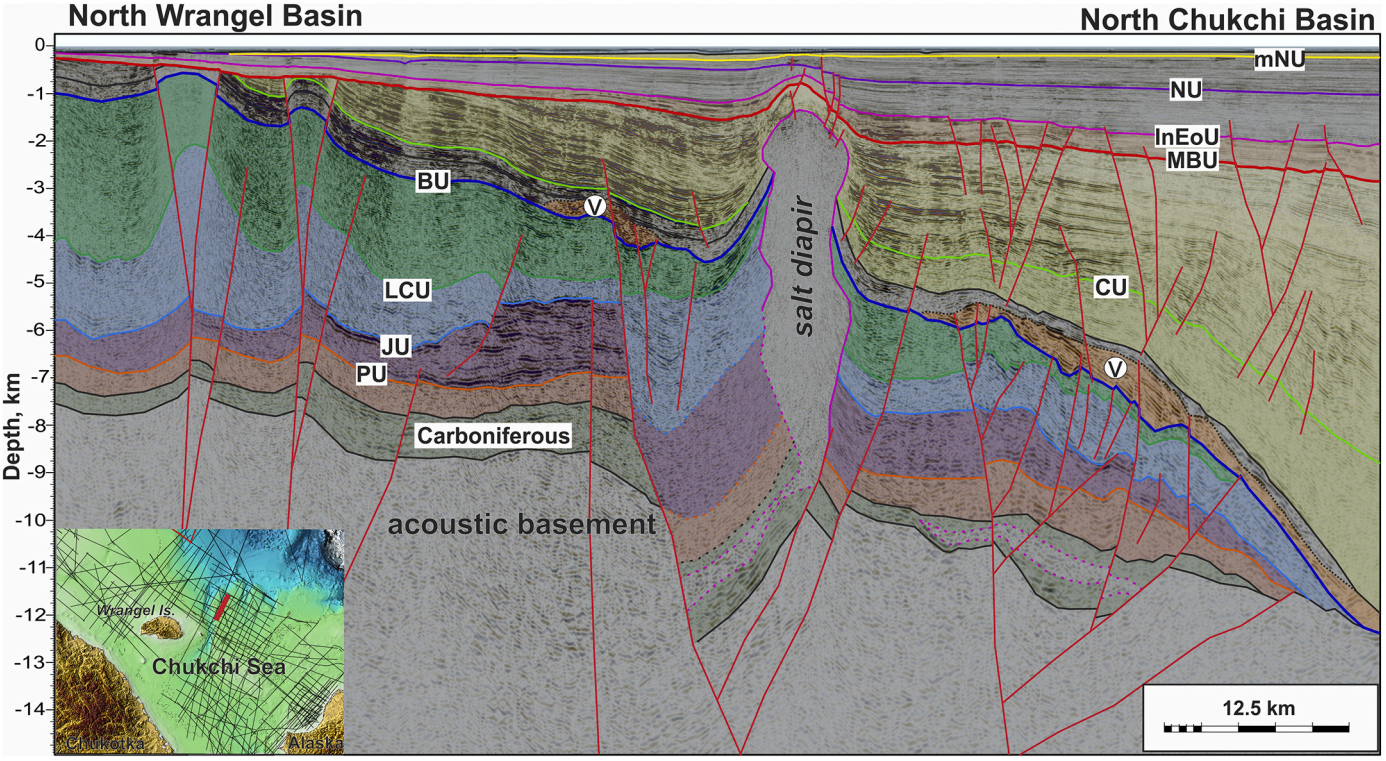

Fig. 19. Fragment of a seismic profile for the Chukchi Sea with geological interpretation. Location of the profile is shown on the map. Modified after Skaryatin et al. (2020). PU – Permian Unconformity, JU – Jurassic Unconformity, LCU – Lower Cretaceous Unconformity, BU – Brookian Unconformity, CU – Cenomanian Unconformity, MBU – Mid-Brookian Unconformity, InEoU – Intra-Eocene Unconformity, NU – Neogene Unconformity, mNU – Mid-Neogene Unconformity, v – unit with volcanics.

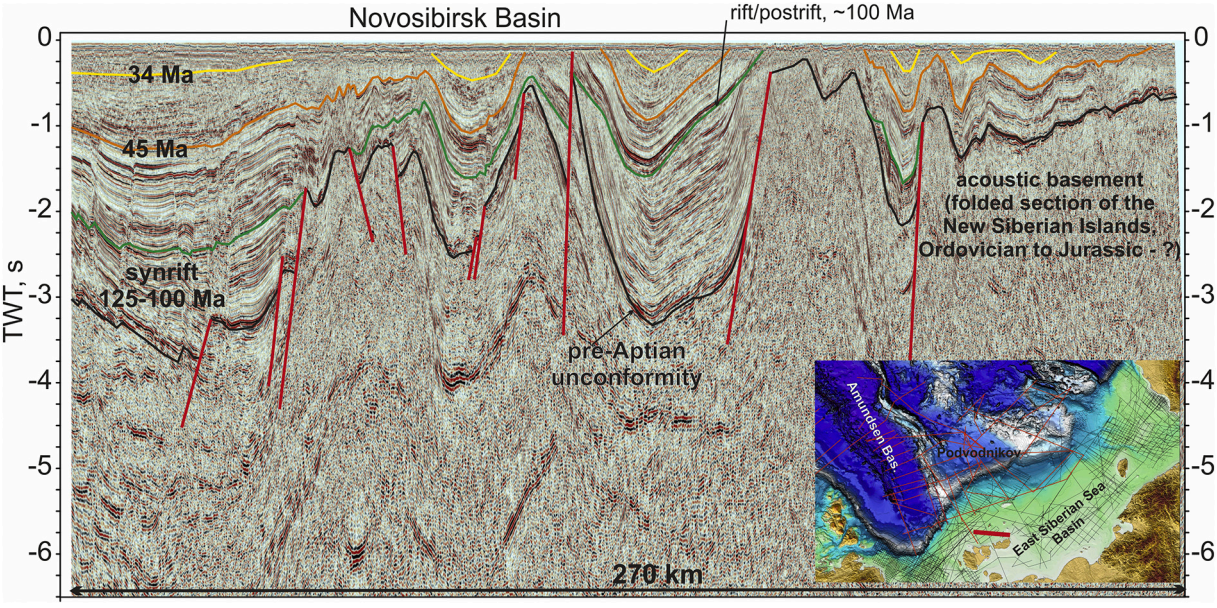

Fig. 20. Interpretation of seismic profile located to the north of the New Siberian Islands. Pre-Aptian or intra-Aptian angular unconformity is well documented for the New Siberian Islands (e.g. Kos'ko and Trufanov, 2002). Location of the profile is shown on the map. Data courtesy of the Ministry of Natural Resources, Russia.

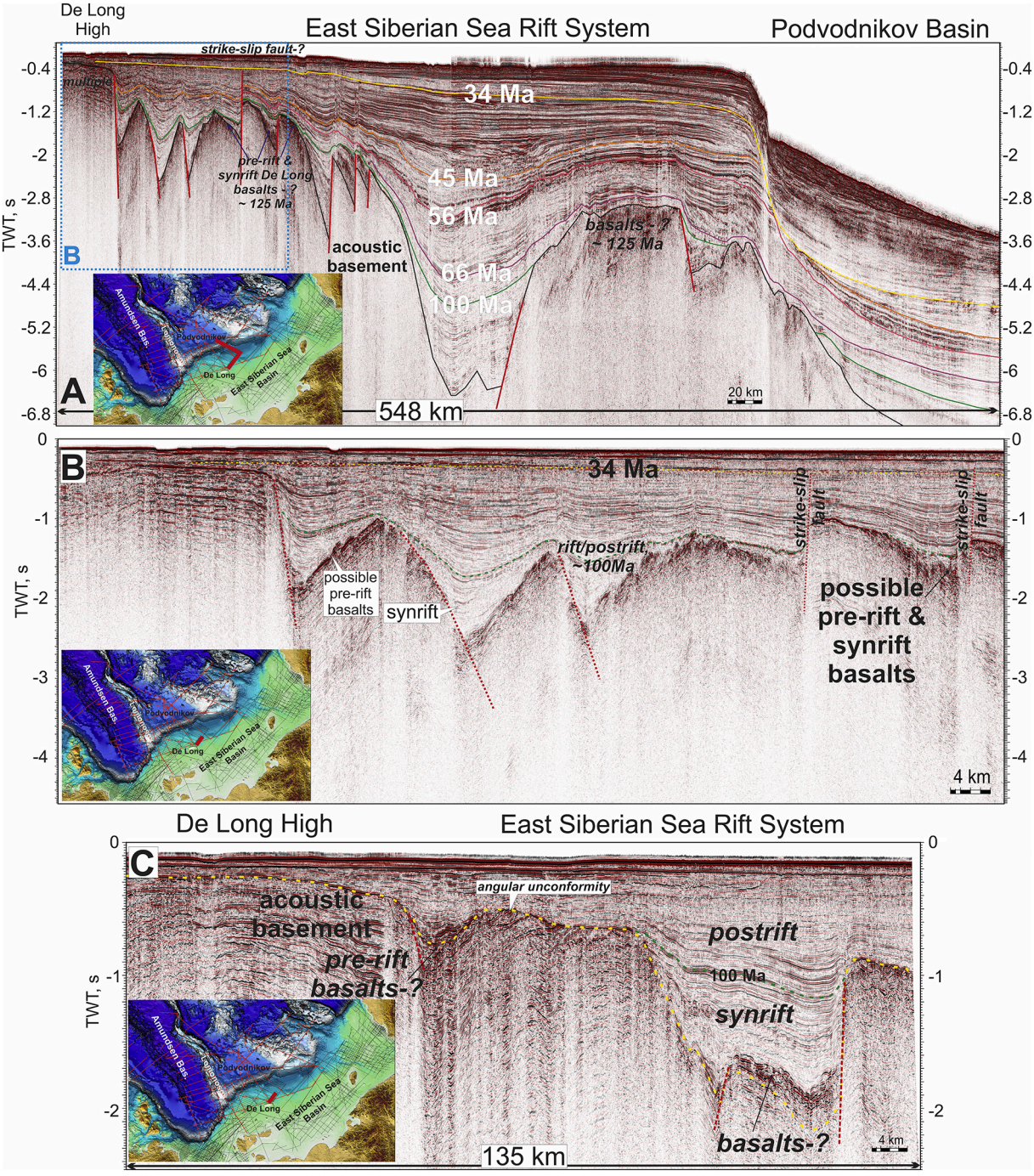

Fig. 21. Interpretation of seismic profiles for the East Siberian Sea Shelf (De Long High). A. Composite seismic profile from the East Siberian Sea Shelf (De Long High) to the Podvodnikov Basin (lines MAGE ESS1611 and MAGE ESS1601). B. Enlarged section of profile ESS1611. C. Seismic profile MAGE ESS1625. Location of the profiles is shown on the map. See also supplementary data, Fig. 21 (seismic profile without interpretation at high resolution).

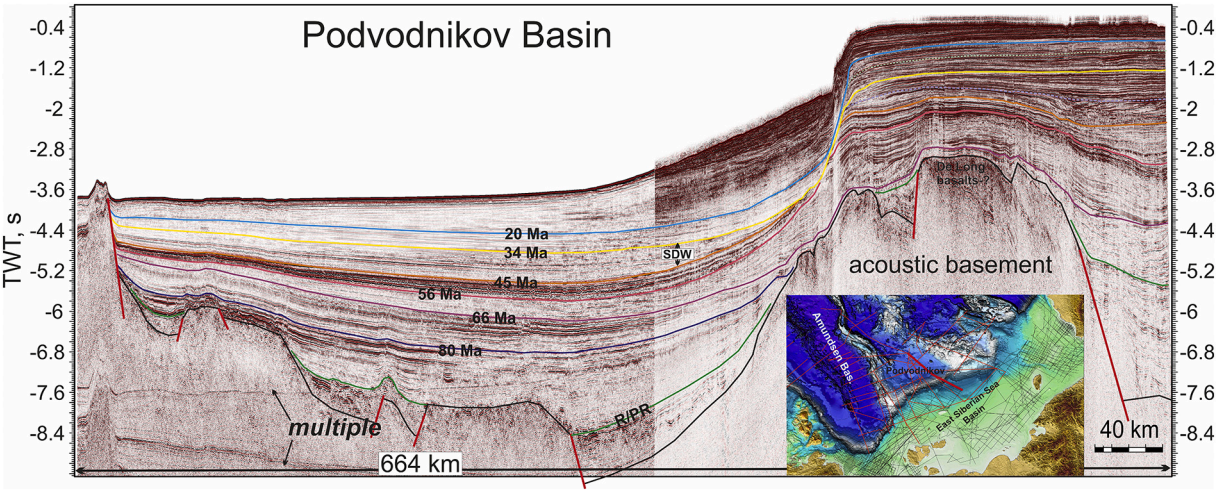

Fig. 22. Interpretation of composite seismic profile running from the East Siberian Sea Shelf to the Podvodnikov Basin (lines ARC 14-06 (fragment) and MAGE ESS1601). Location of the profile is shown on the map. R/PR – rift/postrift boundary. SDW – syntectonic depositional wedge. See also supplementary data, Fig. 22 (seismic profile without interpretation at high resolution).

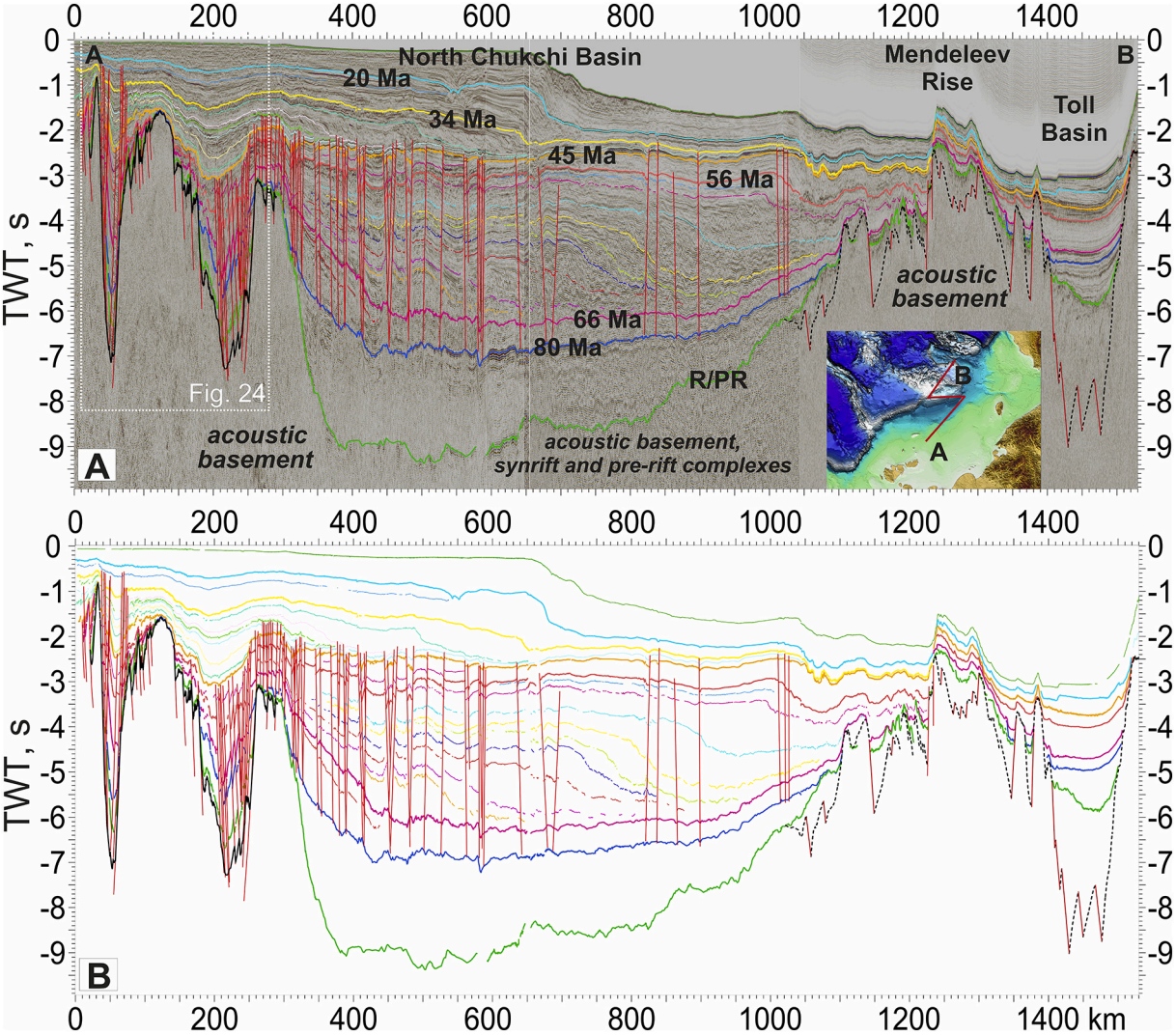

Fig. 23. A. Interpretation of composite seismic profile from the East Siberian Sea and Chukchi Sea Shelf to the Podvodnikov Basin, Mendeleev Rise and Toll Basin (lines ION12_1400, ION11_1400, 5AR, ARC14_P01, ARC12_03). Location of the profile is shown on the map. B. Interpretation without seismic imaging. See also supplementary data, Fig. 23 (seismic profile without interpretation at high resolution).

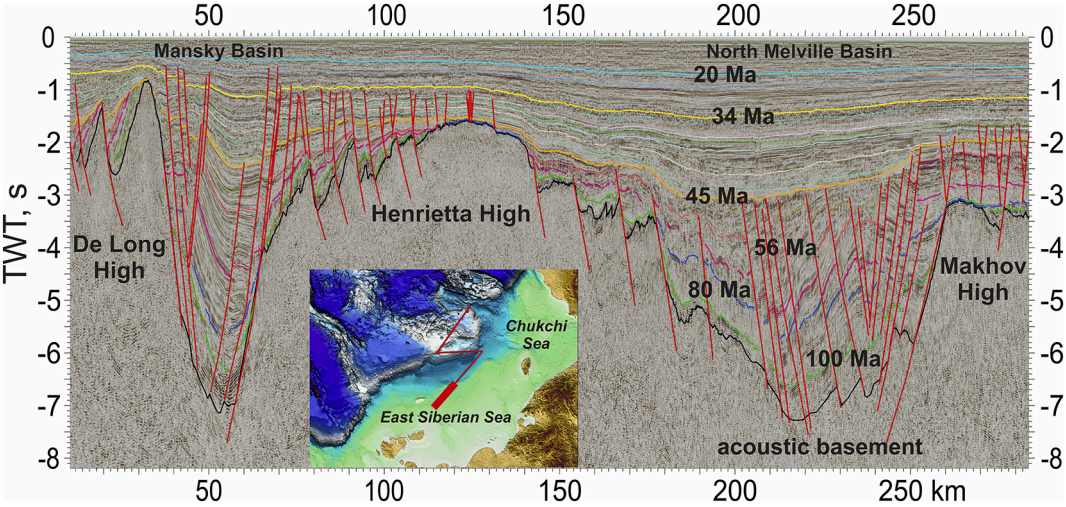

Fig. 24. Interpretation of a fragment of the composite seismic profile for the East Siberian Sea which is illustrated in Fig. 23 (white quadrangle) (line ION12_1400). A large continental rift system can be observed with a number of rift phases between 125 and 45 Ma and later. The correct timing of rifting is difficult to evaluate.

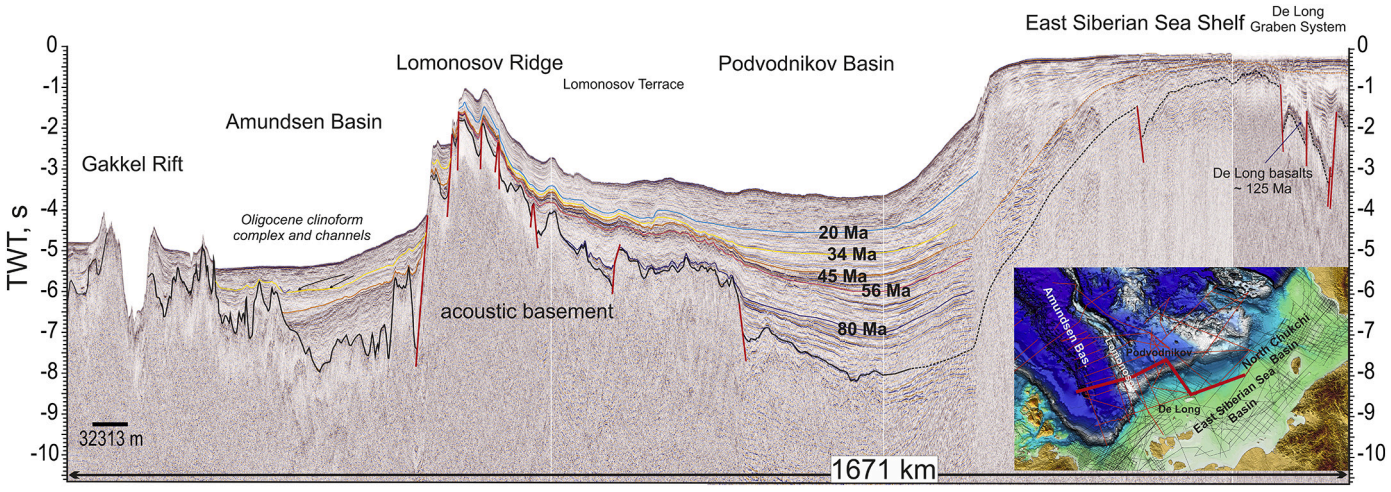

Fig. 25. Interpretation of composite seismic profile from the East Siberian Sea Shelf to the Gakkel Ridge (lines ARC 14-05, ARC 14-13, ARC 14-03, and ARC 12-16). Location of the profile is shown on the map. See also supplementary data, Fig. 25 (seismic profile without interpretation at high resolution).

Kuzmichev, 2009; Amato et al., 2015; Drachev, 2016; Toro et al., 2016; Petrov, 2017).

Mesozoic folding widely occurs on the New Siberian Islands and on the Wrangel Island in the Chukchi Sea. On the New Siberian Islands, the collisional orogeny ended before the Mid Aptian. Upper Aptian deposits unconformably overlie the Paleozoic-Lower Jurassic folded complex with the surface marked by angular discordance (Kos'ko and Trufanov, 2002; Kuzmichev et al., 2009, 2013; Kos'ko et al., 2013). This angular unconformity is well expressed on seismic profiles located in the area of the New Siberian Islands (Drachev et al., 2018; Nikishin et al., 2018; Nikishin et al., 2017; Nikishin et al., 2014) (Fig. 20). The following sedimentary sections have been identified on these islands (Kos'ko et al., 2013; Kuzmichev et al., 2013; Kuzmichev et al., 2009): the Late Aptian-Albian, Upper Cretaceous (Cenomanian-Coniacian), Eocene, and Quaternary. All deposits are represented predominantly by continental sandstones, siltstones and clays, intercalated with coal horizons. The presence of a Mesozoic pre-Aptian orogeny on the New Siberian Islands coupled with considerable pre-Aptian erosion is indicative of the fact that sedimentary complexes of the East Siberian Sea system of rifts are not older than Aptian (Sekretov, 2001; Nikishin et al., 2017; Nikishin et al., 2014). The deposits of the East Siberian Sea rifts can be traced on seismic lines into the Podvodnikov and Makarov basins of the Arctic Ocean (Figs. 21-30).

On Wrangel Island, folded Silurian-Triassic deposits are observed (Kos'ko et al., 1993; Verzhbitsky et al., 2015; Sokolov et al., 2017). It is commonly assumed that the main folding took place in the Late Jurassic-Early Cretaceous ca. 150-120 Ma, whereas a major uplift phase took place at ca. 105-90 Ma and 72-64 Ma (Kos'ko et al., 1993; Miller et al., 2010, 2018a, 2018b,; Verzhbitsky et al., 2015, Verzhbitsky et al., 2012; Sokolov et al., 2017). Examination of seismic lines within the North Chukchi Basin, north of Wrangel Island, reveals that the sedimentary cover of the North Chukchi Basin probably overlies the folded structures exposed on Wrangel Island (Nikishin et al., 2014, 2017) (Figs. 10, 17). This suggests that the formation of the North Chukchi Basin is not older

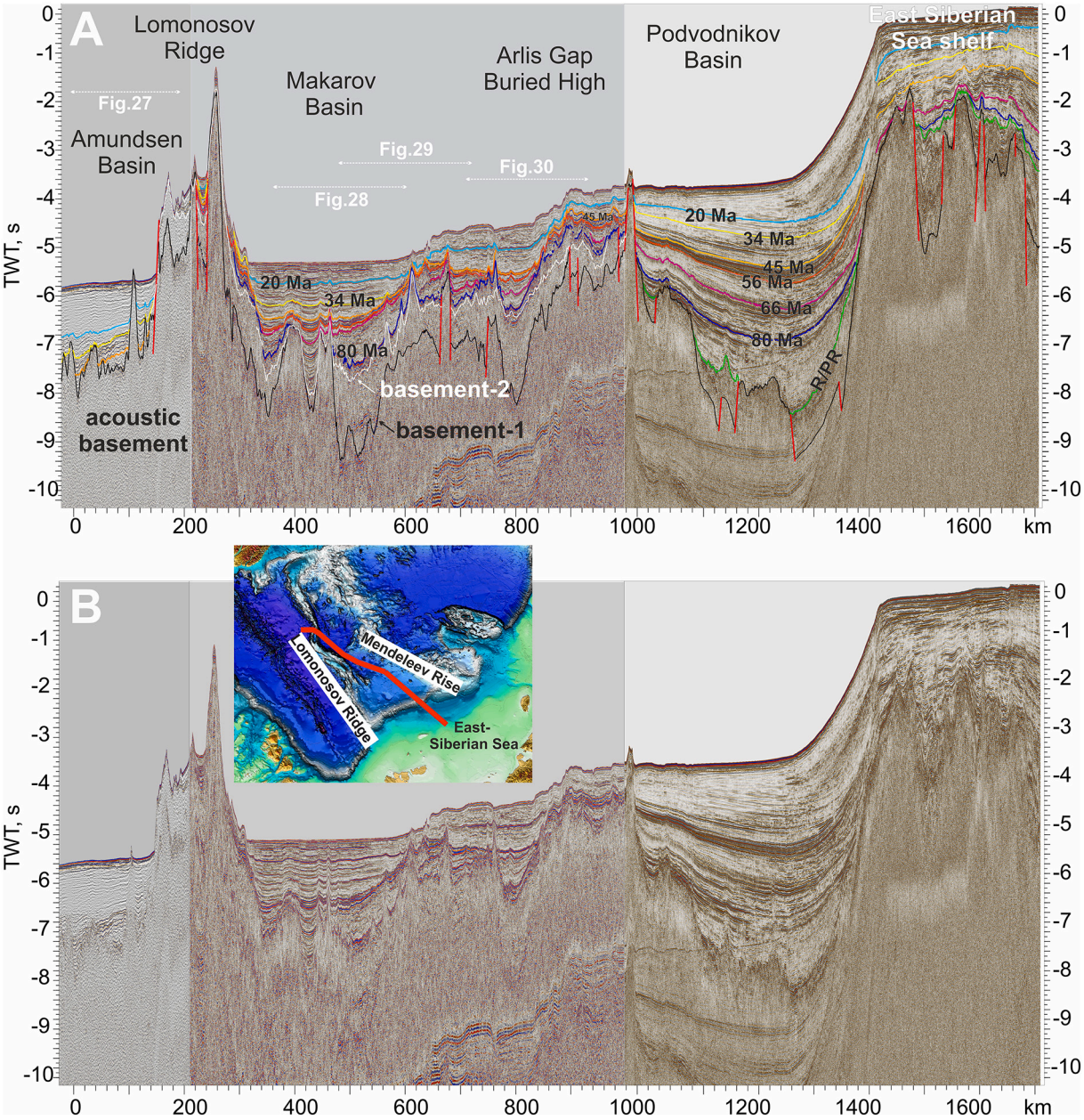

Fig. 26. A. Interpretation of composite seismic profile (lines ARC 14-39a, ARC 14-06, and ARC 14-02) for the region from the East Siberian Sea shelf to the Lomonosov Ridge and North Pole. Location of the profile is shown on the map. Different color lines are seismic horizons and corresponding ages (Ma). B. Seismic profile without interpretation. Basement-1 and basement-2 are two possible boundaries defining acoustic basement in the Arlis Gap-Makarov Basin region. An intermediate unit can be proposed between these boundaries. See also supplementary data, Fig. 26 (seismic profile without interpretation at high resolution).

than Aptian (Nikishin et al., 2014, 2017).

4.5. *Formation history of Late Jurassic to Neocomian (pre-Aptian) foredeep basins in the East Siberian and Chukchi Seas*

The Verkhoyansk-Chukotka Orogen has its possible northern boundary in the East Siberian and Chukchi seas and is expressed as a belt of syn-collisional foredeep basins (e.g., Puscharovsky, 1960; Miller and Verzhbitsky, 2009; Drachev et al., 2010, 2018; Nikishin et al., 2014, 2019; Bird et al., 2017; Popova et al., 2018). The basis of this hypothesis is that a Mesozoic orogeny was known for the New Siberian Islands and Wrangel Island, however, the region of De Long Islands has Early Paleozoic and older crust. Drachev et al. (2010) presented geophysical data for location of this foredeep basin and Nikishin et al. (2014) identified this thrust belt on recent Russian seismic data. Popova et al. (2018) evaluated Rosneft Oil Company data and documented a pre-Aptian foredeep basin, which they named the Zhokhov Basin. Based on the number of recent seismic sections that cross this region (Fig. 31), we recognize a classical foredeep basin with thrusting towards the north. The two-way travel time thickness of the foredeep basin sedimentary fill is ca. 5 secs, with a width of nearly 50-100 km. The Mesozoic orogen together with its foredeep basin is covered by Cretaceous post-

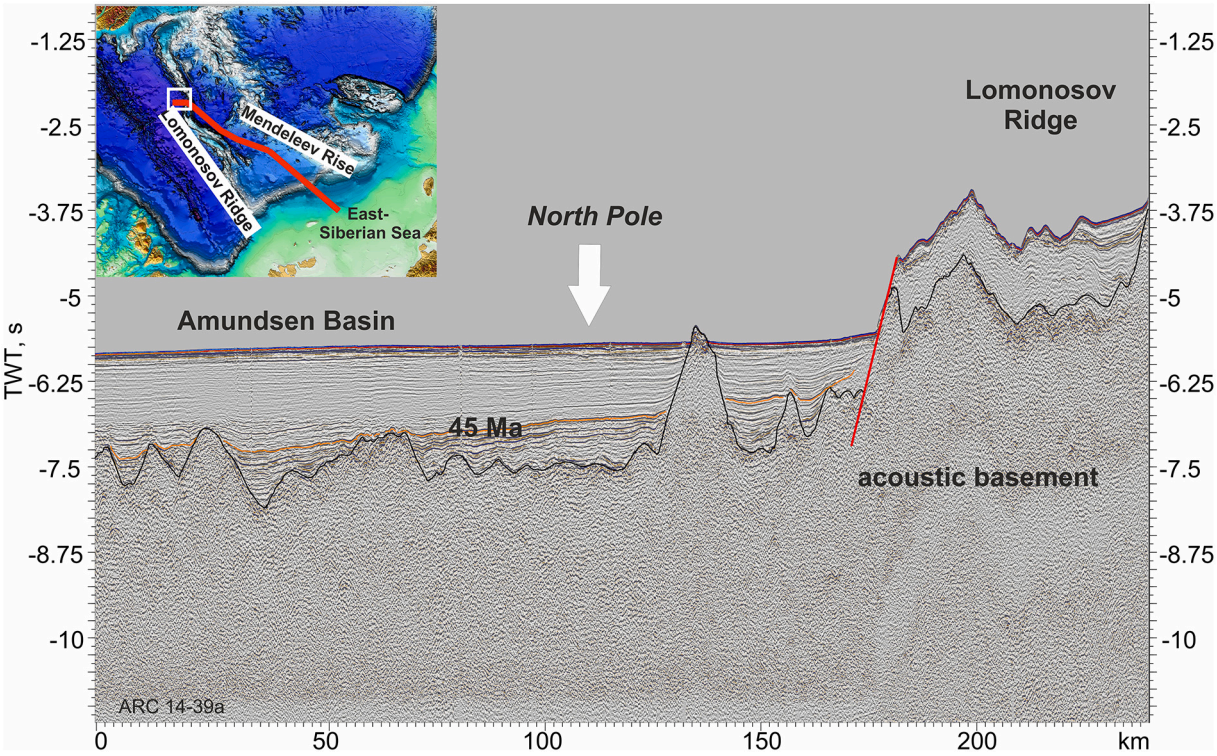

Fig. 27. Fragment of the profile shown in Fig. 26. This profile presents the first data illustrating the geological structure of the North Pole region. The North Pole is located in the Amundsen Basin and close to the Lomonosov Ridge. A key question concerns the position of the continental and oceanic crust boundary on this profile.

Barremian deposits. Some possible grabens can be recognized at the bottom of this Cretaceous section, the age of which is not older that the Aptian.

A pre-Aptian foredeep basin was proposed and documented north of Wrangel Island (Nikishin et al., 2014) and was named the North Wrangel Basin. Recent Rosneft Oil Company seismic data have supported this hypothesis (Skaryatin et al., 2020).

4.6. Formation history of the De Long plateau basalts and of the Alpha-Mendeleev Rise basalts

The De Long Islands are located in the northern part of the New Siberian Islands in the East Siberian Sea. On Bennett Island, one of the De Long Islands, Early Cretaceous plateau basalts are well known and overlie a Lower Paleozoic folded complex (Kos'ko et al., 2013). The age of the basalts is ca. 105-130 Ma (Drachev and Saunders, 2006; Kos'ko et al., 2013; Kuzmichev, personal communication). Below the basalts, Early Cretaceous sandstones with coals are observed (Kos'ko et al., 2013). A strong magnetic anomaly is associated with the De Long Islands, indicative of a possible widespread Early Cretaceous basaltic plateau (Drachev and Saunders, 2006; Drachev et al., 2010; Gaina et al., 2011; Saltus et al., 2011; Nikishin et al., 2014, 2017; Shipilov, 2016). The De Long Plateau forms an uplifted area and is transected by several seismic lines. Several grabens are located within the plateau (Drachev et al., 2010; Nikishin et al., 2014, 2017). At the base of some of the graben fills, packages of high-amplitude reflections are observed (Figs. 6, 21, 22). We assume that these high-amplitude reflections correspond to the De Long basalt complex interbedded with layers of sedimentary deposits (Nikishin et al., 2014, 2017; Shipilov, 2016). The most obvious example is in the Anisin Basin located just north-west of Kotelny Island of the New Siberian Islands where we recognize high-amplitude reflections at the base of the graben and interpret as possible volcanics. In addition we see seismic reflection patterns indicative of the existence of numerous magmatic intrusions below the acoustic basement (Fig. 32). It follows from this hypothesis that the rifting in the East Siberian Sea started at the time of the basaltic volcanism, i.e., the start of the rifting took place not earlier than the Aptian (Nikishin et al., 2014, 2017).

Basalts were penetrated by shallow drilling on the slope of the Trukshin Seamount on the Mendeleev Rise yielding U-Pb ages of 127 Ma derived from zircon samples (Morozov et al., 2013) (see Paper-1, Nikishin et al., 2021a). Basalts of similar age are known in the Canadian Arctic Islands (e.g., Embry and Osadetz, 1989; Evenchick et al., 2015). On the seismic line across the Trukshin seamount these basalts are within the acoustic basement (Nikishin et al., 2014, 2017, 2021a). North of the Chukchi Plateau, basalts were recovered by dredging on slopes of bathymetric highs and have isotopic ages of 118-112 Ma, 105-100 Ma, and 90-70 Ma (Brumley, 2014; Mukasa et al., 2020). On the Mendeleev Rise they either are observed within the acoustic basement or are present as high-amplitude reflections in the cover (Brumley, 2014; Nikishin et al., 2014) These basalts are overlain by the Alpha-Mendeleev sedimentary cover. It should be noted that at the present time there is insufficient data on volcanic rocks of the Alpha-Mendeleev Rise, to allow for robust conclusions. The sedimentary cover possibly starts from the Middle-Upper Cretaceous and includes basalt deposits that form seismically-defined packages characterized by high-amplitude reflections (Nikishin et al., 2014; Rekant et al., 2015; Coakley et al., 2016) (Figs. 33-44).

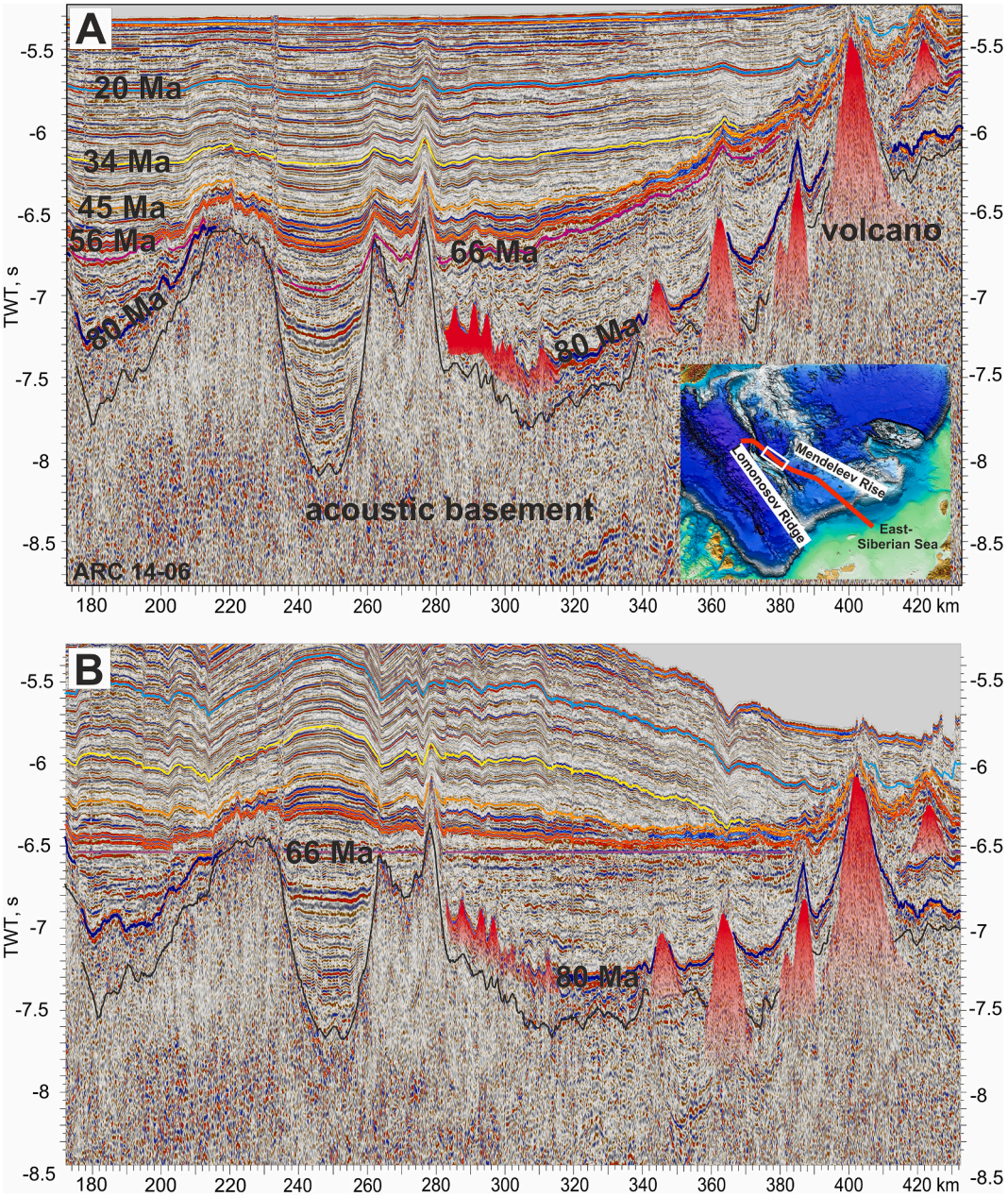

Fig. 28. Fragment of the profile shown in Fig. 26. This profile crosses the Makarov Basin and its southern margin. A. Interpretation of the profile. A V-shape trough is located in the central part of the basin, interpreted as a possible rift basin with a pre-66 Ma age. Possible volcanic structures with Cretaceous pre-80 Ma age are outlined by red lines. B. Section flattened on the 66 Ma horizon.

In 2014 and 2016 rock samples were collected from four scarps on the Mendeleev Rise using a specially-equipped submarine (see Paper-1, Nikishin et al., 2021a). The samples were collected by Skolotnev et al. (2017, 2019,) and four sections were studied, composed mainly of deformed sedimentary rocks with Ordovician to Devonian fauna (see Paper-1, Nikishin et al., 2021a). These sections are pierced by basalt dikes and sills of Early Cretaceous age (105-124 Ma) (Skolotnev et al., 2017, 2019; Skolotnev, unpublished data). The deformed Paleozoic deposits are unconformably covered by Aptian (or late Barremian to Aptian) sandstones in the Trukshin seamount, and basalts and basaltic tuffs with isotopic ages close to 112-124 Ma are observed (Petrov, 2017; Skolotnev et al., 2019; Skolotnev et al., 2017) (see Paper-1, Nikishin et al., 2021a). From these data it appears that the Mendeleev Rise comprises a continental terrane that has experienced strong extension and Cretaceous magmatism.

4.7. Formation history of rifting in the shelf basins of the East Siberian and Chukchi Seas

A large system of continental rifts is present within the shelves of the East Siberian and Chukchi Seas (Drachev et al., 2010; Nikishin et al., 2019; Nikishin et al., 2017; Nikishin et al., 2017; Popova et al., 2018)

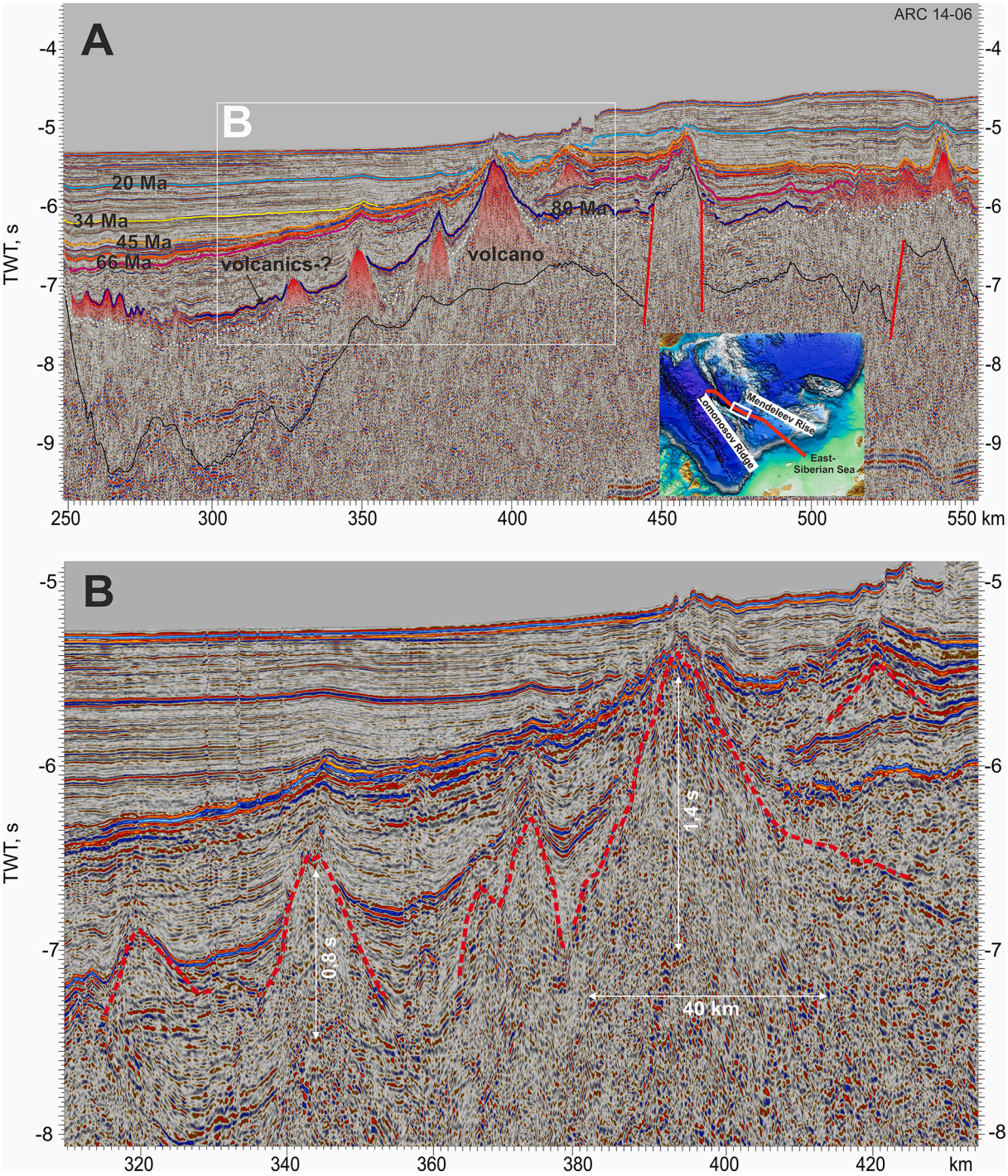

Fig. 29. A. Fragment of the profile shown in Figs. 26 and 28, and detailed fragment of Fig. 28. This profile is located in the region between Arlis Gap Buried Plateau and the Makarov Basin. A number of volcano-like features can be identified. Volcanoes have a Cretaceous pre-80 Ma age. B. Fragment of this profile. Dashed red lines outline possible volcanoes without evidence for subareal erosion, suggesting that these volcanoes originated as submarine structures.

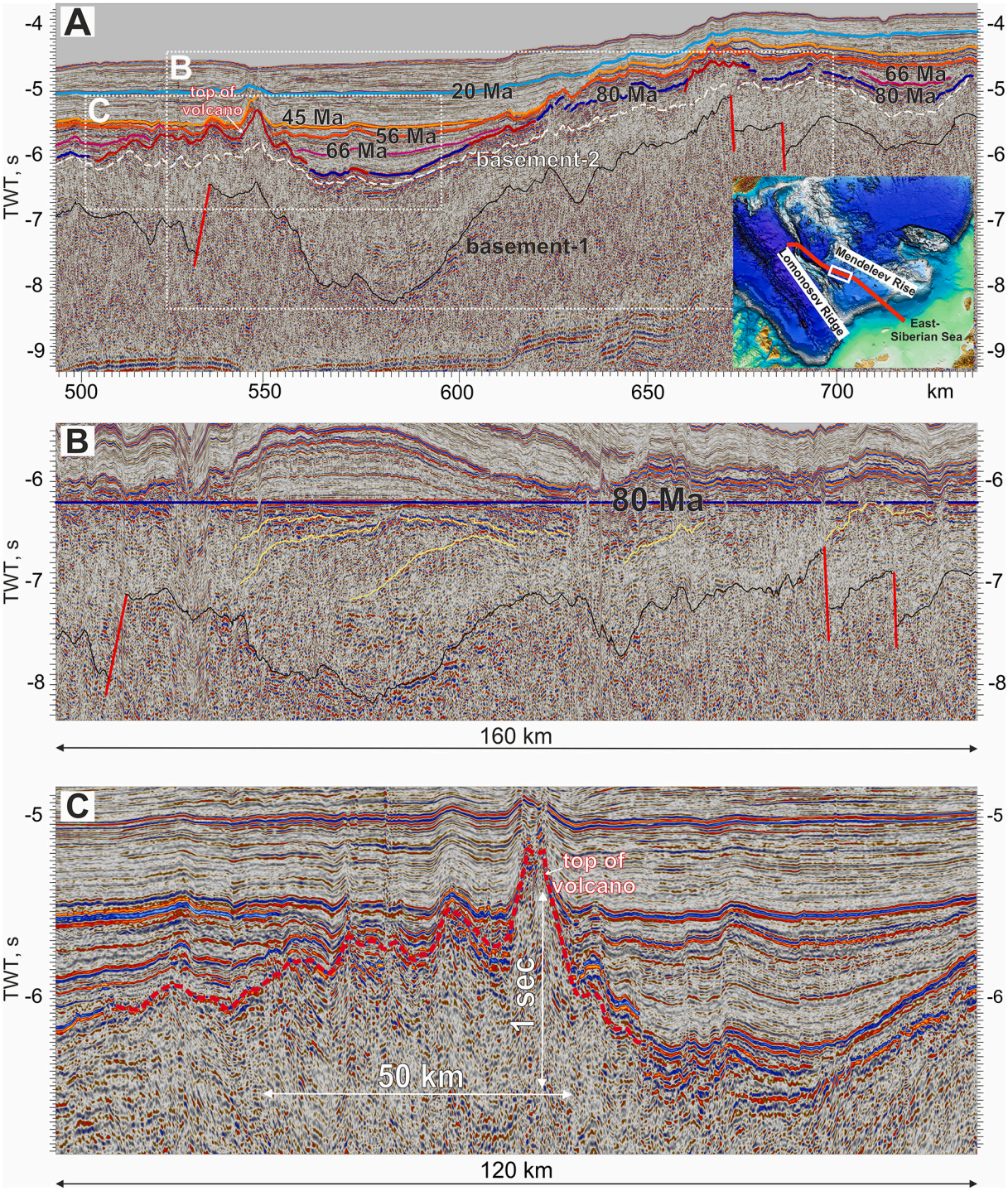

Fig. 30. A. Fragment of the profile shown in Fig. 26. This profile is located in the Arlis Gap Buried Plateau. Red lines are outlines of possible volcanoes. Onlapping of seismic horizons toward 80 Ma surface is observed, implying possible tectonic movements between 80 and 66 Ma and younger. B. Section flattened on the 80 Ma horizon. Possible synrift complex can be observed below 80 Ma horizon. C. Fragment of the seismic line with possible volcanic structures. These structures are of Cretaceous age (older than 80 Ma).

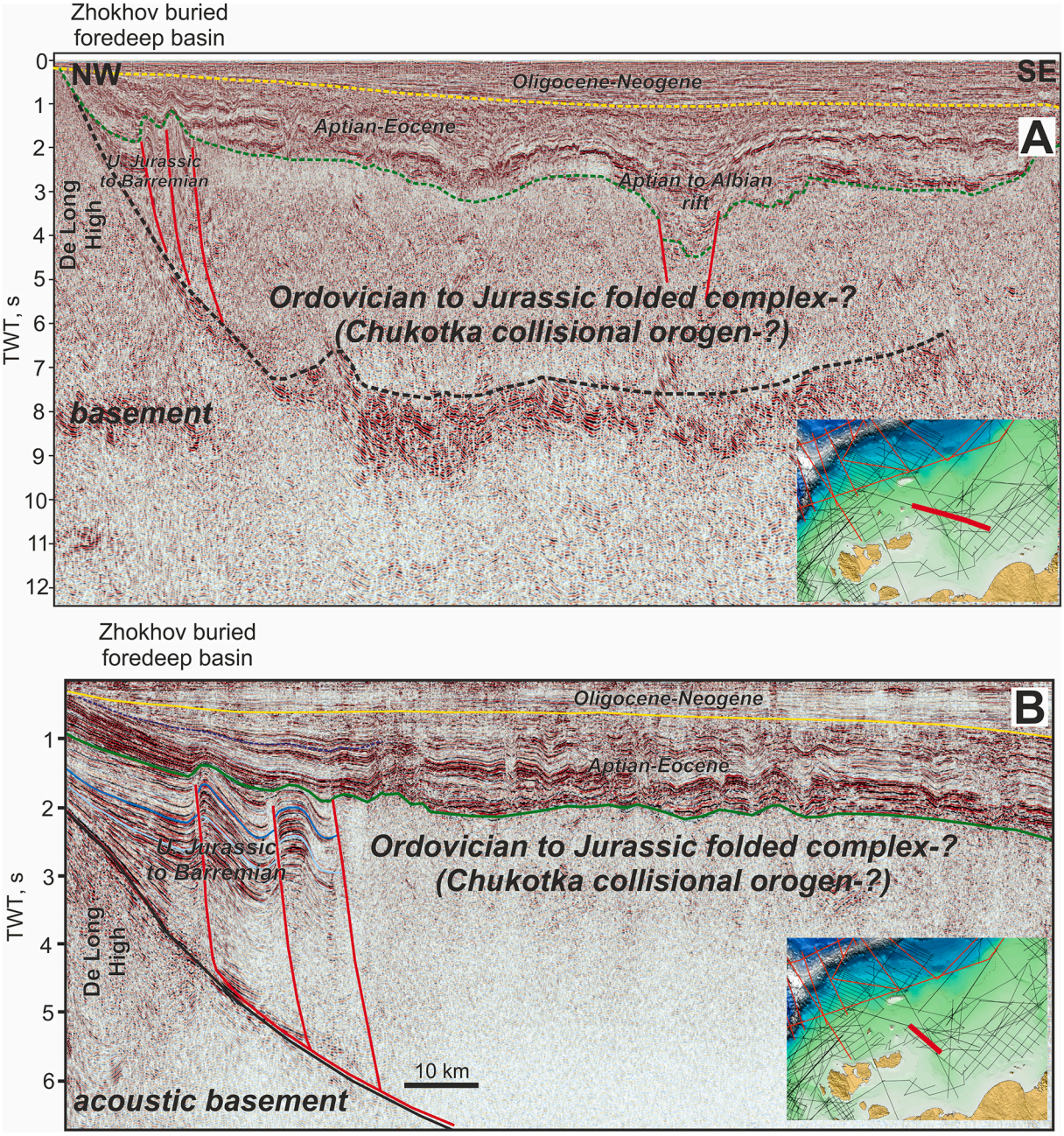

Fig. 31. Seismic profiles for the Zhokhov Foredeep Basin region. A. Modified after Nikishin at al. (2014). B. Fragment of the profile ES1_16ES21 (MAGE, Murmansk, data courtesy of the Ministry of Natural Resources, Russia).

(see Paper-1, Nikishin et al., 2021a). As we pointed out in previous sections the most probable time of rift onset was the Aptian.

Numerous anomalies of apparent intrusive origin are observed on several seismic sections north of Wrangel Island in the Chukchi Sea (Figs. 45, 46). These anomalies, characterized by high-amplitude reflections, all occur below the possible 125 Ma horizon (the base of the Aptian) and are similar to the numerous anomalies in the Barents Sea, which have been interpreted as Cretaceous intrusions (Corfu et al., 2013; Polteau et al., 2016; Minakov et al., 2018). In the North Chukchi Basin, high-amplitude reflections are present at the base of the stratigraphic section, and can be interpreted as alternating basalts and sedimentary rocks (Figs. 46, 47). This probable igneous province in the Chukchi Sea is distinctly identifiable on the magnetic anomaly map (Gaina et al., 2011) in the form of a strong positive anomaly. The age of the magmatism could be Aptian (or HALIP); in this case, the magmatism was approximately synchronous with the magmatism of the De Long Plateau in the East Siberian Sea and with the magmatism on the Alpha-Mendeleev Rise. We propose that at the onset of formation of the North Chukchi Basin, approximately in the Aptian, basaltic magmatism occurred.

Within the East Siberian and Chukchi Sea rifts, a rift/postrift boundary is seismically identified (Figs. 20–26, and 32) though its

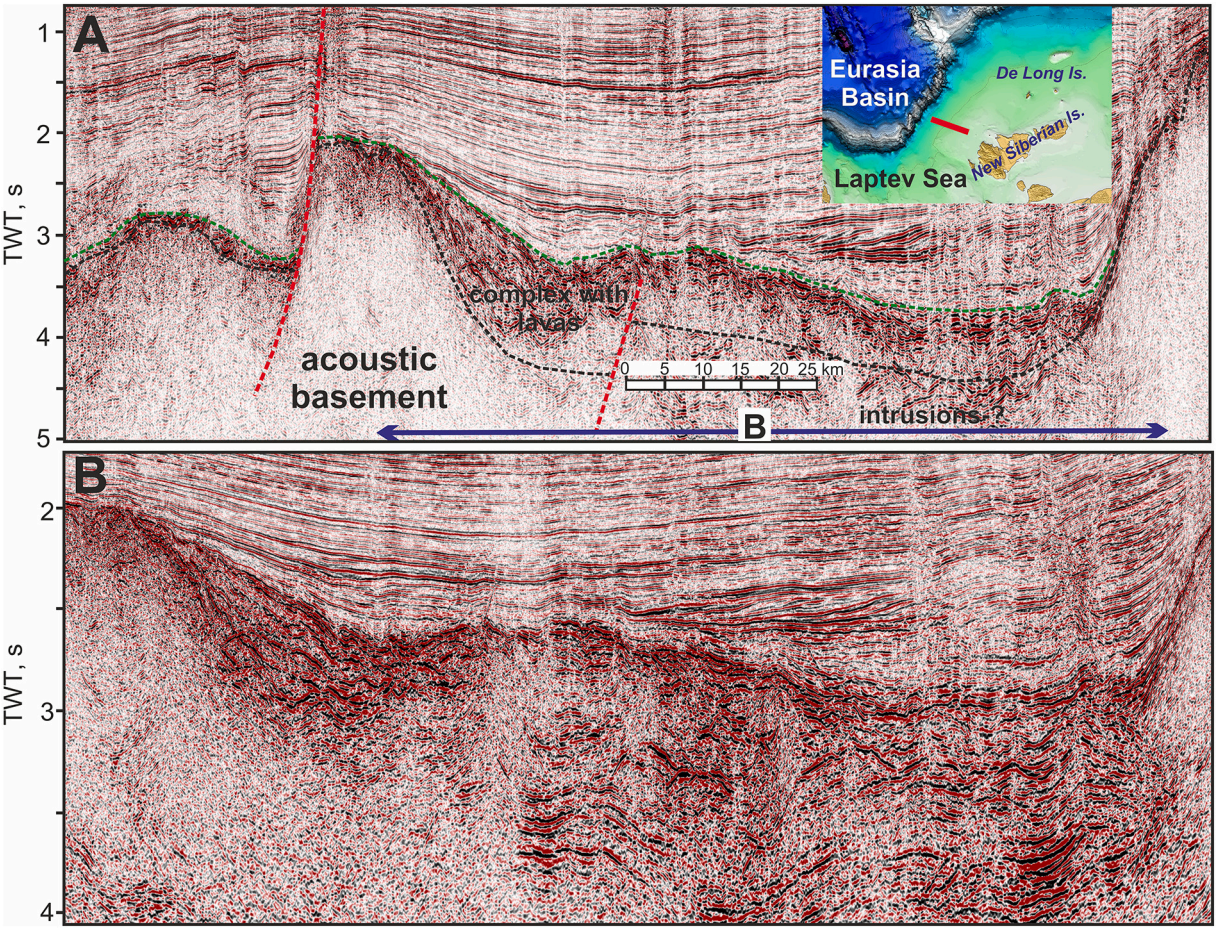

Fig. 32. A. Fragment of seismic profile across the Anisin Basin. Location of the profile is shown on a map. B. Fragment of profile A. Possible volcanic complex and intrusions can be observed. Volcanics are at the base of the rift basin. Data courtesy of the Ministry of Natural Resources, Russia.

precise dating is difficult. Because an unconformity between the Albian and the Cenomanian exists on the New Siberian Islands, we propose as a hypothesis that this boundary corresponds to the rift/postrift boundary and we date it as 100 Ma. Miller et al. (2018b, 2018a) studied a normal fault event possibly related to rifting, on Wrangel Island using U-Pb and AFT dating and concluded that the timing of fault motion was likely 105-100 to 95 Ma, with only a minor uplift after that. These data are consistent with our general model. This unconformity of Cenomanian or Early Cenomanian age also is well documented in the Beaufort-Mackenzie Basin (Embry and Dixon, 1994) and Arctic Alaska (Homza and Bergman, 2019; Ilhan and Coakley, 2018).

New data on the New Siberian Islands history based on low-temperature thermochronology demonstrate that a cooling episode took place at 125-93 Ma (Prokopiev et al., 2018). We interpret this epoch as a rift shoulder uplift event. Our data do not support the hypothesis of Prokopiev et al. (2018) that it was a compressive event with thrusting.

4.8. A breakup unconformity on the Laptev Sea Shelf and on the Lomonosov Ridge

Retraction of the Lomonosov Ridge from the Barents-Kara Shelf is assumed to have occurred in the course of formation of the Eurasia Basin (e.g., Drachev et al., 2010); a breakup unconformity with an age of about 56 Ma corresponds to the time of onset of oceanic crustal spreading in the Eurasia Basin (Drachev et al., 2010; Franke, 2013; Nikishin et al., 2014; Weigelt et al., 2014). This boundary is observed in the Laptev Sea (Figs. 48, 49) and on the slopes of the Lomonosov Ridge (Figs. 7, 8, 9, 50), and can be correlated with boundaries of seismic sequences in the Arctic Ocean.

New data on the New Siberian Islands history based on low-temperature thermochronology demonstrate that a cooling episode took place at ca. 53 Ma (Prokopiev et al., 2018). We interpret this epoch as a rift shoulder uplift event.

4.9. Seismic stratigraphy of the Laptev Sea Basin

The Laptev Sea basin is traditionally considered a single rift system (Drachev et al., 2010; Franke, 2013; Weigelt et al., 2014). Interpretation of the new grid of seismic lines shows that this is probably not correct (Nikishin et al., 2017, 2018). In the eastern part of the Laptev Sea in the area of the Anisin Basin, complex rifting probably started in the Aptian. There are two main constraints for this hypothesis: (1) At the base of the rift fill sections in the area of the De Long High, packages of high-amplitude reflections are observed, which are interpreted as basalts (Figs. 21, 32). These basalts are present on the nearby De Long Islands and have been dated at ca. 130-105 Ma (Barremian-Aptian) (Kos'ko and Trufanov, 2002; Drachev and Saunders, 2006;Kos'ko et al., 2013). (2)

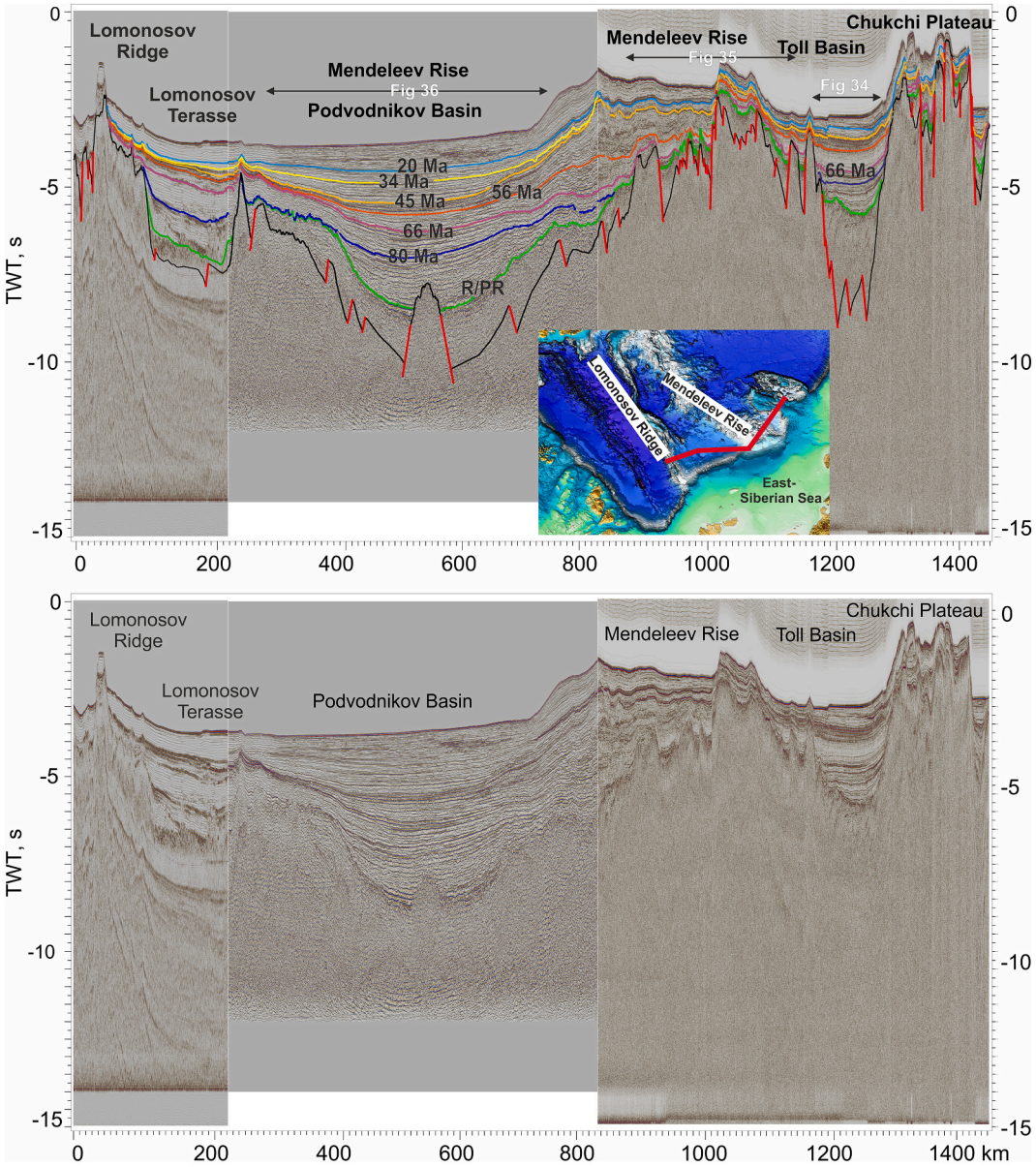

Fig. 33. Interpretation of composite seismic profile (lines ARC 12-03, ARC 14-01 and ARC 11-053) for the region from Lomonosov Ridge to Chukchi Plateau. Location of the profile is shown on the map. Different color lines are seismic horizons and corresponding ages (Ma), R/PR - rift/postrift boundary. See also supplementary data, Fig. 33 (seismic profile without interpretation at high resolution).

An angular unconformity at the base of the rift complex is observed on some seismic lines in the area of the De Long High (Nikishin et al., 2014). This unconformity probably corresponds to the known regional unconformity on the New Siberian Islands, which lies at the base of the Aptian and is substantiated in many studies (Kos'ko and Trufanov, 2002;Kuzmichev et al., 2009, 2013;Kos'ko et al., 2013; Nikishin et al., 2017).

In the western part of the Laptev Sea Basin in the area of the Ust' Lena Basin, a breakup boundary is clearly observed, which is dated at 56 Ma (Fig. 48). Below this boundary, a synrift sediment complex is observed, which can be dated as Paleocene (or Cretaceous-Paleocene). That is, continental rifting in the Ust' Lena Basin took place in the Paleocene before the onset of the Eurasia Basin opening.

Numerous intrusive type anomalies associated with volcanic sills and dykes are observed in the western part of the Laptev Sea on some seismic sections (Fig. 48). These probable intrusions occur below the breakup boundary (56 Ma). High-amplitude reflections, which can be interpreted as volcanics, are identified below the Eocene section as well. The timing of magmatism is likely close to the Paleocene/Eocene boundary. The presence of a likely igneous province is confirmed by the presence of a strong positive anomaly on the magnetic anomaly map (Gaina et al., 2011). It is likely that a period of basaltic magmatism took place before the onset of opening of the Eurasia Basin – we call this magmatic area the Faddey Magmatic Province. Based upon magnetics and seismic data, a very similar province with possible volcanoes is located on the other side of the Eurasia Basin at the transition between the Lomonosov Ridge and the shelf region (Figs. 7, 9). We name this magmatic area the

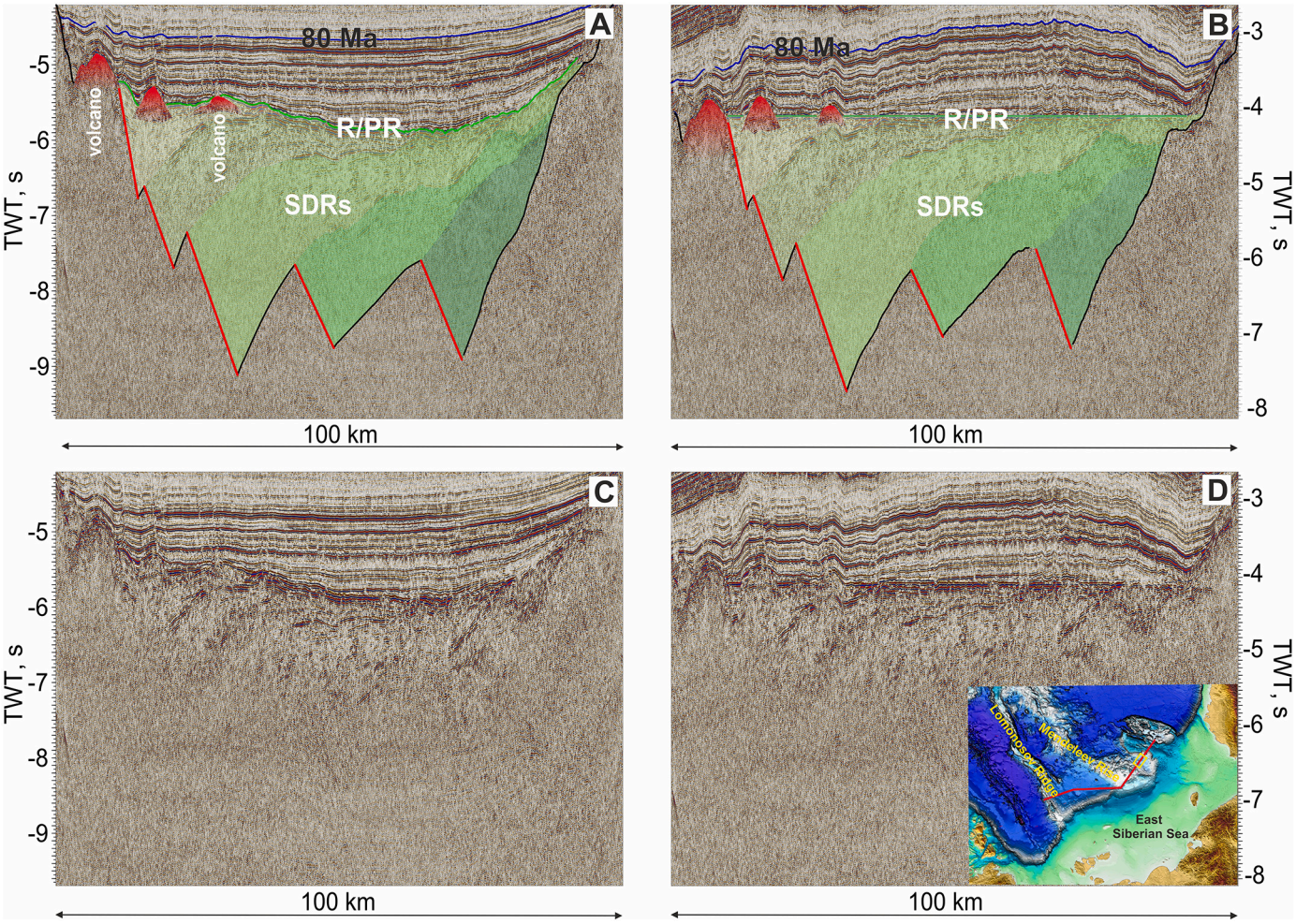

Fig. 34. A. Interpretation of a fragment of seismic profile (lines ARC 12-03) from the Toll Basin (Fig. 33). Location of the profile is shown on the map. Different color lines are seismic horizons and corresponding ages (Ma). SDR complexes and volcanoes on a top of SDRs are interpreted. B. Flattening on the rift/postrift boundary. C and D – profiles without interpretation.

Lomonosov-Anisin Magmatic Province.

New data show that in the eastern part of the Laptev Sea, the main rifting was in the Aptian-Albian. These rifts should be assigned to the system of rifts of the East Siberian and Chukchi Seas rifts and were connected with the Podvodnikov Basin (Nikishin et al., 2017). The Ust' Lena Rift in the western part of the Laptev Sea was associated with the subsequent opening of the Eurasia Basin.

Eocene-Quaternary normal faults are common in the Laptev Sea Basin (Figs. 51, 52). Their formation has traditionally been interpreted as the continuation of the Gakkel Mid-Oceanic Ridge (Drachev et al., 2010; Franke, 2013; Nikishin et al., 2018).

4.10. SDR complexes in the Mendeleev Rise and Podvodnikov and Toll basins

The Toll Basin is located between the Chukchi Plateau and the Mendeleev Rise. The Toll Basin has one significant feature in its lower part: there is a probable rift-postrift boundary below which packages of reflections dip uniformly towards the Mendeleev Rise (Nikishin et al., 2014) (Fig. 34). They are interpreted as possible Seaward Dipping Reflectors (SDRs) and are typical of volcanic passive continental margins (e.g., Geoffroy, 2005). Recently, American investigators published a profile that lies southward and almost parallel to our profile (Ilhan and Coakley, 2018). It clearly shows similar SDRs with the same polarity. SDRs are primarily composed of synrift basalts that are emplaced during continental rifting over mantle plumes (e.g., Geoffroy, 2005) (this is a very specific topic which we will not discuss in detail here). Based upon our grid of seismic data, apparent SDR-like units are very common for the Mendeleev Rise (Figs. 34, 35, 36, 37, 38, 39, 40, and 41). They could be classical SDRs with basalts, though we cannot conclusively rule out the possibility that these reflections are indicative of sedimentary deposits within half grabens. The Mendeleev Rise appears to be divided into two parts, each of which characterized by a consistent and contrasting dip. Reflections dip toward the Toll Basin on the eastern slope of the Mendeleev Rise and toward the Podvodnikov Basin on its western slope. The presence of SDR-like units also is proposed for the Podvodnikov Basin. These units are observed along the eastern and western slopes of this basin (Figs. 33, 35, 36, 37). The rift/postrift boundary (or top of SDR complex) seems to be at nearly the same stratigraphic level in the regions of the Podvodnikov Basin, Mendeleev Rise, and Toll Basin (Figs. 33-42). Although this is not precisely determined, we cannot find evidence for moving this boundary to different stratigraphic levels. Our

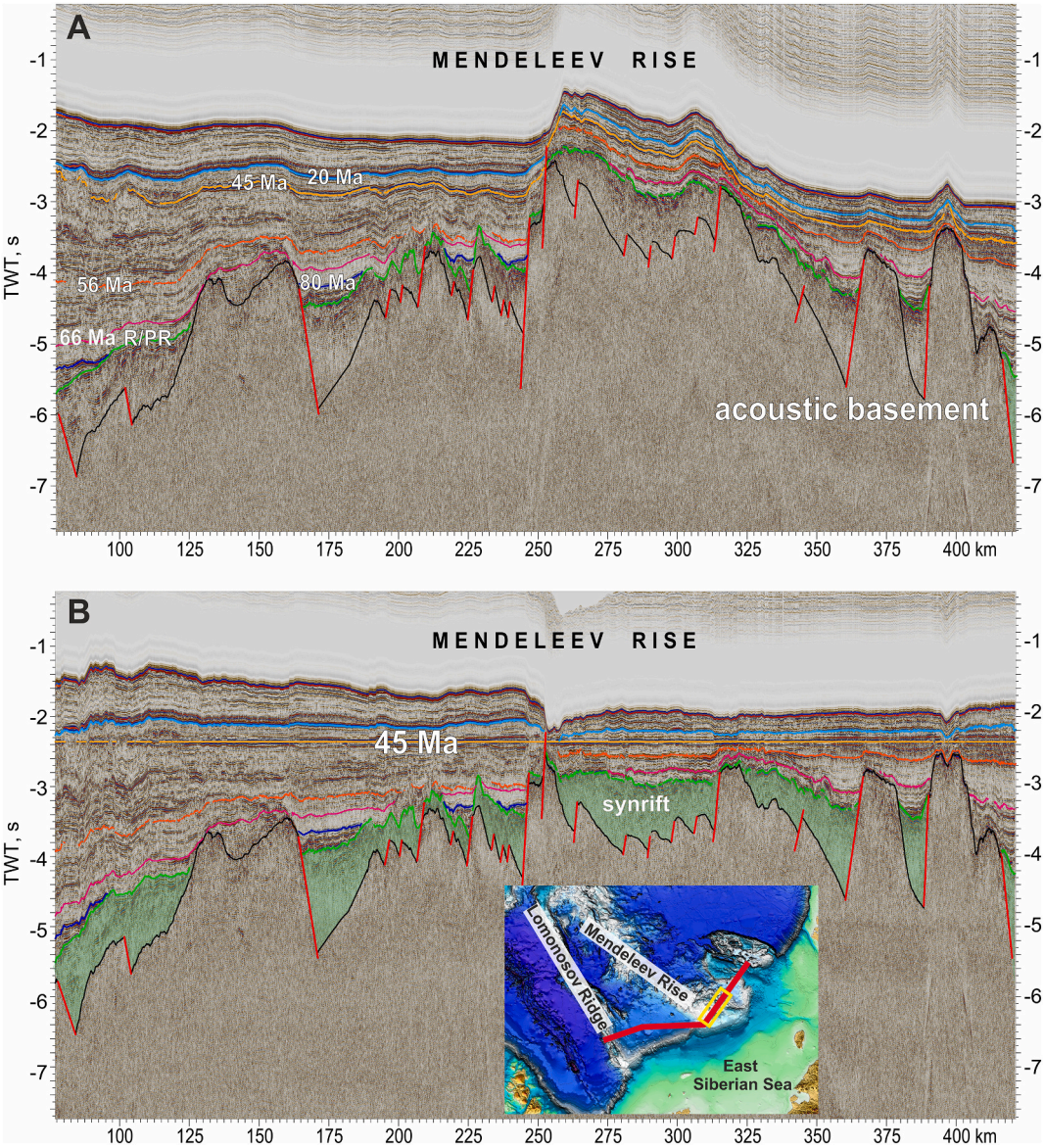

Fig. 35. A. Fragment of seismic profile shown in Fig. 33. The line ARC 12-03 for the Mendeleev Rise. Location of the profile is shown on the map. Different color lines are seismic horizons and corresponding ages (Ma). B. Profile flattened on the 45 Ma horizon. Horst/graben structure on the Mendeleev Rise acoustic basement can be observed.

seismic data suggests that SDR-like units and/or half-grabens are characterized by strike that is approximately parallel to the Mendeleev Rise and Toll Basin (Figs. 33, 37). This implies that the orientation of extension was orthogonal to the Mendeleev Rise. We observe on 2D seismic sections volcano-like conical seismic structures at the top of the SDR complexes along 2D seismic lines (Figs. 34, 36).

As discussed above, Skolotnev et al. (2017, 2019) studied samples collected on the Mendeleev Rise (see also Paper-1, Nikishin et al., 2021a). These authors documented the presence of Aptian (or Barremian-Aptian) shallow-marine sandstones, Cretaceous basalt lavas and Cretaceous tuffs. The Paleozoic section is associated with basaltic Cretaceous intrusions. Associated Cretaceous volcanic extrusives occurred in sub-aerial and shallow-marine conditions. The isotopic age of magmatism was close to 105-125 Ma (Skolotnev et al., 2019; Skolotnev et al., in preparation). Our seismic data together with the Skolotnev et al. (2019) data demonstrate that the Mendeleev Rise contains multiple half-grabens and/or SDR units. Half-grabens and/or SDRs are characterized by continental basement enriched with basalt intrusions.

A rift/postrift boundary is observed at nearly the same stratigraphic level in the region of the Podvodnikov Basin, Mendeleev Rise, and Toll Basin as discussed above. We dated the rift/postrift boundary for shelf basins in the Laptev, East-Siberian Sea and Chukchi Sea as ca. 100 Ma. Although this is a speculative conclusion, it seems most reasonable to correlate this rift/postrift boundary on the shelf with the same boundary in the Mendeleev Rise region and dating to ca. 100 Ma, or younger.

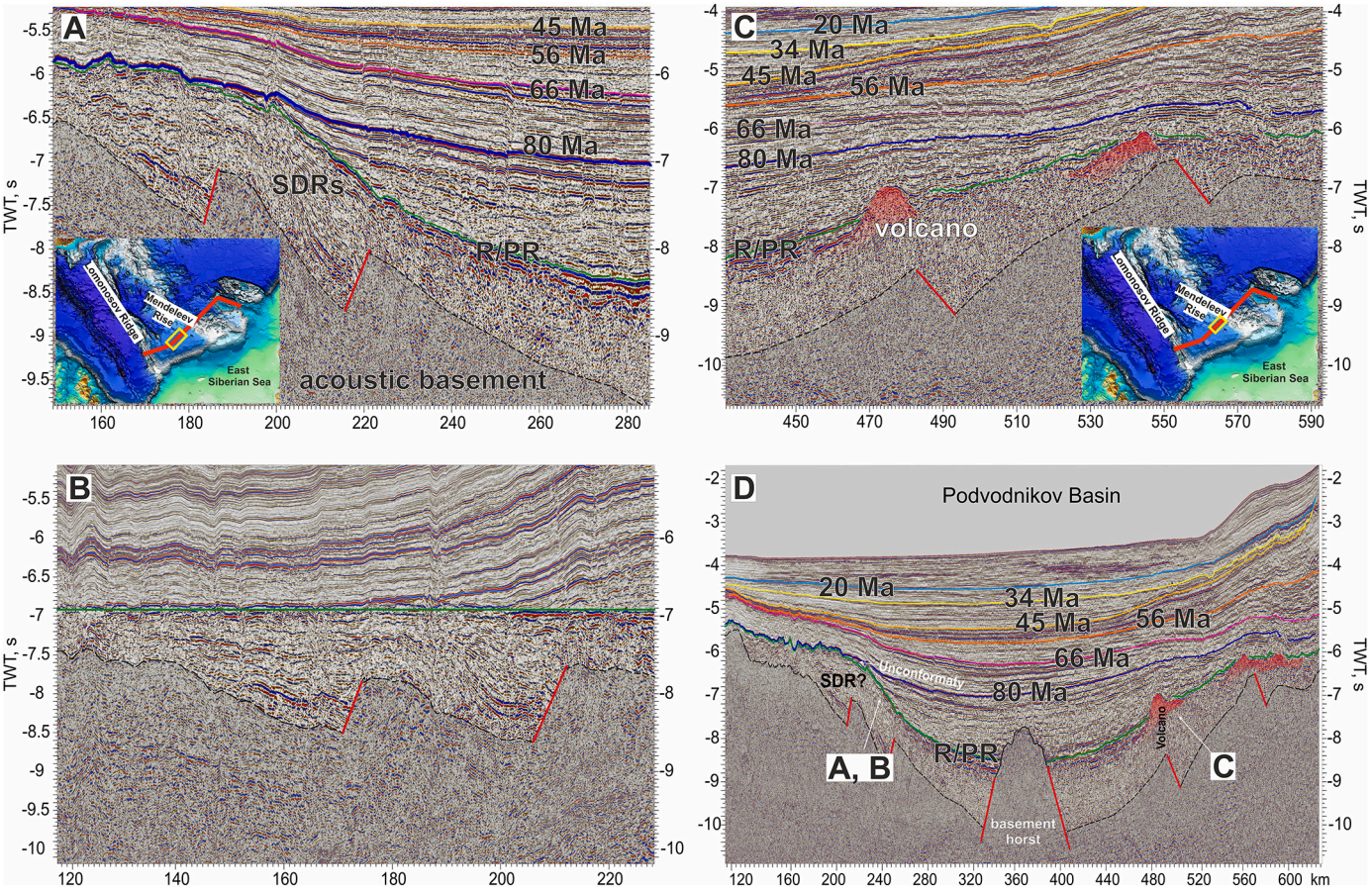

Fig. 36. Fragment of seismic profile shown in Fig. 33. Some details of the Podvidnikov Basin are shown. A. Western slope of the Podvodnikov Basin. SDR-complex can be observed below rift/postrift (R/PR) boundary. B. Profile flattened on the rift/postrift boundary. C. Possible volcanic structures at top of synrift complex in the south-eastern slope of the Podvodnikov Basin (top of volcanoes is outlined by red line). D. Fragment of seismic profile across the Podvodnikov Basin (Fig. 33)

4.11. Cretaceous seismic stratigraphy of the Laptev Sea-East Siberian Sea-North Chukchi Sea system shelf basins and Cretaceous seismic stratigraphy of adjacent deep-water Arctic basins and rises

Rift basins in the eastern part of the Laptev Sea and in the East Siberian Sea and the North Chukchi Basin are characterized by a rift/postrift boundary at ca. 100 Ma (Figs. 6, 17, 18, 20, 21, 22, 23, 24, 26 and 32). Sediment thickness in the North Chukchi Basin is characterized by a TWT up to 9-11 secs (up to 20-22 km). The stratigraphic base of the North Chukchi Basin is relatively flat lying as was observed on a number of seismic profiles (Figs. 10, 11, 12, 13, 14, 23, and 53). We subsequently mapped that seismic horizon from the North Chukchi Basin into the Laptev and East Siberian Seas (Figs. 10, 12, 13, 14, 16, 23, and 53). We conclude that the stratigraphic base of the North Chukchi Basin comprises either a possible rift/postrift boundary or marks the top of SDR units for the Podvodnikov and Toll basins as well as for the Mendeleev Rise. We propose that synrift and pre-rift complexes are strongly stretched and represent the acoustic basement. Two possible explanations for these observations could be: (1) synrift hyperextension of a continental crust with possible exhumation of the lower crust, or (2) synrift exhumation of the mantle. Drachev et al. (2018) suggested the possibility of local mantle exhumation. However, we prefer hyperextension of the continental crust as a causal mechanism. Our interpretation is based on the calculated crustal structure of the North Chukchi Basin as presented by Poselov et al. (2019) and Savin (2020).

The rift/postrift (or top of SDRs complex) boundary is at nearly the same stratigraphic level in the region of the Podvodnikov Basin, Mendeleev Rise, and Toll Basin as we discussed above. There are two important consequences of this observation: (1) the Podvodnikov and Toll basins together with the Mendeleev Rise have a nearly similar timing of development and originated as a single geodynamic system with extension orthogonal to the Mendeleev Rise; (2) the rift/postrift boundary for this system could be 100 Ma or younger; a younger age could be proposed due to the general hypothesis that the end of rifting events in the shelf areas is typically older than the end of rifting in adjacent deep-water basins (the South China Sea is an example; e.g., Yang et al., 2018).

4.12. Climatostratigraphy

Our correlations of seismic lines show that the boundary of ca. 45 Ma separates different seismic facies (Figs 5-16, 54). Above this boundary, weak seismic reflections prevail, while below this boundary high-amplitude reflections dominate (Weigelt et al., 2014; Nikishin et al., 2014). We associate this boundary with a sharp climatic cooling as has been proposed earlier (Backman et al., 2008; Moran et al., 2006).

The Paleocene-Eocene Thermal Maximum (PETM) is well substantiated for the Canadian Archipelago (West et al., 2015), Spitsbergen

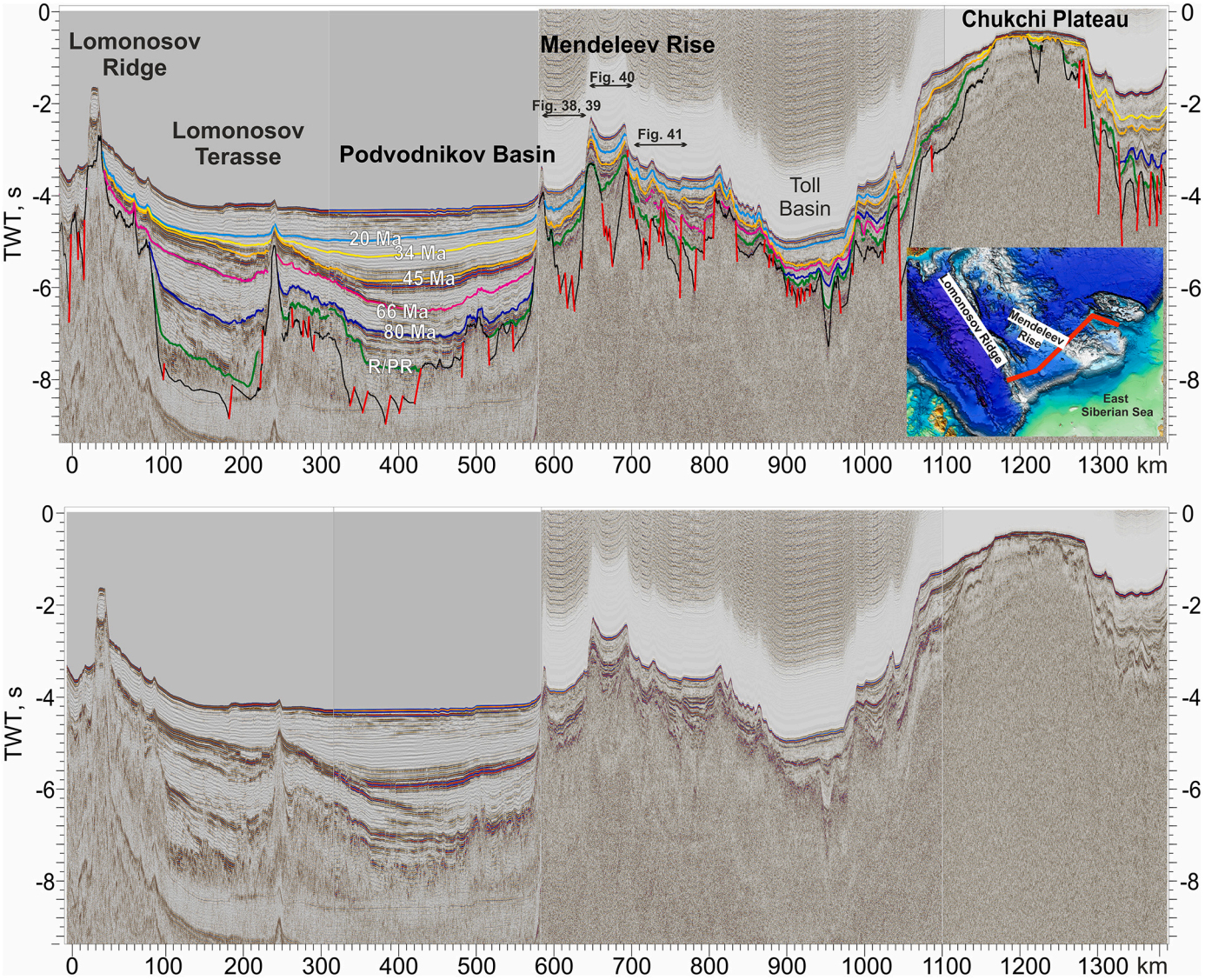

Fig. 37. Interpretation of composite seismic profile (lines ARC 11-53, ARC 12-04, ARC 11-65 and ARC 12-18) for the region from Lomonosov Ridge to Chukchi Plateau. Location of the profile is shown on the map. Different color lines are seismic horizons and corresponding ages (Ma). See also supplementary data, Fig. 37 (seismic profile without interpretation at high resolution).

(Harding et al., 2011), and West Siberia (Akhmet'ev et al., 2010). Our boundary of 56 Ma in the Arctic Ocean probably corresponds to a phase of rapid warming. The Early Eocene is characterized by several phases of rapid warming (Cramer et al., 2009; Gradstein et al., 2012), which are observed for the Lomonosov Ridge as well (Stein et al., 2015). Deposition in the Arctic Ocean in general between 56-45 Ma is possibly associated with these rapid warming phases and expressed on seismic lines by the packages of high-amplitude reflections (Figs. 5-16).

A section characterized by high-amplitude reflections also is observed below our proposed boundary of 80 Ma (Figs. 6, 10, 11, 12, 13, 14, 16, 22, 23, 25, 26, 33, 37, 44, and 53). We refer to this high-amplitude reflector sequence as HARS-2. This sequence has widespread distribution and can be mapped across the Podvodnikov Basin and in the North Chukchi Basin. We interpret the 80 Ma boundary to have specific climatic significance. Recently acquired paleontological and isotopic data show that during late Cretaceous time (close to 80-90 Ma) the Arctic climate was relatively warm with relative cooling close to Campanian time (Herman and Spicer, 1996; Jenkyns et al., 2004; Zakharov et al., 2011; Pugh et al., 2014; Schröder-Adams, 2014; Schröder-Adams et al., 2014; Herman et al., 2016). Other recent data show a relatively cool climate during early Cretaceous time with some short-lasting cooling events (Galloway et al., 2015; Herrle et al., 2015; Rogov et al., 2017). These data correlate with the record of global climatic history (O'Brien et al., 2017) (Fig. 55). We propose that our HARS-2 sequence was formed during the late Cretaceous warm climate epoch. In any case, the climatic history of the Arctic region requires further investigations.

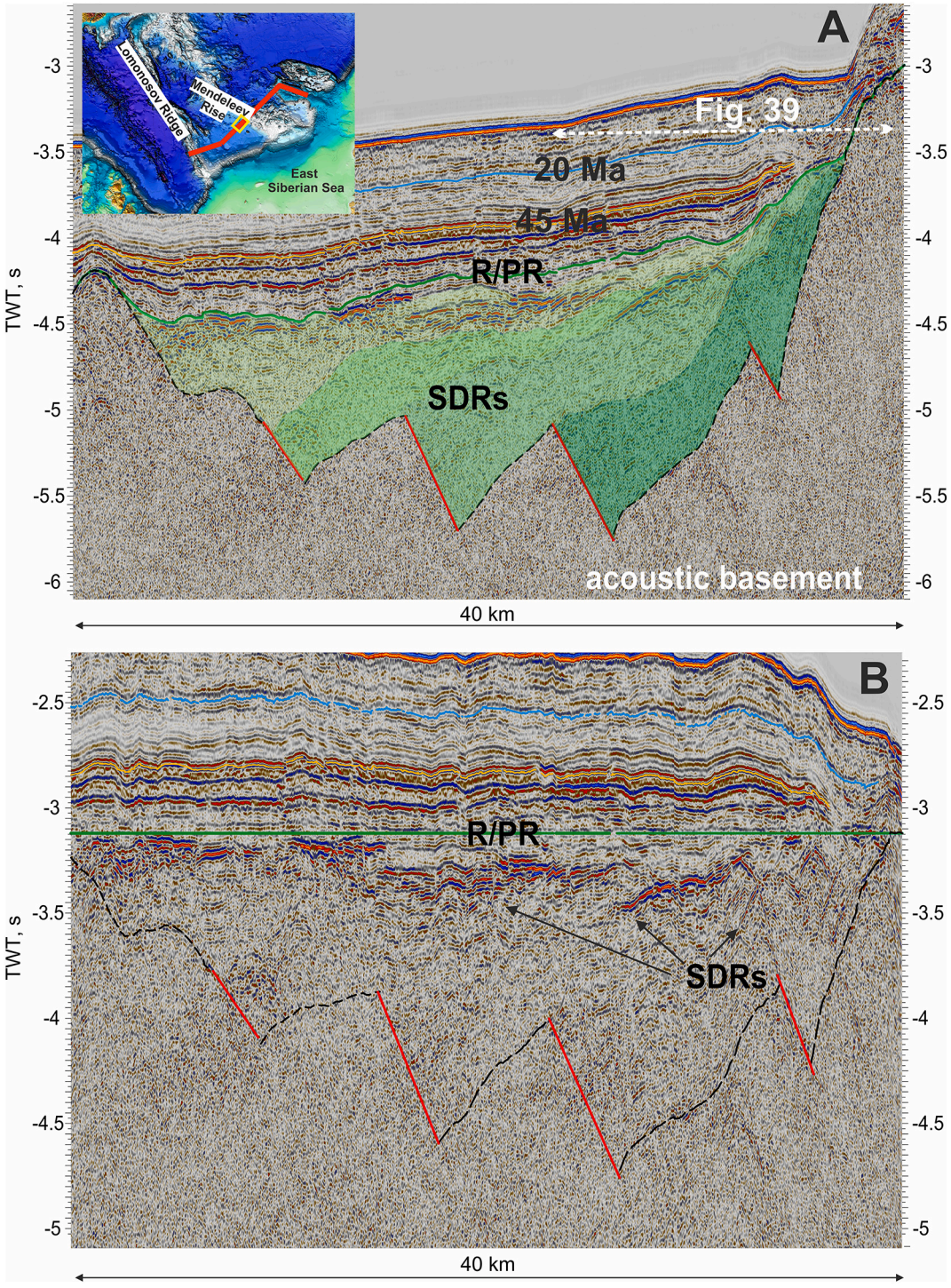

Fig. 38. A. Fragment of seismic profile shown in Fig. 37. Rift/postrift (R/PR) boundary and synrift SDR complex are interpreted. B. Profile flattened on the rift/postrift boundary.

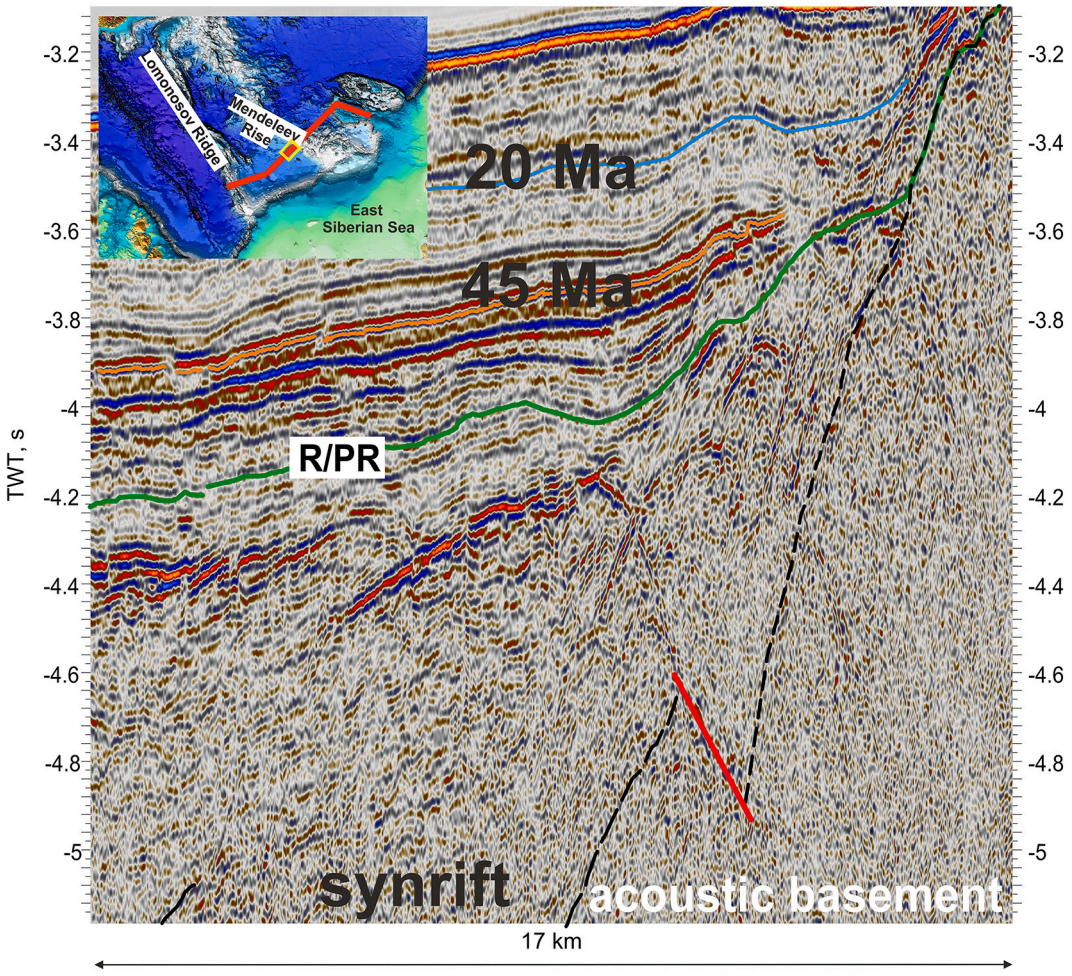

Fig. 39. Fragment of seismic profile shown in Fig. 37 and 38. Rift/postrift (R/PR) boundary and synrift complex are interpreted. A detailed image of possible SDR unit.

4.13. Identification of new igneous provinces on the shelf

We have found evidence for two new magmatic provinces in the region of the Laptev Sea (Figs. 7, 9, 48, 50). The age of the magmatism likely is close to the Paleocene-Eocene boundary. Additional evidence for the existence of volcanism associated with a rifted continental margin of the Eurasia Basin in the Laptev Sea is evidently needed. Our findings based on our newly acquired seismic data seem to contradict conventional assumptions concerning the formation dynamics of the Eurasia Basin (Drachev et al., 2010; Franke, 2013). A possible large magmatic province is identified for the southern part of the North Chukchi Basin with a possible Aptian (or HALIP) age (Figs. 45, 46, 47). Further, our new seismic data demonstrate that the De Long magmatic province has a substantially larger size than proposed before (Figs. 6, 21, 25, and 32).

The occurrence of Cretaceous basalt magmatism is well known for the Barents Sea region. The magmatism has been studied for Franz Josef Land (e.g., Dobretsov et al., 2013) and has been dated to ca. 122-125 Ma (Corfu et al., 2013; Polteau et al., 2016). A key question is the correct age and extent of this magmatic province (e.g., Shipilov, 2016). South and southeast of Franz Josef Land, approximately at the base of the horizontally-layered Aptian sequence, a package with high-amplitude and chaotic reflections is observed (Fig. 56). Its typical thickness is ca. 50-100 msec. In our view, this package of high-amplitude reflections correlates with the basalt strata of Franz Josef Land. Based on borehole data tied to the 2D seismic grid our interpretation of the age of these reflections is close to the Barremian-Aptian boundary. Within the East Barents Megabasin a number of intrusions principally within Triassic shales have been observed (e.g., Dobretsov et al., 2013; Polteau et al., 2016; Shipilov, 2016). The precise age of the intrusions is not known but likely is the same as that of the lavas (Polteau et al., 2016). In association with the intrusions, we observe coeval forced folding (Fig. 56), implying that the intrusions occurred simultaneously with the basaltic volcanism and structuration. Recently acquired regional data demonstrate that magmatism took place nearly simultaneously in the Barents Sea, East Siberian Sea and Chukchi Sea with a possible age close to 125 Ma.

4.14. Identification of regional seismic horizons

Based on the comprehensive data set reviewed here and in Nikishin et al. (2021a), we propose the following tectonostratigraphic model for the Arctic Ocean based on several key seismic horizons (Figs. 57, 58, 59):

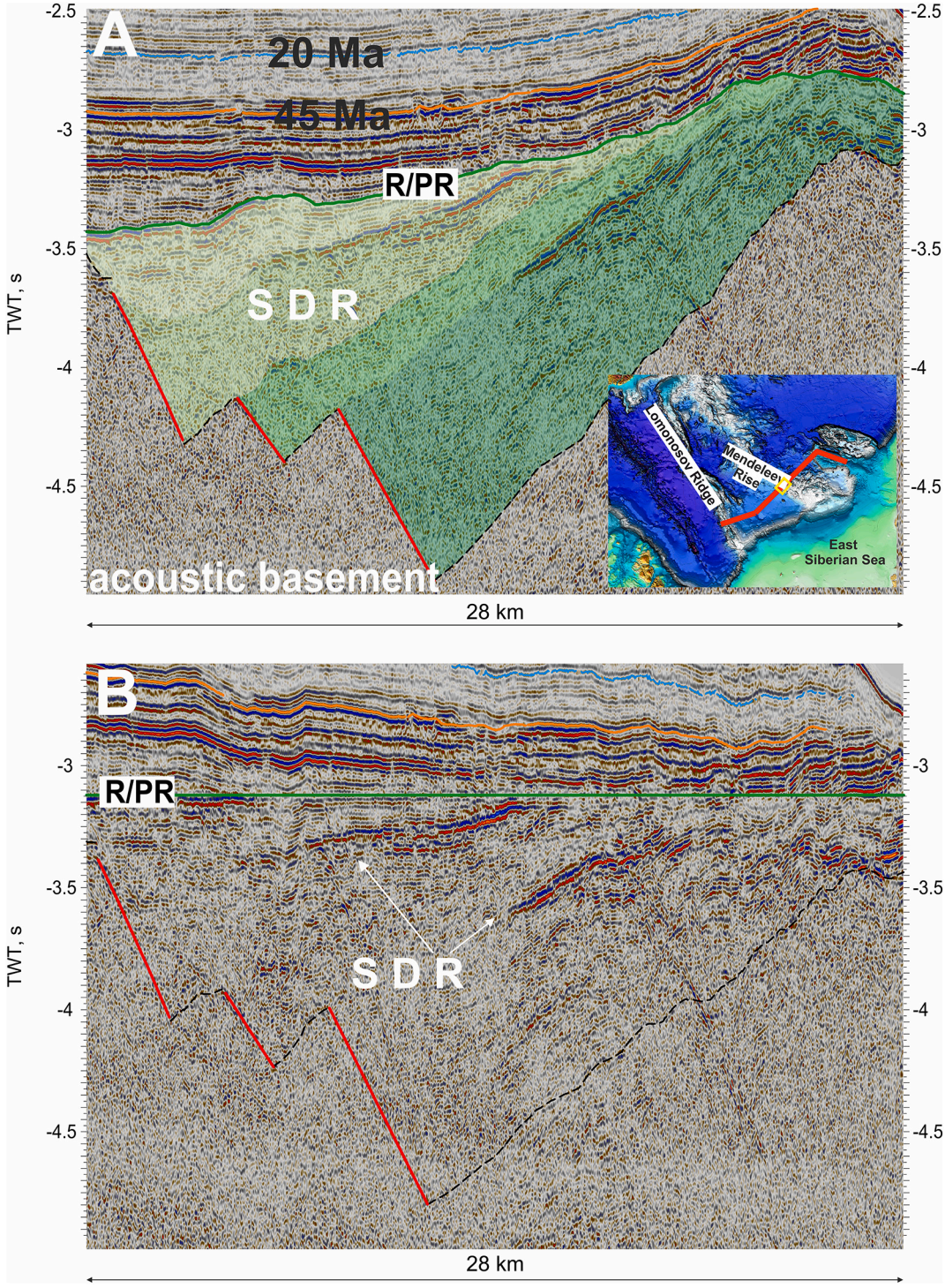

Fig. 40. A. Fragment of seismic profile shown in Fig. 37. Rift/postrift (R/PR) boundary and synfirt SDR complex are supposed. B. Profile flattened on the rift/postrift boundary.

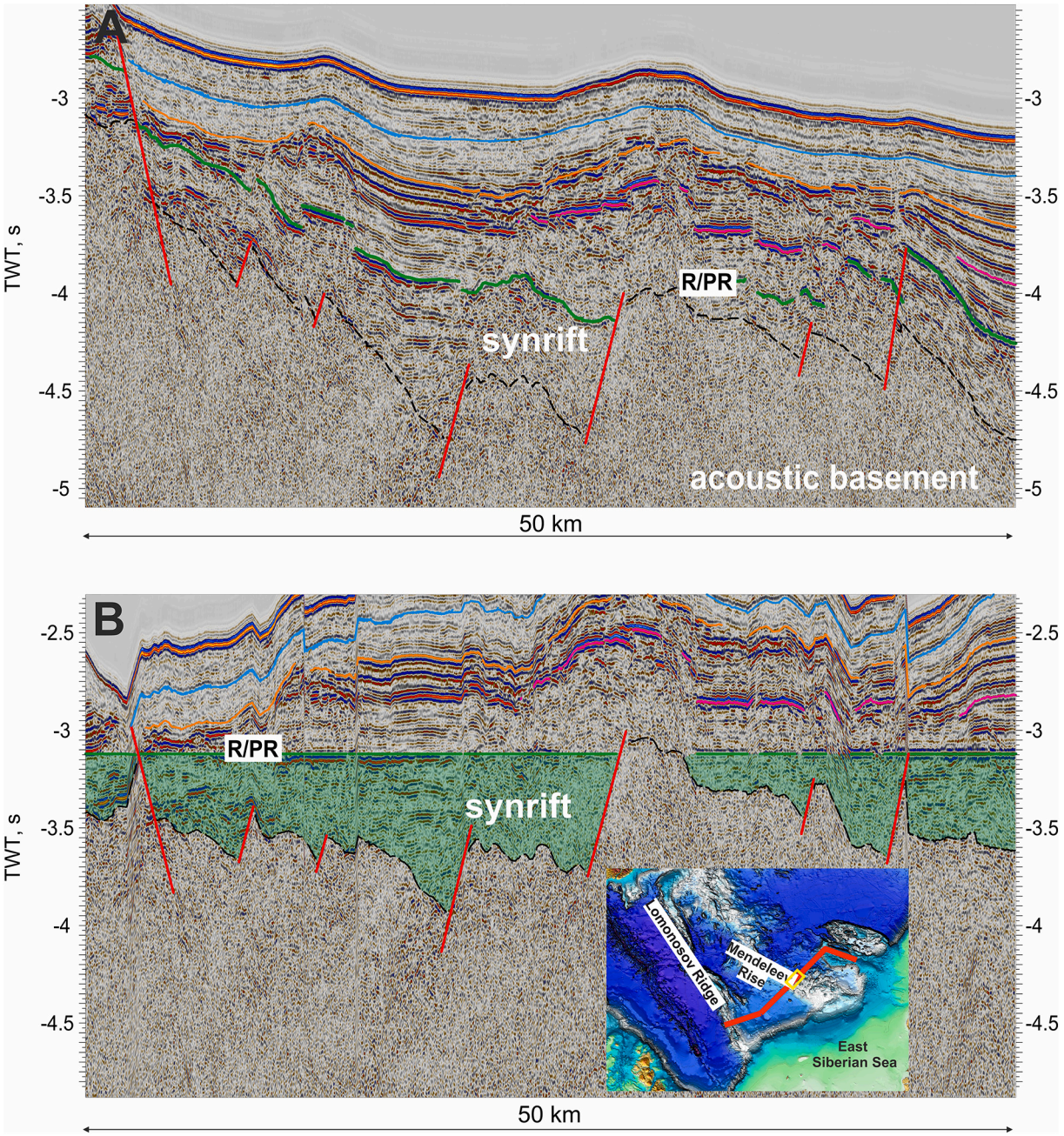

Fig. 41. A. Fragment of seismic profile shown in Fig. 37. Rift/postrift (R/PR) boundary and synrift complex are supposed. B. Profile Flattened on the rift/postrift boundary.

1. The base of the stratigraphic section correlates with the onset of rifting on the shelves of the East Siberian and Chukchi Seas, which occurred during the Aptian-Albian. Consequently, we propose that the Podvodnikov Basin originated at this time (between ca. 100 Ma and 125 Ma). Any older deposits, if present, are included in the acoustic basement.
2. The rift/postrift boundary in the East Siberian Sea is tentatively dated as the boundary between the Upper and Lower Cretaceous (ca. 100 Ma). We can trace the rift/postrift boundary in the Podvodnikov Basin and in the area of the Lomonosov Ridge (Figs. 6, 20, 21, 22 and 26). We cannot date the age of the rift/postrift boundary in the deep-water part of the Arctic Ocean. It could be 100 Ma or younger. The HARS-2 is readily traceable above this boundary (Figs. 6, 10, 11, 12, 13, 14, 16, 22, 23, 25, 26, 33, 37, 44, and 53).
3. Volcanism ended within the Mendeleev Rise approximately 80 Ma ago (Brumley, 2014; Coakley et al., 2016). This boundary approximately corresponds to the upper boundary of the seismic package associated with high-amplitude reflections (HARS-2). This 80 Ma horizon can be readily traced in the Mendeleev Rise and the Arlis Gap Buried High areas (Figs. 23, 26, 28, 29, 30, 33, 35, 37, and 44).

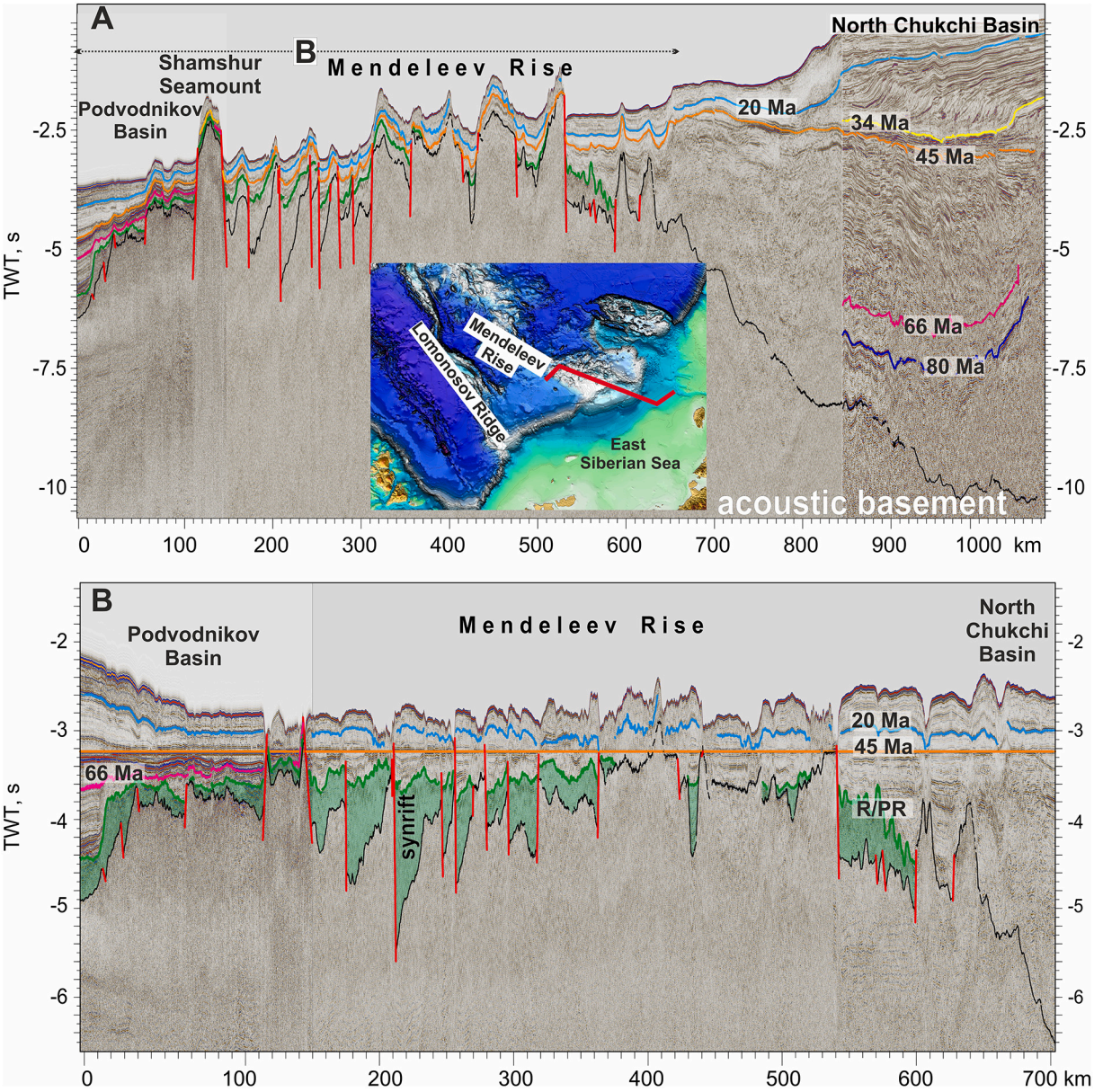

Fig. 42. A. Interpretation of composite seismic profile (lines ARC 12-17, ARC 12-01 and ARS 10F-24) for the region from the North Chukchi Basin and along the Mendeleev Rise.
Location of the profile is shown on the map. Different color lines are seismic horizons and corresponding ages (Ma). B. Profile flattened on the 45 Ma horizon. Horst/graben structure on the Mendeleev Rise acoustic basement can be observed. See also supplementary data, Fig. 42 (seismic profile without interpretation at high resolution).

4. The 66 Ma boundary corresponds to the bottom of the clinoform complex observed in the North Chukchi Basin and to the MBU boundary on the Alaskan Shelf. This boundary was subsequently mapped into the deep-water part of the ocean (Figs. 10, 11, 12, 13, 14, 15, and 16).
5. The 56 Ma boundary corresponds to a breakup unconformity. It has the characteristics of a rift/postrift boundary on seismic sections. This boundary is clearly expressed on the slopes of the Eurasia Basin – in particular, on the Lomonosov Ridge and in the Laptev Sea (Figs. 7, 8, 9, 48, 49, 50, 51) and can be traced in most parts of the Arctic Ocean along the base of the high-amplitude reflection sequence (HARS).
6. The 45 Ma boundary is primarily defined by the age of associated linear magnetic anomalies in the Eurasia Basin. It is also defined on the basis ACEX well borehole data (although different researchers disagree on age dating of the well sections that tie to this seismic horizon). This boundary corresponds to the top of the high-amplitude reflection sequence (HARS). We correlate this horizon with the timing of the onset of cooling and a concomitant sharp change in ocean sedimentation (the transition from more siliceous sediments to clays). The 56 Ma to 45 Ma section contains many high-

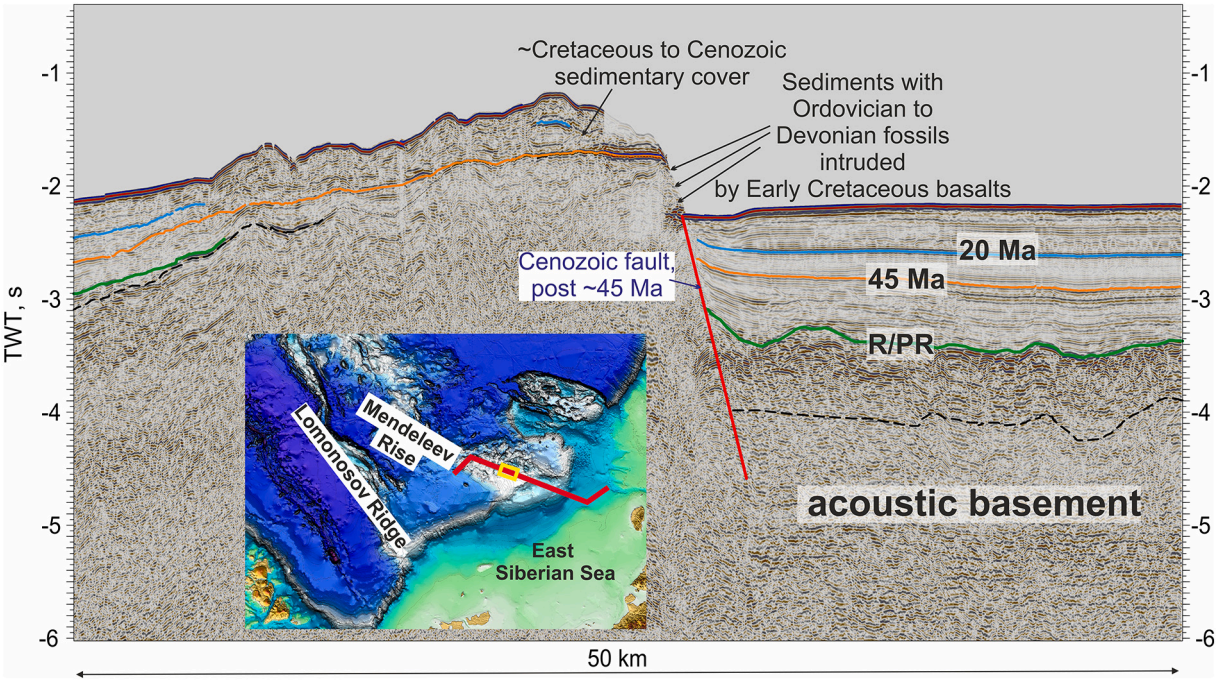

Fig. 43. Interpretation of a fragment of seismic profile (lines ARC 12-01) (Fig. 42) for the Mendeleev Rise region. Location of the profile is shown on the map. Different color lines are seismic horizons and corresponding ages (Ma). The escarpment was formed due to Cenozoic post-45 Ma extension. Samples were collected using special equipment on this scarp. Data from Skolotnev et al. (2019, 2017).

amplitude reflections. We associate this section with a warming epoch in the Eocene and hence – with an epoch of warmer-water sedimentation. The 45 Ma boundary corresponds to the base of the upper clinoform complex of the North Chukchi Basin. The 45 Ma seismic horizon is one of the most continuous reflections in the Arctic Ocean.

7. The 34 Ma boundary also is identified by age of associated linear magnetic anomalies in the Eurasia Basin. Clinoform complexes originating from the side of the Lomonosov Ridge are identified above this boundary in the Amundsen Basin (Fig. 25). On the East Siberian Sea and Chukchi Sea Shelf, activation of some thrust faults are approximately associated with this boundary (Nikishin et al., 2019; Nikishin et al., 2014) (Fig. 60).
8. The 20 Ma boundary is again mainly identified by age of associated magnetic anomalies in the Eurasia Basin. The erosional character, sometimes associated with responses to gravity tectonics (landslides, channels, and slope erosion), are commonly observed with this surface, which suggests that oceanic currents changed sharply in the Arctic Ocean at this time (Figs. 12, 13, 23, 53). Our data support an early Miocene onset of a ventilated circulation regime in the Arctic Ocean that was attributed to the opening of the Fram Strait as proposed by Jakobsson et al. (2007).

4.15. *Vertical intraplate tectonic movements at 45-20 Ma*

Our analysis of a grid of seismic lines shows that either syntectonic depositional wedges (SDW) or syntectonic deposition lenses with ages of 45-20 Ma are present in the Podvodnikov Basin and in the Makarov Basin (Figs. 6, 12, 13, 14, 25, 26, 28, 29, 30, 33, 37, and 61). These deposits progressively pinch out toward the Lomonosov Ridge from the side of the Podvodnikov Basin. This seismic sequence also pinches out toward the Arlis Gap Buried High from the side of the Makarov Basin and is absent in the ACEX wells on the Lomonosov Ridge.

In many instances, onlapping onto the 45 Ma surface is observed. It is likely that differential vertical movements started at 45 Ma. At that time, relative subsidence was initiated in the Podvodnikov and Makarov basins with the onset of relative uplift at the Lomonosov Ridge (this corresponds to the hiatus in the ACEX wells). A phase of relative uplift is also noted for the North Janette Basement High at the border of the North Chukchi and Podvodnikov basins (Figs. 11, 12, 14). On the East Siberian Sea-Chukchi Sea shelves and in the Amundsen Basin, a pronounced phase of low-amplitude normal faulting appears to have occurred around 45 Ma ago (Figs. 14, 15, 23, 24, 62) when activation of normal faulting was established for the area of the Lomonosov Ridge (Figs. 4, 5, 6, 8, 11, 61). As a result of these vertical movements, the Makarov Basin became a separate basin. Phases of relative uplift possibly took place for the Mendeleev Rise as well at this time (Figs. 33, 37). A major normal fault between the Mendeleev Rise and the Podvodnikov Basin probably was activated between 45-20 Ma (Figs. 35, 37, 44). Further, we can unambiguously identify additional substantial vertical movements and phases of normal faulting between 45-20 Ma in this area. The principal driver behind these structural events can be explained by normal oceanic crustal spreading which then passed into ultra-slow spreading at ca. 45 Ma along the Gakkel Ridge (Glebovsky et al., 2006). The transition to ultra-slow spreading and the ultra-slow spreading itself probably occurred synchronously with the onset of super-regional intraplate. The cause of these processes is discussed in detail in Paper 3 (Nikishin et al., 2021b).

4.16. *Comparison of different seismic stratigraphic frameworks*

The seismic stratigraphic scheme for the area of the Podvodnikov Basin presented in Weigelt et al. (2014) is most widely accepted. This scheme is based on data from the ACEX wells as well as on correlation

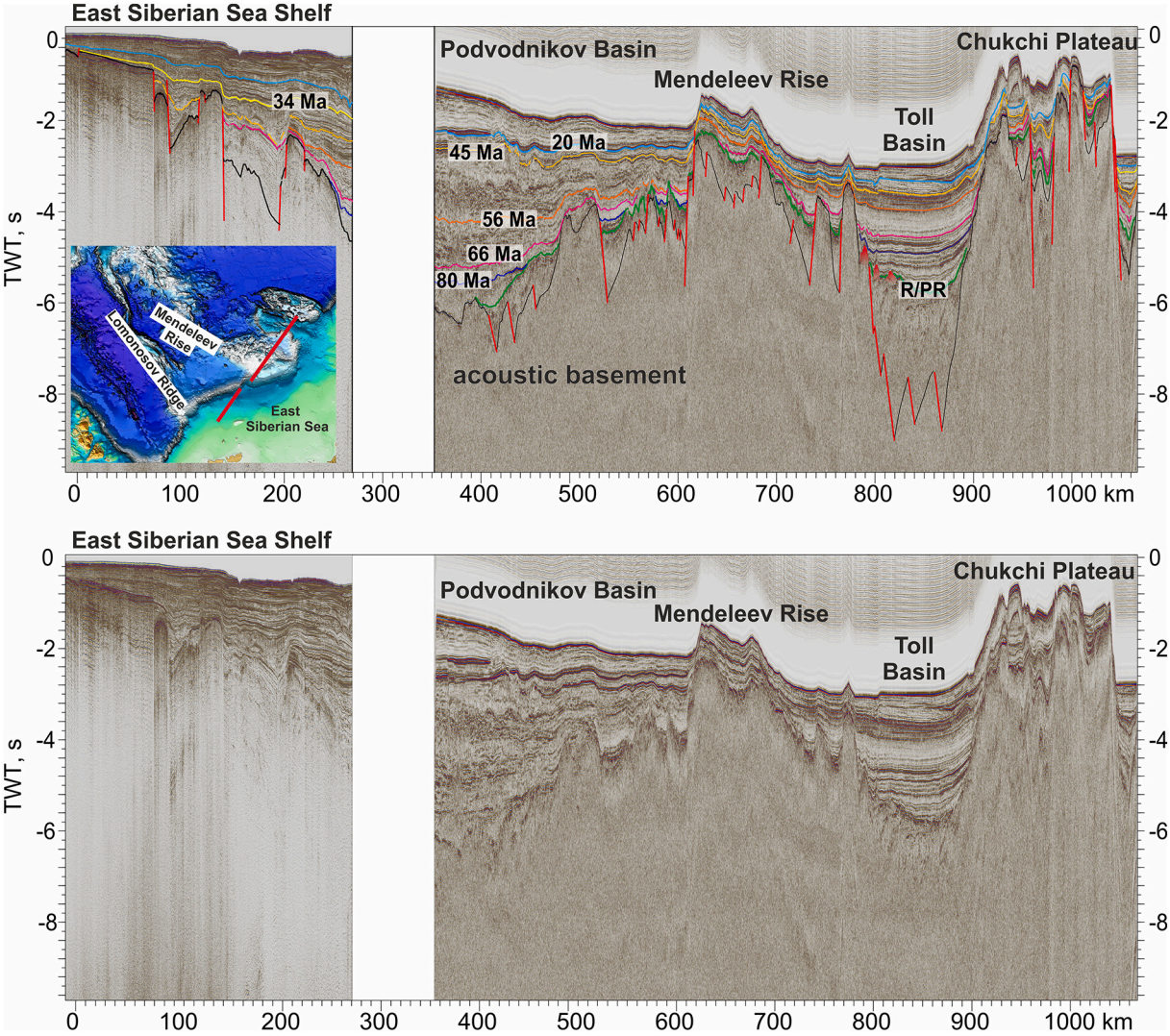

Fig. 44. Interpretation of composite seismic profile from the East Siberian Sea Shelf to the Chukchi Plateau (lines MAGE ESS1620 and ARC 12-03). Location of the profile is shown on the map. Rift systems of East Siberian Sea, Podvodnikov Basin, Mendeleev Rise, Toll Basin, and Chukchi Plateau possibly constitute a single geodynamic system with nearly synchronous history. See also supplementary data, Fig. 44 (seismic profile without interpretation at high resolution).

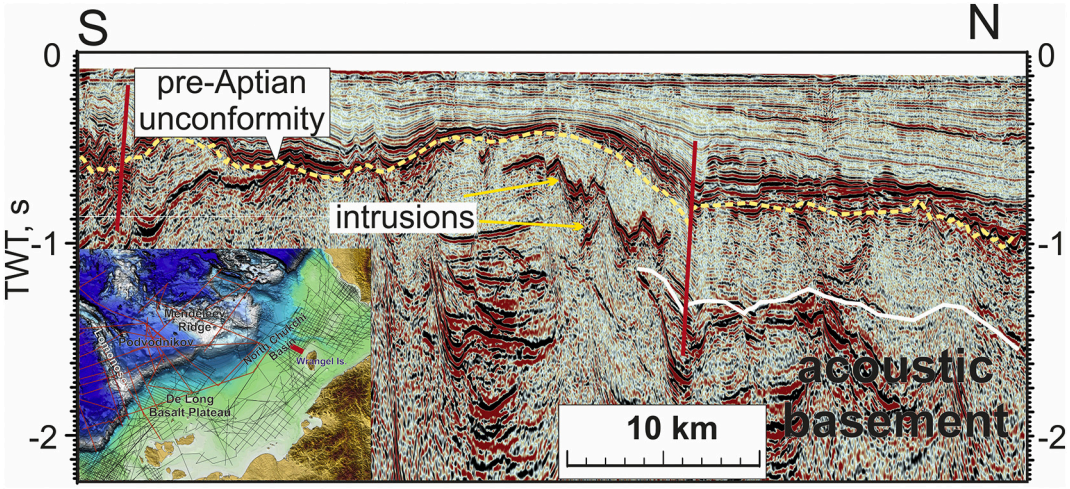

Fig. 45. Interpretation of a fragment of seismic profile. Location of the profile is shown on the map. A number of seismic anomalies can be interpreted as magmatic intrusions. All intrusions are located below horizon 125 Ma. Data courtesy of the Ministry of Natural Resources, Russia.

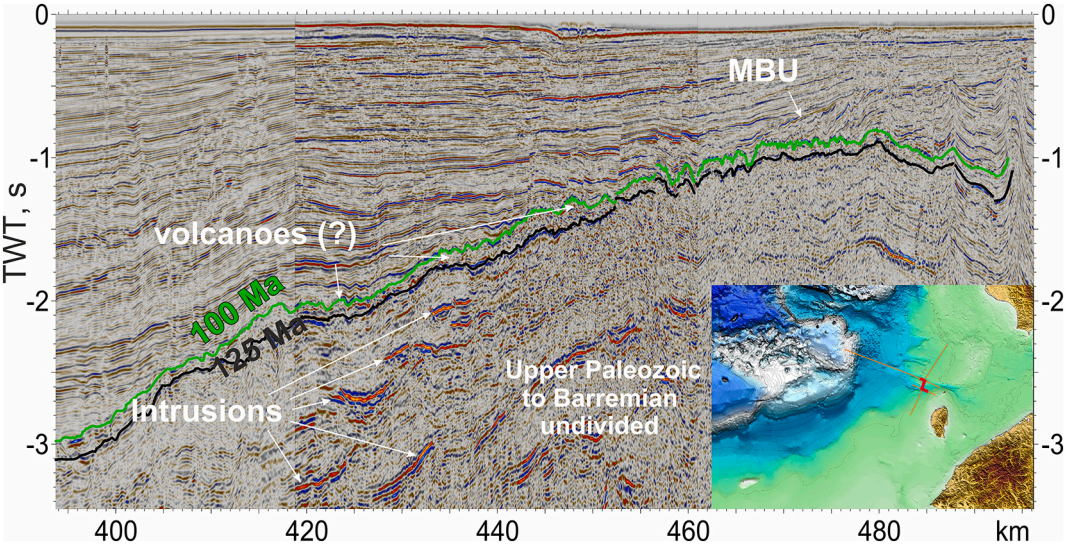

Fig. 46. Interpretation of a composite seismic profile (lines ION11_4200A, ION15_2000, ION15_4225). Location of the profile is shown on the map. A number of high-amplitude reflections below 125 Ma boundary can be identified. These can be magmatic intrusions within Paleozoic to Lower Cretaceous deposits. A chaotic seismic unit above 125 Ma can be a sequence containing volcanoes.

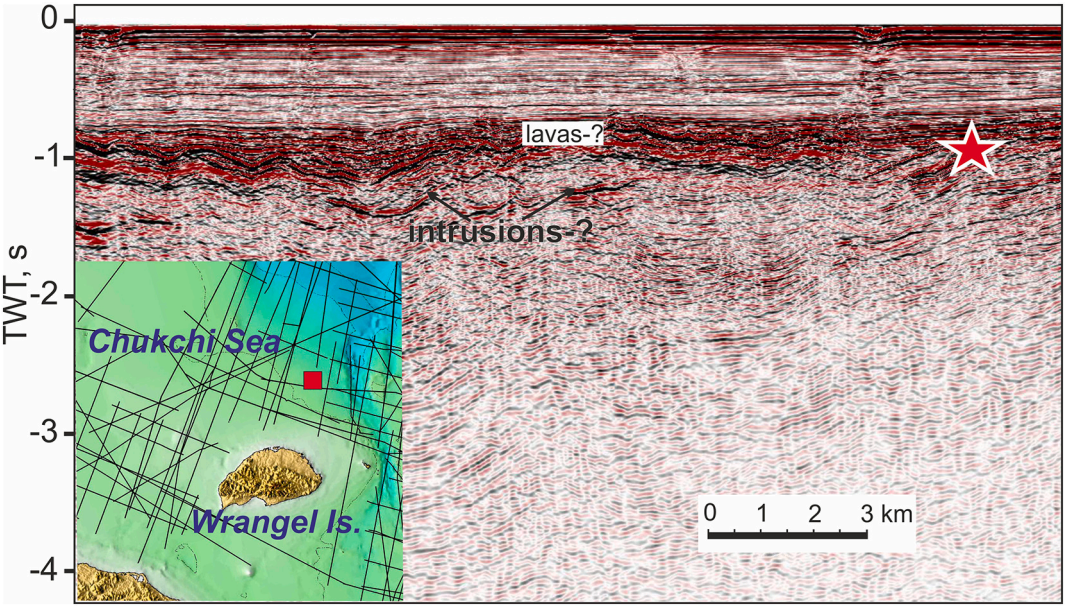

Fig. 47. Fragment of seismic profile for southern slope of the North Chukchi Basin. See map for location. Star shows a top of calculated magnetic bodies at depth close to 700 meters. A volcanic complex and intrusions can be recognized. Data courtesy of the Ministry of Natural Resources, Russia.

with major events in the Arctic. In general, our seismic stratigraphic scheme is similar that presented by Weigelt et al. (2014). However, one fundamental difference is that our 45 Ma boundary corresponds to their 23 Ma horizon. Weigelt et al. (2014) substantiated their age determination by arguing that a major regression took place at the end of Oligocene with which the hiatus in the ACEX wells is associated. In contrast, we argue that the correlation of the 45 Ma boundary with linear magnetic anomalies in the Eurasia Basin and with the clinoform complex in the Chukchi Sea places this boundary at 45 Ma. Another difference is that our boundary of 100 Ma, again based primarily on recognition of linear magnetic anomalies, compared with an age of 66 Ma (Base Tertiary) according to Weigelt et al. (2014) scale. Nonetheless it is noteworthy that irrespective of age differences, we have identified the same main seismic stratigraphic units.

For the Makarov Basin, the seismic stratigraphic framework in Evangelatos and Mosher (2016) in general coincides with our time scale. Nonetheless, differences are likely for interpretation of lower horizons.

A new seismic stratigraphic framework for the North Chukchi Basin

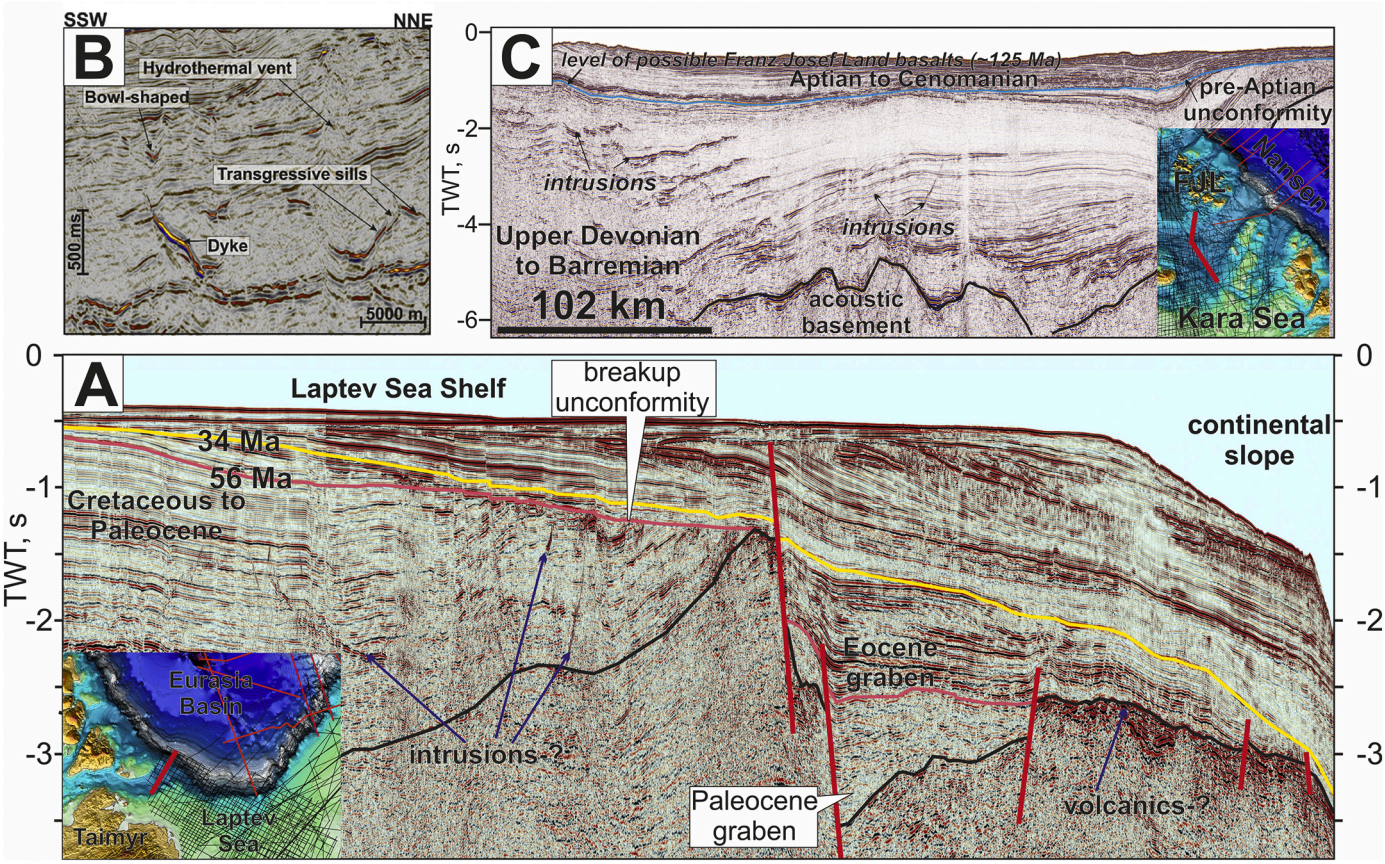

Fig. 48. A. Interpretation of seismic profile MAGE ESS1409. Location of the profile is shown on the map. Breakup unconformity is clearly observed (56 Ma). A number of seismic anomalies can be interpreted as magmatic intrusions. All intrusions are located below horizon 56 Ma. Bright reflection package at the basement could be interpreted as possible volcanics. B. Example of seismic expression of well documented intrusions in Stappen High, SW Barents Sea (Omosanya et al., 2016). Bowl-shaped sills are found above extrusive deposits. Dykes are vertical to sub-vertical positive impedance reflections, which acted as conduits for emplacement of other sills in this area. The extrusive rocks are parallel to sub-parallel to layered positive high amplitude anomalies. C. Fragment of seismic profile for the northern part of the Barents Sea. Intrusions are clearly observed. The profile is located close to Franz Josef Land where Early Cretaceous intrusions and basalt lavas are well documented.

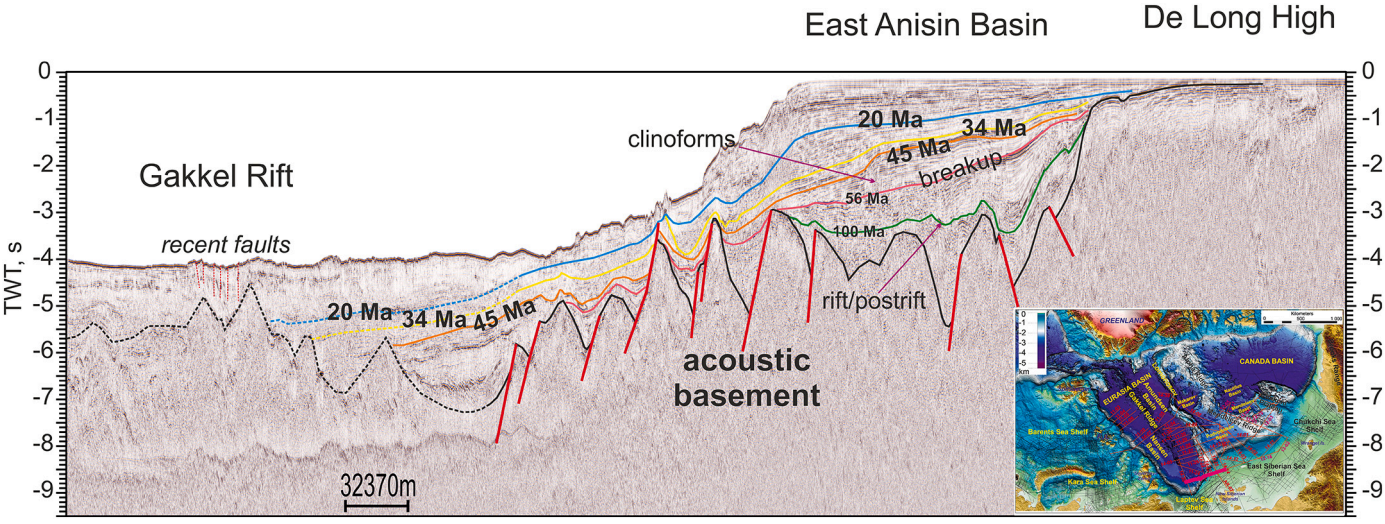

Fig. 49. Interpretation of seismic profile ARC-12-16 (western part) for area from the Laptev Sea Shelf to Eurasia Basin margin and Gakkel Rift (Nikishin et al., 2018, with additional interpretation). See also supplementary data, Fig. 49 (seismic profile without interpretation at high resolution).

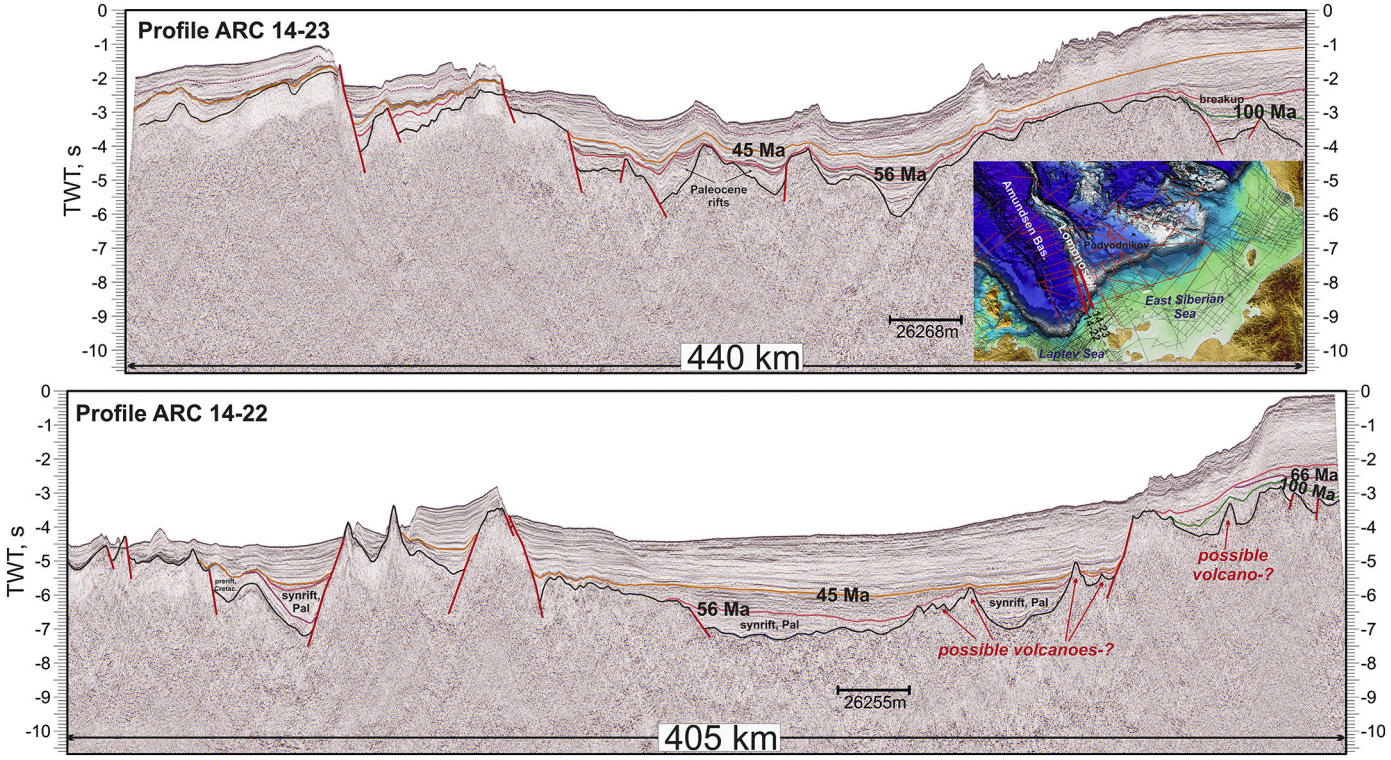

Fig. 50. Interpretation of seismic profiles ARC 14-23 and ARC 14-22 for the southern part of the Lomonosov Ridge and adjacent shelf area. See also supplementary data, Fig. 50 (seismic profile without interpretation at high resolution).

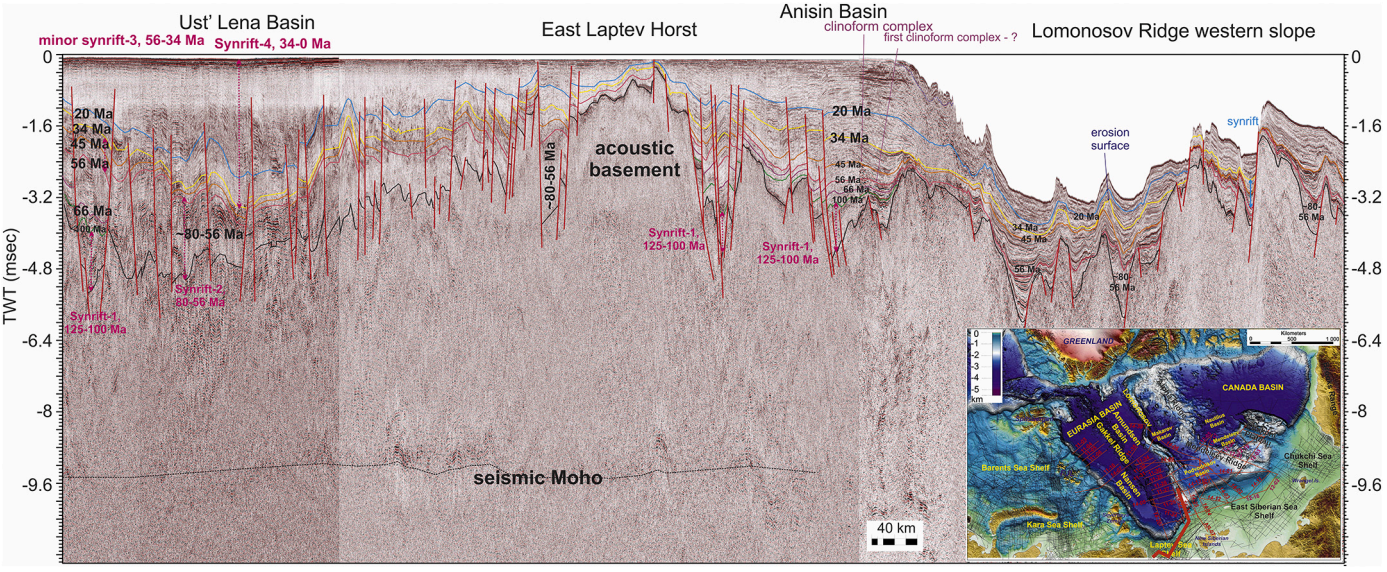

Fig. 51. Interpretation of composite seismic profile (lines ION11-1700, ION11-4600 and ARC 14-23) for the Laptev Sea Shelf and along the Lomonosov Ridge slope. Location of the profile is shown on the map. Different color lines are seismic horizons and corresponding ages (Ma). See also supplementary data, Fig. 51 (seismic profile without interpretation at high resolution).

has been proposed by Ilhan and Coakley (2018). Our stratigraphic schemes are very similar for the Aptian to Cenozoic deposits and we reach similar conclusions (Nikishin et al., 2017; Nikishin et al., 2014). There is, however, one important difference is in the age of the lower synrift unit. Ilhan and Coakley (2018) recognized a synrift complex in the Toll Basin characterized by SDRs. They interpreted the rift/postrift boundary as a condensed section with an age approximately between Middle Jurassic and Neocomian (up to Barremian) with rifting having taken place during Jurassic time. We observe a similar situation in the Toll Basin with SDRs infilling a half graben (Nikishin et al., 2019, Nikishin et al., 2014) (Figs. 33, 34). We observe a number of SDR-like units in the Mendeleev Rise region as well, but according to our interpretation Aptian or Aptian-Albian rifting was followed by late Cretaceous postrift subsidence with the rift/postrift boundary close to 100

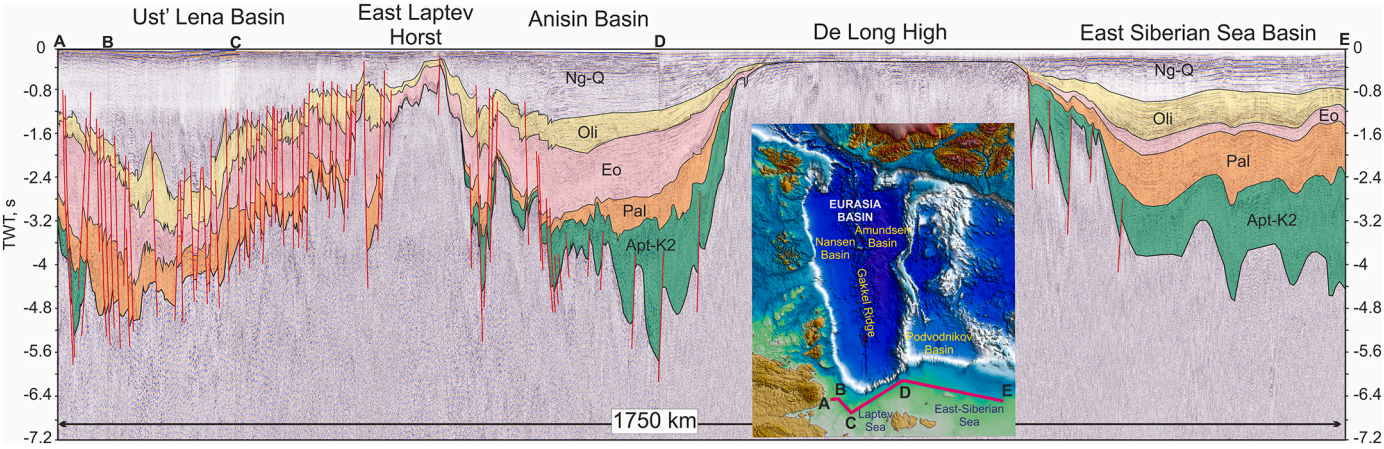

Fig. 52. Interpretation of composite seismic profile from the Laptev Sea Shelf to the East Siberian Sea Shelf (lines ION 11-1700, ION 11-4600 and ARC 12-16). Location of the profile is shown on the map. See also supplementary data, Fig. 52 (seismic profile without interpretation at high resolution).

Ma. We have no evidence for the presence of condensed sections between synrift and postrift complexes in the Podvodnikov-Mendeleev-Toll area (Figs. 33, 34, 35, 36, 37, 38, 39, 40 and 41). This rift/postrift boundary is very similar to well-known examples in other passive continental margins.

Hegewald and Jokat (2013) have prepared a seismic stratigraphy for the Chukchi Abyssal Plain (Toll Basin). In total, six horizons with ages between Barremian/Hauterivian and Top Miocene were identified. The age control on seismic data was based on five exploration wells located on the northwest coast of Alaska coupled with additional seismic reflection lines from the Chukchi Shelf. Their oldest horizon is the Lower Cretaceous unconformity (Barremian-Hauterivian). In any case, they concluded that it was not possible to map each horizon through the entire new multi-channel seismic grid because of the presence of basement highs, faults, unconformities, and variations in sediment thickness. They interpret the Chukchi Abyssal Plain (Toll Basin) to have evolved in Jurassic to Early Cretaceous time during the opening of the Canada Basin. We have performed a similar study, correlating seismic horizons with exploration wells located on the northwest coast of Alaska. On the whole, correlations of our seismic lines with the wells on the Alaskan Shelf were ambiguous and as a result, unreliable. Five different teams from Moscow State University, Geological Survey of Russia, and Rosneft Oil Company suggested different correlations with different ages. Hegewald and Jokat (2013) and Ilhan and Coakley (2018) reported the same problem. The key driver in this conundrum lies in the selection of a regional geodynamic model. Hegewald and Jokat (2013) and Ilhan and Coakley (2018) proposed that the Chukchi Abyssal Plain evolved during the opening of the Canada Basin. They used the well-known rotation model of the Amerasia Basin opening with simultaneous opening of the entire basin (e.g. Embry, 1990; Grantz et al., 2011; Grantz and Hart, 2012). According to our geodynamic model, however, the Toll Basin is not older than the rift system in the East Siberian and Chukchi Seas shelf. Hence, these rift systems are not older than Aptian. Nikishin et al. (2014) and Ilhan and Coakley (2018) recognized a synrift complex in the Toll Basin presented by SDRs. New data show that SDR-like units are common for the Mendeleev Rise and Podvodnikov Basin. According to our model, these SDRs have a HALIP age (not older than ±130 Ma).

A number of geologists use the Arctic Alaska Basin stratigraphy for

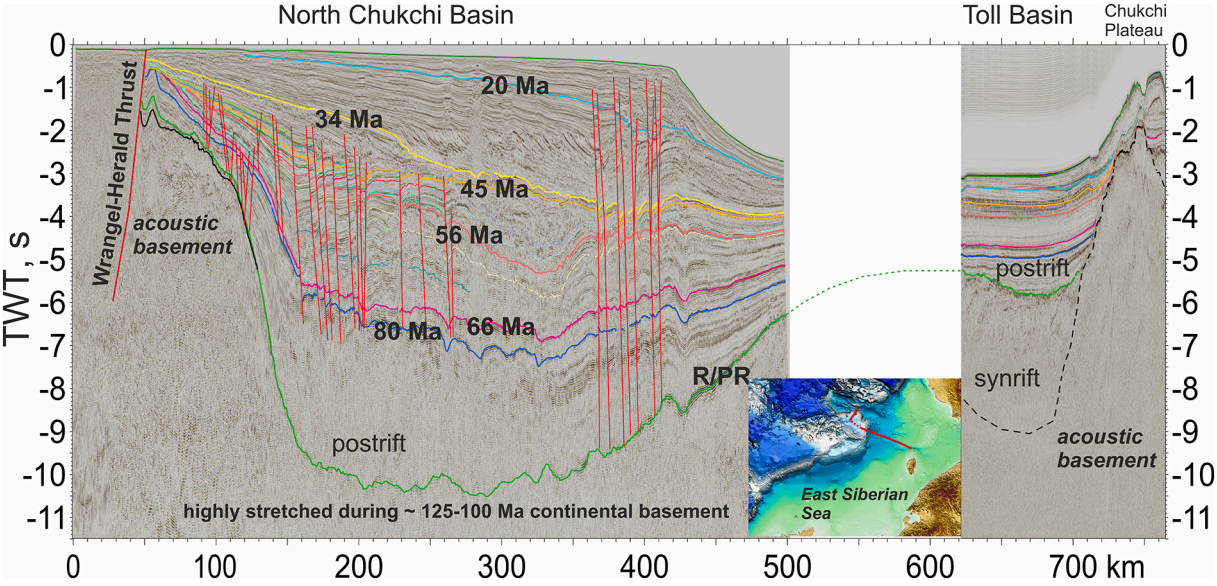

Fig. 53. Interpretation of composite seismic profile from the Chukchi Sea Shelf to the Toll Basin (lines ARC12_03, ION11_4200A). Location of the profile is shown on the map. Rift/postrift boundary in the Toll Basin possibly coincides with the base of sedimentary cover of the North Chukchi Basin, implying that the flattened bottom of the North Chukchi Basin is a rift/postrift boundary (green line). See also supplementary data, Fig. 53 (seismic profile without interpretation at high resolution).

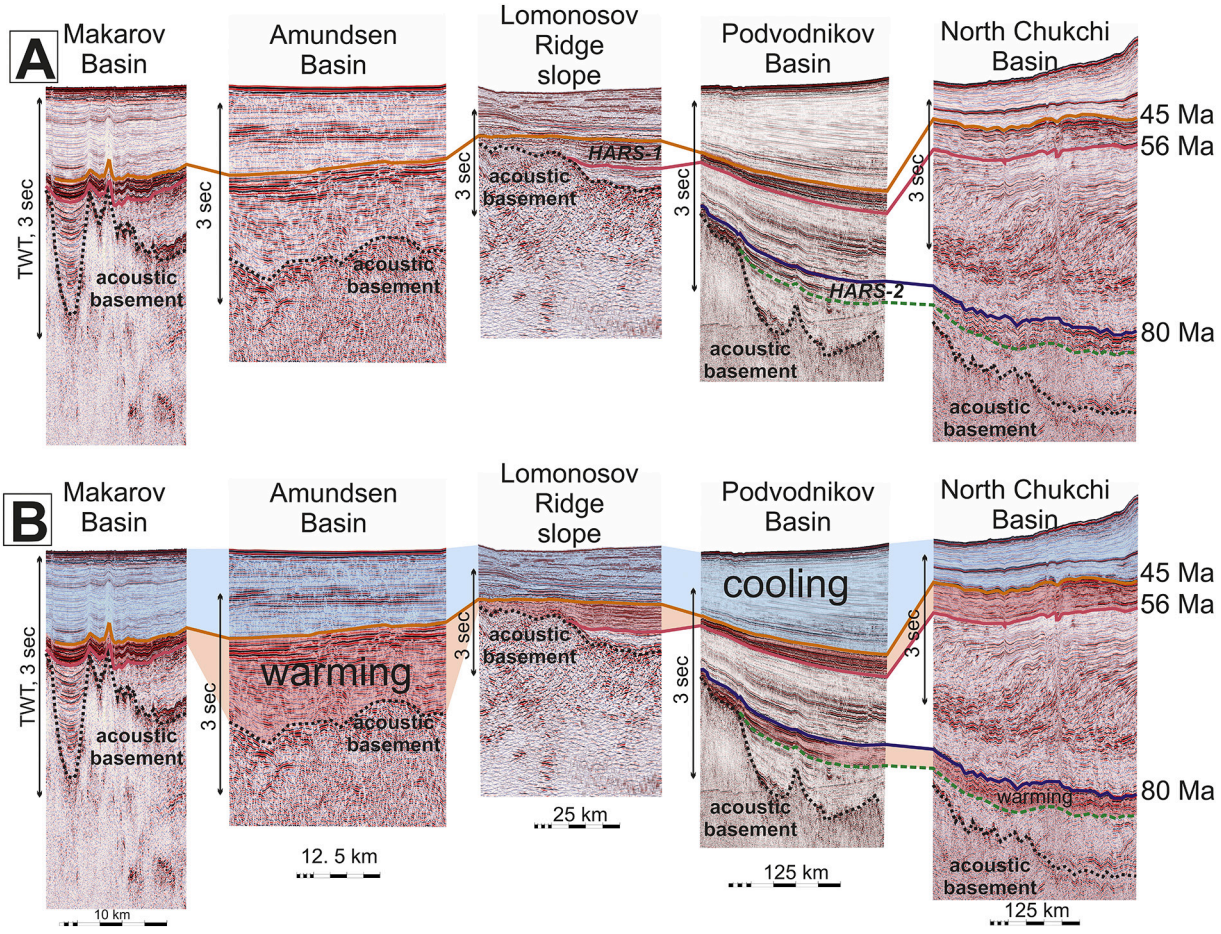

Fig. 54. Possible climatic seismic boundaries in different basins of the Arctic Ocean. A. Fragments of seismic profiles. B. Possible seismic units with anomalous climatic warming or cooling significance.

the North Chukchi Basin (e.g., Hegewald and Jokat, 2013; Ilhan and Coakley, 2018). They propose that the North Chukchi Basin has a Jurassic section and originated during Jurassic rifting. We constructed a geological section for the Arctic Alaska Basin and the North Chukchi Basin (Fig. 63). Clearly, the basins are not characterized by a similar stratigraphy. The Arctic Alaska Basin has a Beaufortian unit (Jurassic-Valanginian-?) with transport of clastic material from the North (Houseknecht, 2019a, 2019b). The North Chukchi Basin has no such unit at the base. The Arctic Alaska Basin has a condensed section between the Lower Cretaceous Unconformity (~intra-Valanginian) and GRZ (gamma-ray zone) (Aptian to Albian). The thickness of this unit is minimal (Fig. 63) (Houseknecht, 2019a, 2019b) and the time of deposition is close to 10-20 million years. This unit is absent in the North Chukchi Basin. Consequently, our conclusion is that it is not reasonable to apply the timing of events in Arctic Alaska to those of the North Chukchi Basin.

Within our collective of co-authors, as is to be expected, different teams have used somewhat different stratigraphic boundaries for the shelf basins. These differences are not significant and discussions remain ongoing about precise ages of horizons within the Cretaceous and Cenozoic. Some variants of the stratigraphy were published by Popova et al. (2018) and Skaryatin et al. (2020). Evidently in the absence of wells, we have not yet seen the establishment of an unequivocal stratigraphic scheme for the Arctic Ocean at large.

5. Discussion

5.1. Correlation of major tectonic events in the geological history of the Arctic Ocean

Our new data allow for the refinement of existing hypotheses regarding the chronology of events in the history of the Arctic Ocean. Below we focus on the formation history of the major basins and uplifts.

The new data confirm many previously held assumptions concerning the history of the Eurasia Basin. Opening of the basin started at ca. 56 Ma (Glebovsky et al., 2006; Gaina et al., 2011; Pease et al., 2014; Coakley et al., 2016; Nikishin et al., 2017, 2018; Weigelt et al., 2020). Our data show that the opening of the Eurasia Basin was preceded by continental rifting in the western part of the Laptev Sea Basin (Figs. 48, 49) and on the western slopes of the Lomonosov Ridge (Figs. 7, 8, 9, 50, and 51). In the area of the Laptev Sea, basaltic magmatism probably preceded the opening of the Eurasia Basin (Fig. 48). If this is the case, the dynamics of Eurasia Basin opening is similar to the dynamics of the opening of the North Atlantic as proposed, for example, by Gaina et al. (2017), Wilkinson et al. (2017), and Foulger et al. (2020).

A remaining question concerns the model for the geological structure and history of the Amerasia Basin. Data presented in this paper demonstrate that the North Amerasia Domain (the Mendeleev Rise together with adjacent deep-water basins) together with the Mesozoic rift system in the Laptev-East Siberian-Chukchi seas comprise a single geodynamic system and originated during the Aptian-Albian. The North Amerasia Domain is separated from the South Amerasia Domain (or

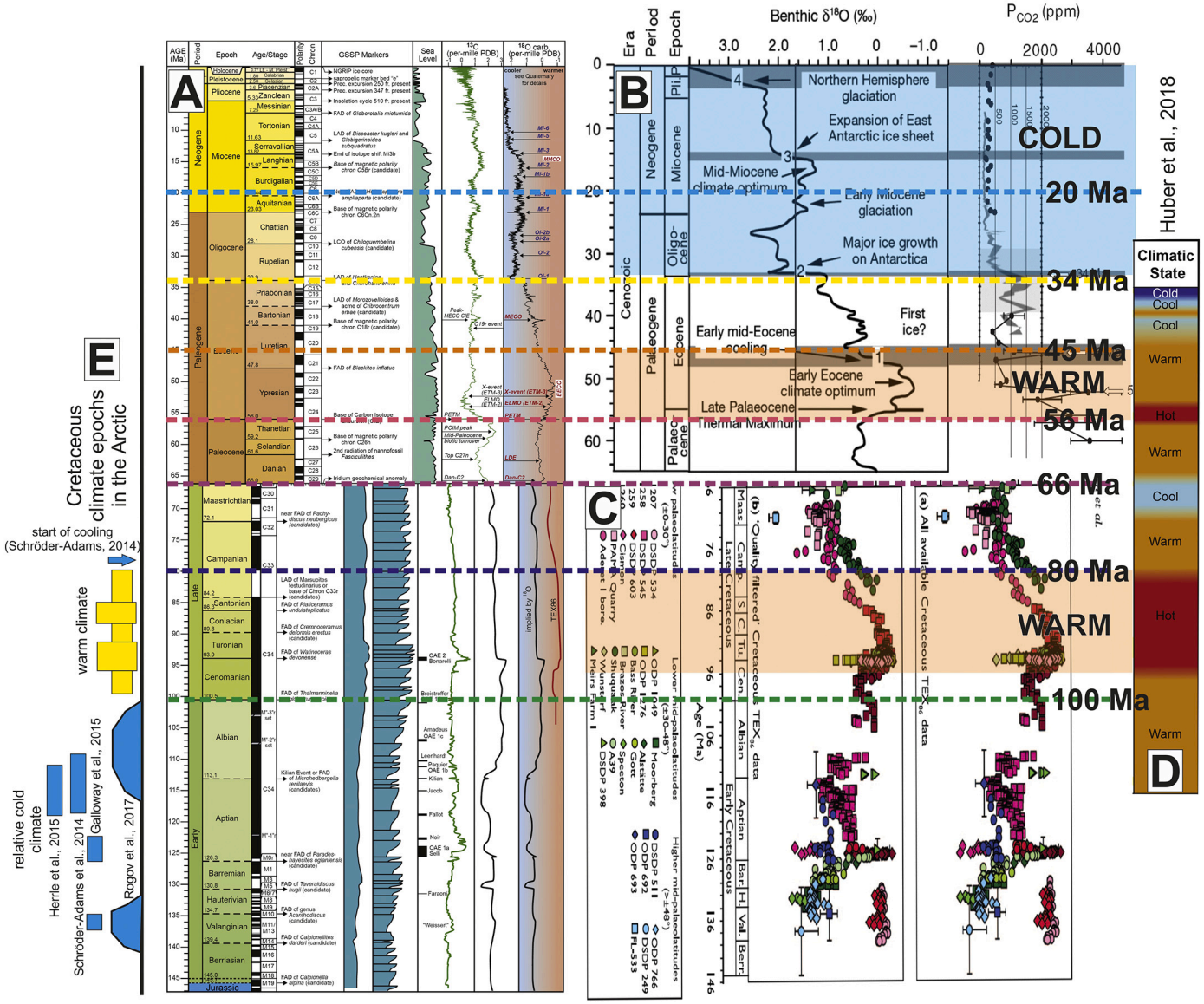

Fig. 55. Cretaceous to Cenozoic global climatic events and climatic stratigraphy of the Arctic Ocean. A. Global time scale (Ogg et al., 2016). B. Main climatic events in the Arctic Ocean in the Cenozoic (Stein, 2008). C. Main global Cretaceous climatic events (O'Brien et al., 2017). D. Global climatic stages (Huber et al., 2018). E. Cretaceous climatic epochs in the Arctic region (Schröder-Adams, 2014; Galloway et al., 2015; Herrle et al., 2015; Rogov et al., 2017). Horizontal colored dashed lines with ages represent seismic horizons.

Canada Basin Domain) by a proposed Amerasia transform fault (Fig. 2) (Nikishin et al., 2014). We include the Arctic Alaska Basin within the South Amerasia Domain comprising the margin of the Canada Basin. We propose here that the South Amerasia Domain had a different geodynamic history and timing of evolution than the North Amerasia Domain.

Regional seismic data without borehole control can lead to different interpretations with different models of proposed ages for different seismic horizons and units. Nonetheless, the seismic 2D grid demonstrates definitively a sequence if not the precise timing of geological events. We can recognize sequences of seismic complexes that originated within the context of uniform tectonic environments and can therefore be described as tectonostratigraphic units. Tectonostratigraphic units and their associated sequences form the basis of our tectonic restorations.

The first mega-tectonostratigraphic or seismic megasequence is the Paleozoic to Jurassic unit. It is located to the north of the Zhokhov-Wrangel-Herald-Brooks thrust belt. We do not further discuss this megasequence in detail here. This unit is documented in the Arctic Alaska Basin as Ellesmerian and Beaufortian (e.g., Homza and Bergman, 2019; Houseknecht, 2019a, 2019b). Our work suggests it as possible Ellesmerian and Beaufortian to the north of Wrangel Island (Figs. 10, 19).

The second proposed seismic megasequence is Late Jurassic to Neocomian in the North Amerasia Domain and Beaufortian in the South Amerasia Domain. We have mapped the distribution and characteristics of these seismic megasequences (Fig. 64), which are expressed as foredeep seismic megasequence in the Russian shelf. We can recognize a belt of foredeep basins north of the Zhokhov-Wrangel-Herald thrust belt (Figs. 2, 31). The Verkhoyansk-Chukotka Late Jurassic to Barremian collisional orogen was formed south of this thrust belt. These foredeep basins could be similar to the Verkhoyansk Foredeep Basin observed in Siberia. The age of the foredeep seismic megasequence likely is similar to the age of orogeny and close to Late Jurassic to Barremian.

The Arctic Alaska Basin is characterized by another type of seismic

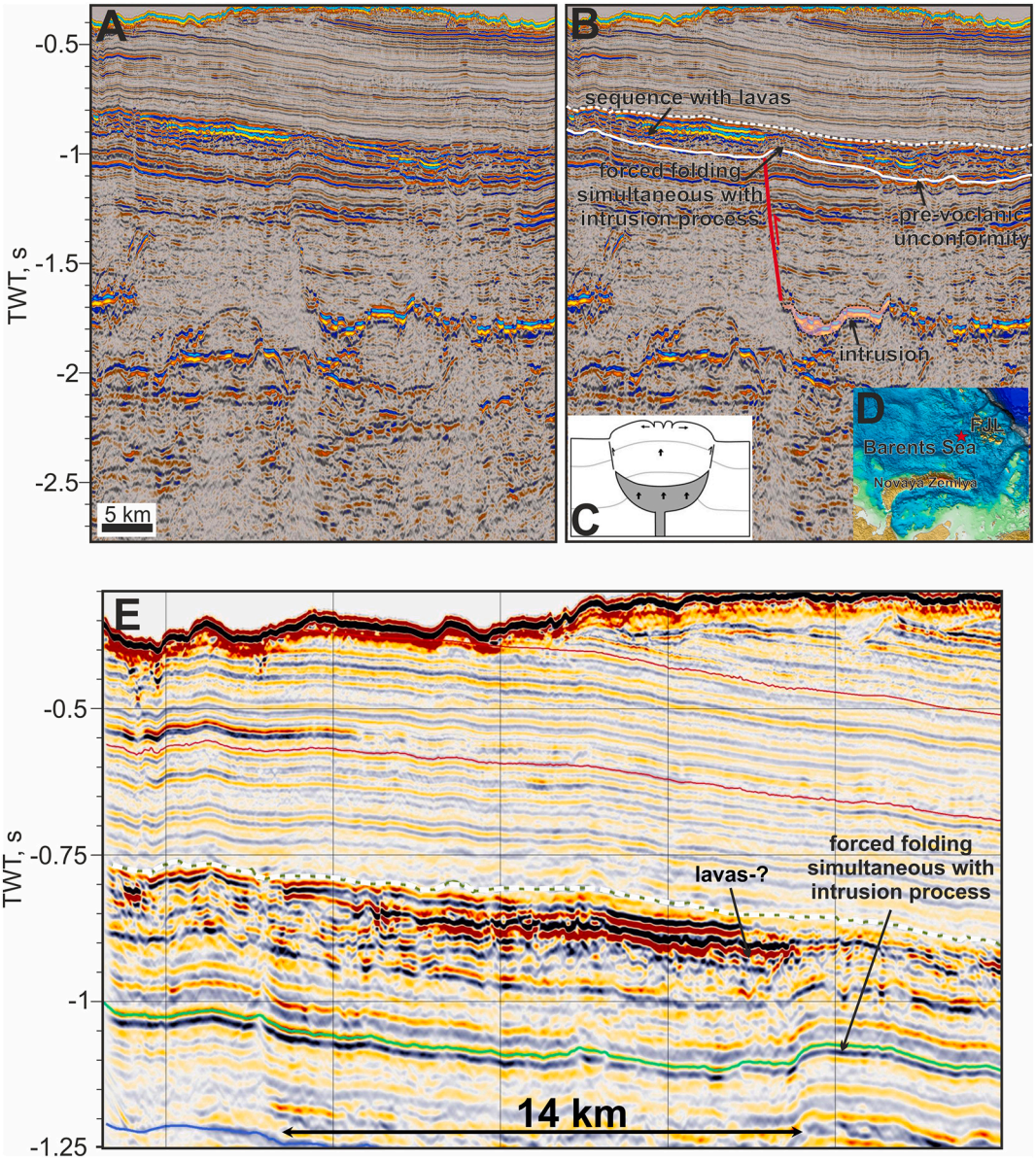

Fig. 56. A. Fragment of seismic profile for the Barents Sea. B. Interpretation of this seismic profile with possible lavas and intrusions. Correlations of seismic data with boreholes show that the age of lavas is close to the Barremian-Aptian boundary. C. Model of intrusion propagation and forced folding above the intrusion (Mathieu et al., 2008). D. Location of seismic profile (star). E. Fragment of the same profile with details. Data courtesy of the Ministry of Natural Resources, Russia.

megasequence for this time interval (Fig. 64). A shelf basin existed in this region during the time from Jurassic to Hauterivian with transport of clastic material from the north (possible Beaufort rift shoulder) (Houseknecht, 2019a, 2019b). Pre-Hauterivian (LCU) erosion took place in northern and western parts of the basin (Houseknecht, 2019a, 2019b). The uplift of the Beaufort High could be connected with rift shoulder uplift or a forebulge rise. The Colville Basin subsidence could be influenced by tectonic loading due to the start of Brookian orogenesis (e.g., Homza and Bergman, 2019; Houseknecht, 2019a, 2019b). The Lower Cretaceous Unconformity (LCU) was interpreted as being associated with continental break-up (Helwig et al., 2011) or as a result of flexural uplift related to Brookian orogenesis (Homza and Bergman, 2019).

We can observe a pronounced difference between the Russian and Alaskan parts of the basins for Late Jurassic to Neocomian time. We do not have any evidence for the existence of the North Chukchi Basin during this time and have proposed a strike-slip Neocomian fault between the South Amerasia and North Amerasia domains (Fig. 64) (Nikishin et al., 2014).

The third significant seismic megasequence is the package of proposed Aptian to Albian units. We have mapped the distribution and characteristics of these seismic megasequences (Fig. 65). Continental synrift and postrift seismic sequences, which spread from the Laptev Sea to the Chukchi Sea, are typical of the Russian shelf (Figs. 6, 10, 11, 20, 21, 22, 23, 24, 25, 26, 32, 44, and 52). The associated rift basins contain continental basalts. The De Long basalts have an isotopic age of ca. 105-130 Ma as we discussed above. We propose that the North Wrangel and Anisin basalts have a possible similar HALIP age. There are three key arguments for an Aptian-Albian age of continental rifting: (1) some rifts are located above the Neocomian collision orogen and could be interpreted as collapse structures; (2) seismic data demonstrate that synrift complexes overlap foredeep seismic megasequences with possible Late Jurassic to Barremian age (Fig. 31); (3) HALIP basalts lie at or near the base of a number of rifts (Figs. 21, 32). We can trace a rift/postrift

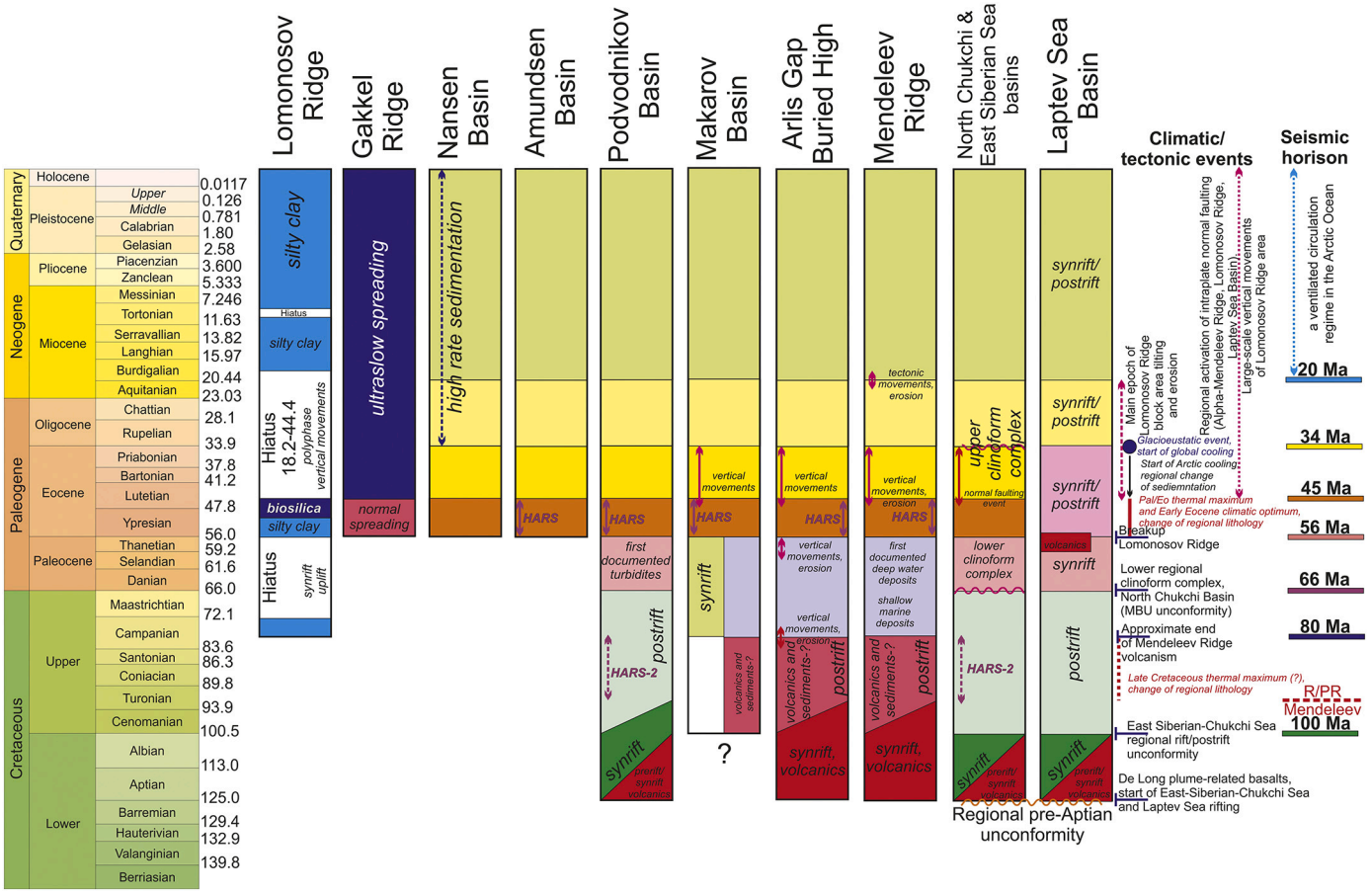

Fig. 57. Chronostratigraphic chart for the Arctic Ocean and Laptev Sea-Chukchi Sea Shelf. Lomonosov Ridge stratigraphy after Moran et al. (2006), Backman et al. (2008), Backman and Moran (2009). Gakkel Ridge spreading history after Glebovsky et al. (2006). Climatic events mainly from Moran et al. (2006), Backman et al. (2008), Stein (2008) and Stein et al. (2015). R/PR – possible rift/postrift boundary for the Mendeleev Rise and Podvodnikov Basin.

Cretaceous boundary at ca. 100 Ma from the shelf area toward the Podvodnikov and Toll basins and Mendeleev Rise (Figs. 6, 10, 11, 12, 13, 14, 16, 22, 23, 25, 26, 44, and 53). All rifts or half-grabens have nearly the same rift/postrift boundary on the shelf and in deep-water areas. We discussed above that the age of this boundary could be younger in the deep-water area. Graben structures are typical for the Podvodnikov and Toll basins. SDR-like units are common features for these basins. The Mendeleev Rise has a typical structure of half-grabens and highs. Many half-grabens have SDR-like complexes. We recognized a number of possible volcanoes in the region of the Mendeleev Rise, Podvodnikov Basin and Arlis Gap (Figs. 16, 28, 29, 30, 34, and 36). The Mendeleev Rise has an axial line that separates SDRs or half-grabens with different polarity (Figs. 33, 34, 35, 36, 37, 38, 39, 40, 41, and 44). The Toll Basin has an axial rift or trough in the northern part (Figs. 65, 66, 67), which trends along the axial part of the basin. This trough directly coincides with a strong magnetic anomaly (see, e.g., Gaina et al., 2011). One possible explanation for this trough is that it represents an aborted start of lithospheric separation. Basalts close to 127-100 Ma in age are documented for the Mendeleev Rise. The Mendeleev Rise forms a single geodynamic system together with the Podvodnikov and Toll basins and originated due to extension orthogonal to the Mendeleev Rise as discussed above. The age of the basalts could be close to the age of rifting. As a consequence, we propose that the main rifting and extension took place close to the Aptian-Albian time. We do not exclude the possibility that rifting in the deep-water part of the Arctic Ocean could have continued after the termination of rifting in the shelf region. A possible age of the rift/postrift boundary could be from 100 Ma and up to 90-80 Ma. Our key conclusion is that rift systems in the shelf region originated together and nearly simultaneous with the systems of the Mendeleev Rise and adjacent Podvodnikov and Toll basins.

Multiple depositional environments can be recognized for the Arctic Alaska Basin (Fig. 65). The Aptian to Albian is represented by the Torok and Nanushuk stratigraphic units (e.g., Homza and Bergman, 2019; Houseknecht, 2019a, 2019b). Condensed deposits are located at the base of this sequence (Houseknecht, 2019a, 2019b) (Fig. 63). Clinoform complexes within the Torok unit are common and well known (e.g., Houseknecht, 2019a, 2019b) with transport of clastic sediments from the Chukotka region and the Brooks Orogen (Fig. 65) toward the Canada deep-water basin, which possibly existed at that time.

A major difference in tectonic environment during the Aptian-Albian for South Amerasia and North Amerasia domains can be recognized. In this context, we propose the hypothesis that the Canada Basin originated before the Aptian time as a deep-water basin.

A significant tectonic event took place close to 80 Ma in the North Amerasia Domain. Sediments with an age younger than 80 Ma commonly have uniform thicknesses in the Podvodnikov and Toll basins

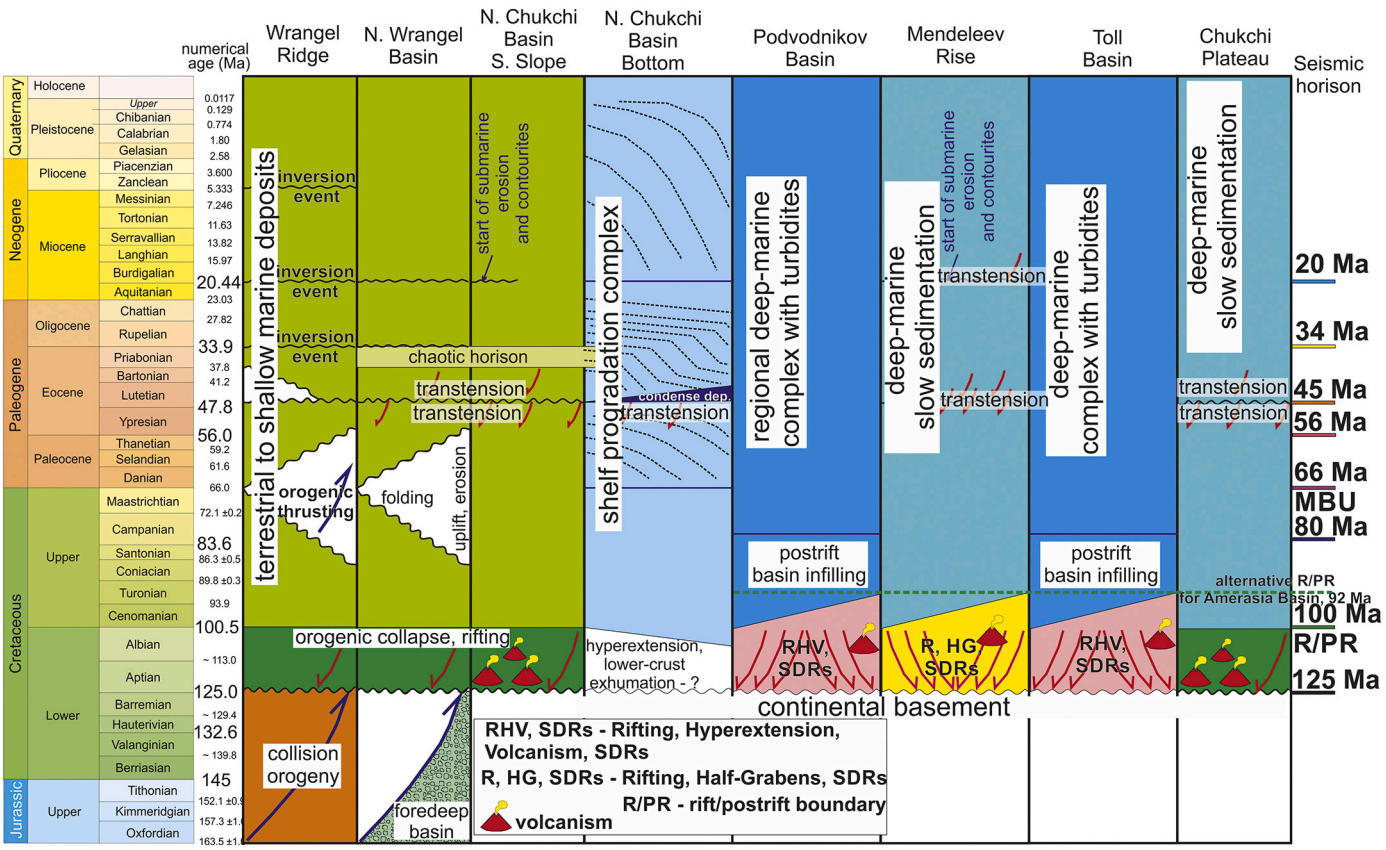

Fig. 58. Chronostratigraphy and main seismic complexes of the Chukchi Sea and adjacent region of the Arctic Ocean. Time scale is from http://www.stratigraphy.org/index.php/ics-chart-timescale.

region and commonly cover all highs (Figs. 6, 11, 12, 13, 14, 16, 22, 23, 25, 26, 33, 36, 37, 44, 53, and 61). This suggests that the formation of the Amerasia Basin occurred close to 80 Ma and regional uniform thermal subsidence proceeded afterwards.

The seismic stratigraphy of the Podvodnikov Basin as a whole is similar with that of the North Chukchi Basin and the East Siberian Sea Basin (Figs. 6, 10, 11, 12, 13, 14, 21, 22, 23, 25, 26, 44, 53, and 61). Isolated rifts can be observed at the base of the basin (Figs. 12, 13, 14, 16, 22, 33, 36, 37, and 44). Synrift sedimentary wedges, which are typical for continental rifting, can be identified in these rifts. Therefore, it is likely that the Podvodnikov Basin has a strongly extended continental crust (Nikishin et al., 2017; Nikishin et al., 2014; Petrov et al., 2016). Similar conclusions were presented by Weigelt et al. (2014), Jokat and Ickrath (2015), and Lebedeva-Ivanova et al., 2019, Lebedeva-Ivanova et al., 2011.

The seismic stratigraphy of the Lomonosov Ridge is characteristic of numerous rifts in the region. On the eastern slope of the Lomonosov Ridge, a rift system forms the Lomonosov Terrace (Figs. 6, 33, 37). This zone is typical of continental rifts that have an Early Cretaceous, Aptian-Albian age according to our scheme (older than 100 Ma at least). On the western slope of the Lomonosov Ridge, synrift deposits are observed below the 56 Ma boundary (Figs. 7, 8, 9, 50, 51), probably corresponding to Paleocene rifts. This rifting preceded the onset of opening of the Eurasia Basin.

The new seismic data across the Mendeleev Rise (Figs. 33, 35, 37, 42, 44) reveals that structure of the Mendeleev Rise is almost identical to the structure of the Alpha Ridge as reported by Brumley (2014) and Evangelatos et al. (2017). Jokat and Ickrath (2015) noted that the Mendeleev Rise does not seem to be associated with horst-graben basement structure. However, in contrast, our seismic lines, which run across and along the Mendeleev Rise (Figs. 33, 35, 37, 42, 44) clearly indicate the presence of basement grabens and horsts.

A key question remains with regard to how the irregular basement relief should be interpreted. We interpret this irregular relief as apparent horsts and grabens punctuating the acoustic basement surface of the Mendeleev Rise. It is likely that the interpreted horsts are not volcanic edifices and that they do, in fact, constitute horst-and-graben topography associated with rifting. We flattened the 45 Ma horizon on seismic lines (Figs. 35, 42). With this procedure, post-depositional structure is removed, and original topography is restored, thus affording an ambiguous view of the paleo-geography. Whereas alternative interpretations are possible, we lean toward the horst-and-graben model of Brumley (2014) and Nikishin et al. (2014).

We identified the Arlis Gap Buried High, which separates the Podvodnikov and Makarov basins, on seismic lines (Figs. 11, 26, 30). With respect to the acoustic basement relief, the Arlis Gap Buried High looks similar to the Mendeleev Rise. Consequently, we consider this high to be a continuation of the Mendeleev Rise structure. The magnetic anomalies, which characterize the Mendeleev Rise, generally are analogous to the anomalies of this high (Gaina et al., 2011; Oakey and Saltus, 2016). The lower seismic stratigraphic unit contains many high-amplitude reflections and extends into the Makarov Basin as described by Evangelatos and Mosher (2016) and Evangelatos et al. (2017). This unit can be interpreted as interbedded volcanic and sedimentary deposits formed at the end of a volcanic epoch in the area of the Alpha-Mendeleev Rise (Evangelatos and Mosher, 2016). We interpret several possible volcanic structures as expressed on 2D seismic profiles (Figs. 26, 28, 29, 30). The 80 Ma horizon boundary, characterized by reflection onlap terminations and a small angular unconformity, is observed in the area of this high (Figs. 26, 28, 30). This suggests that just after deposition at 80 Ma,

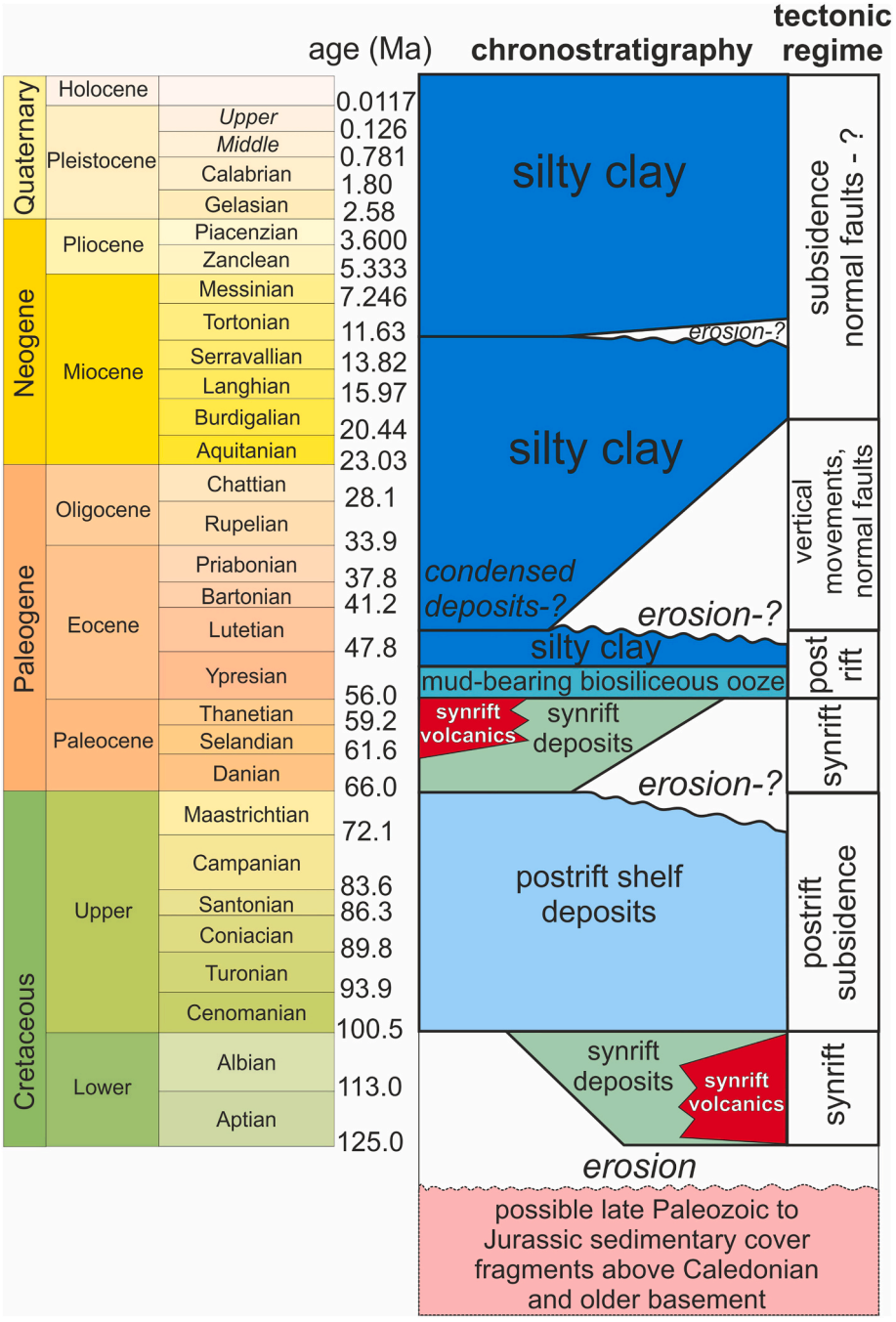

Fig. 59. Tectonostratigraphy for the Lomonosov Ridge.

vertical movements took place, ending at ca. 56 Ma. The 80-56 Ma seismic stratigraphic unit is characterized by variable thickness (Fig. 30), which is indicative of tectonic movement during the time of its deposition.

In the Makarov Basin, two domains, the West Makarov Basin and the East Makarov Basin, can be identified on the basis of acoustic basement characteristics. This is consistent with the interpretation of Evangelatos and Mosher (2016) and Evangelatos et al. (2017). Two of our seismic lines cross the East Makarov Basin, one from the side of the Alpha Ridge and one from the side of the Arlis Gap Buried High (Figs 5, 68, 26 and 28). The acoustic basement relief there is strikingly similar to that of the Alpha-Mendeleev Rise. The lower seismic stratigraphic unit contains high-amplitude reflections and can be mapped from the Makarov basin onto the Arlis Gap Buried High and probably onto the Alpha Ridge as well. This is confirmed by Evangelatos and Mosher (2016) who mapped along another seismic line that crossed the Makarov Basin and the Alpha Ridge. This high-amplitude reflection package probably corresponds to a succession of volcanic and sedimentary deposits with an age greater than 80 Ma. We propose that the East Makarov Basin is a more subsided part of the Alpha-Mendeleev Rise. The West Makarov Basin has pronounced grabens at the base of the section (Figs. 28, 68 and Evangelatos and Mosher, 2016). Unfortunately, with a loose 2D seismic grid, we have no reliable data regarding the trend of these grabens. A small angular unconformity, which can be interpreted as a rift/postrift unconformity, was observed near the 66 Ma boundary (Figs. 28, 68). It follows from this that rifting in the West Makarov Basin took place just before the

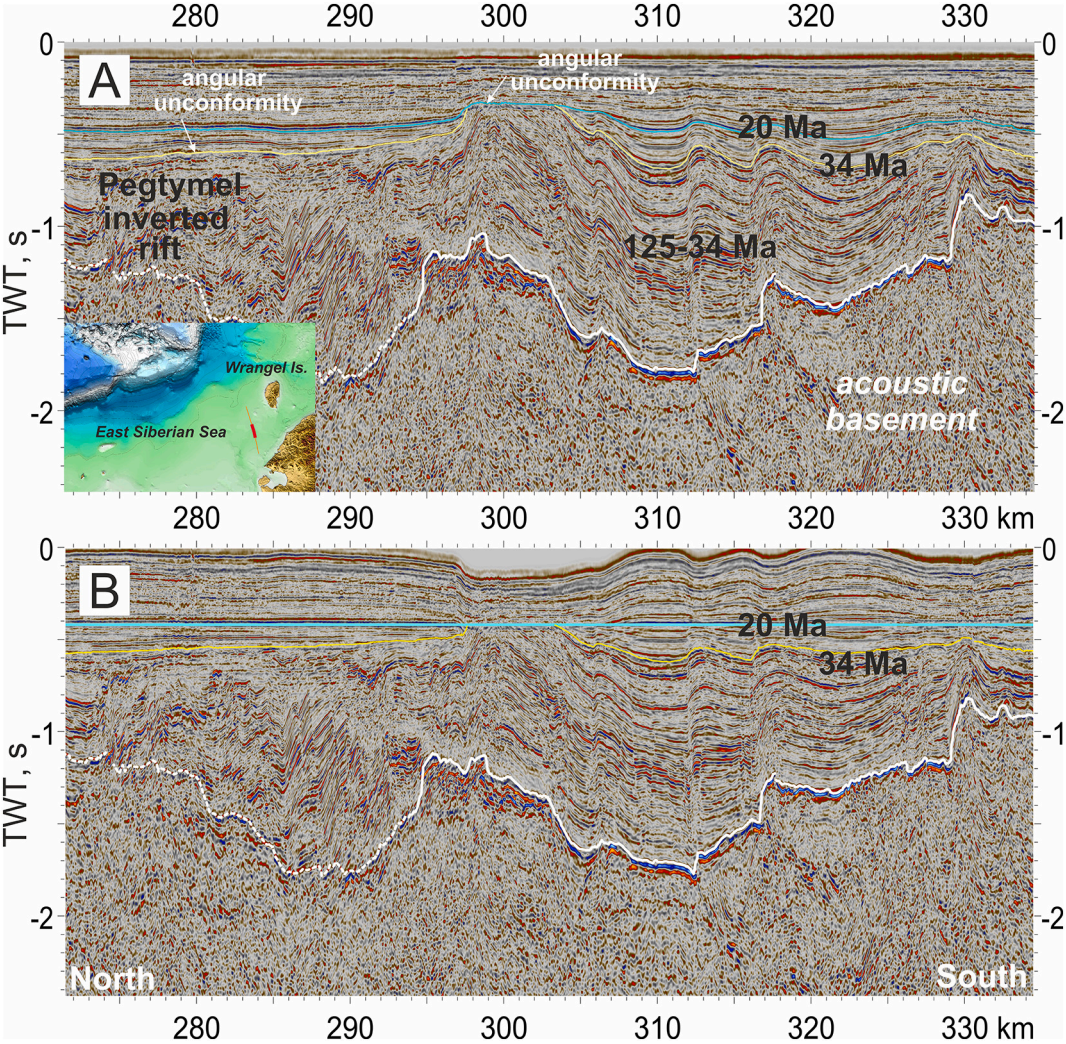

Fig. 60. A. Interpretation of fragment of seismic profile ION15_4410 via Pegtymel Basin, located to the south of Zhokhov-Wrangel-Herald Thrust Belt (Fig. 2 and supplementary data, Fig. 1). The rift basin originated not earlier than the Aptian as it has pre-Aptian orogenic basement. B. Profile flattened on horizon 20 Ma. The rift basin was inverted with main events prior to 34 Ma and 20 Ma. As seismic stratigraphy for this region is badly constrained, ages of inversion could be younger. Modified after Nikishin et al. (2019).

Paleocene. Our seismic stratigraphic correlations indicate no clear base to the rift basin fill. Consequently, the best we can surmise is that the rifting occurred sometime during the Late Cretaceous-Paleocene. The key conclusion is that this rift event is nonetheless younger than the Aptian to Albian rifting in the East Siberian and Chukchi seas shelf and Podvondikov Basin.

We have noted the presence of evidence for likely vertical movement dating to 80-56 Ma in the area of the Arlis Gap Buried High. These vertical movements probably were synchronous with the rifting that occurred in the West Makarov Basin. The main rifting probably took place within the confines of the Lomonosov Ridge slope and was probably associated with strike-slip faults. Probably the West Makarov Basin was formed at 80-66 (or 80-56) Ma as a pull-apart basin. This hypothesis was discussed by us earlier in preliminary form (Nikishin et al., 2014, 2017,). Our interpretation likewise is consistent with the conclusion of Evangelatos and Mosher (2016) that the West Makarov Basin was formed as a pull-apart structure, though these authors argue that the basin was formed earlier than 80 Ma.

5.2. 2D seismic data and crustal structure of some basins and rises

The crustal structure of the Arctic Ocean is the subject of much debate. A number of reviews have been presented (see, e.g., Pease et al., 2014, Lebedeva-Ivanova et al., 2019). The North Chukchi Basin is a prominent example of a super-deep sedimentary basin. It has a sedimentary fill thickness of up to 20-22 km. We document evidence of super-stretching of its basement but an open question remains concerning the type of the basin's basement. According to our model and the recent calculated model of Savin (2020), this could be hyper-extended continental crust. At present, however, we lack the data to unequivocally establish the crustal structure. Hopefully, future numerical modelling can potentially offer greater insight.

The Ust' Lena Basin of the Laptev Sea has a sedimentary cover thickness of the up to 7.5 secs TWT (nearly 15 km). The seismically-

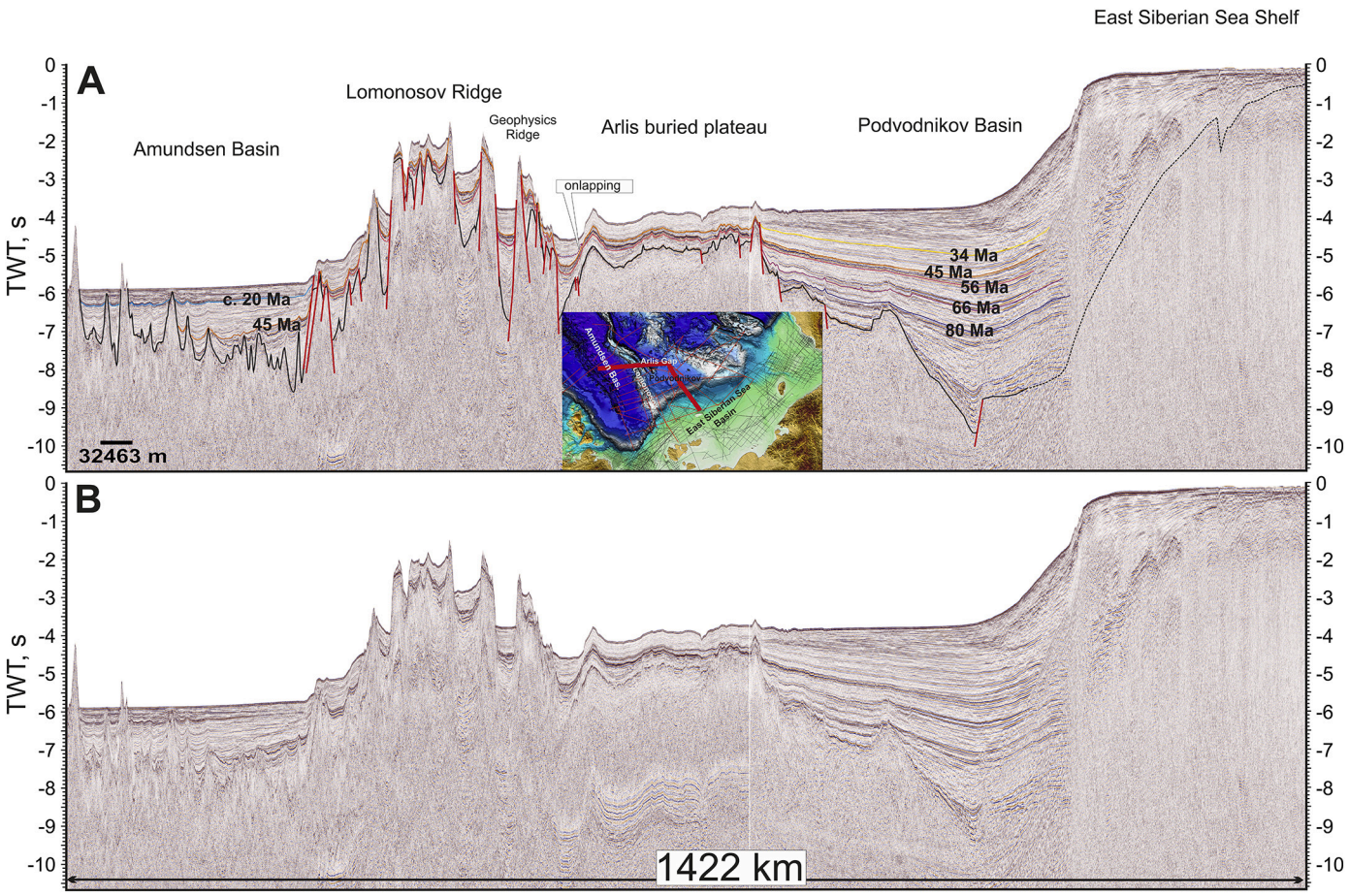

Fig. 61. A. Interpretation of composite seismic profile from the Amundsen Basin to the East Siberian Sea Shelf (lines ARC 14-09 and ARC 14-03). Location of the profile is shown on the map. The trough/ridge topography of the Lomonosov Ridge could be due to Cenozoic normal faulting. B. Seismic profile without interpretation. See also supplementary data, Fig. 61 (seismic profile without interpretation at high resolution).

identified Moho is elevated to approximately 28 km calculated depth. Seismic data suggest that the Moho is for the most part flattened (see Paper-1, Nikishin et al., 2021a). Drachev et al. (2018) proposed mantle exhumation below the sedimentary cover in this basin, however, our grid of seismic lines does not show any unusual features. Consequently, our data and new calculations of the crustal structure of the Laptev Sea (Savin, 2020) do not support the hypothesis by Drachev et al. (2018).

Drachev et al. (2018) proposed mantle exhumation below the sedimentary cover in the East Anisin Basin, located between the continental shelf and the Lomonosov Ridge (Fig. 2). We present a few seismic lines for this area (Figs. 7, 8, 9, 22, 49, 50, and 51) and observe that the thickness of the sedimentary cover is less than 5 secs TWT. We conclude that there is no seismic evidence for the Khatanga-Lomonosov fault as an important active structure (Figs. 7, 8, 9, 22, 49, 50, and 51). We refer the reader to Nikishin et al. (2018) for further discussion of Drachev et al. (2018) hypothesis.

We present new data and a novel geological model for the Mendeleev Rise. The key element is the presence of SDR-like units and half-grabens. Basalts are well documented there as well. We propose that the Mendeleev Rise has a stretched continental crust enriched with basalt intrusions. A similar model was proposed for the mid-Norwegian volcanic continental margin (e.g., Abdelmalak et al., 2016). Skolotnev et al., 2019, Skolotnev et al., 2017 studied four scarps in the Mendeleev Rise, and for every scarp Paleozoic samples were collected. Basalts and dolerites were collected at stations close to the Paleozoic outcrops. As a consequence, they surmise that the total relative volume of intrusions could be up to 10-30% of the pre-Cretaceous basement. This clearly represents is an intriguing case of a combination of extension, volcanism, rifting and intrusive magmatism.

The southern part of the Toll Basin is characterized by SDR complexes within half-grabens (Figs. 33, 34). This is typical for inner SDRs of volcanic passive continental margins with continental basement (e.g., Foulger et al., 2020). The northern part of the Toll Basin (or Mendeleev Basin) has a narrow axial rift or trough (Figs. 66, 67). We propose that this trough could be explained as a failed start of lithospheric separation. The Toll Basin could be a good example of aborted oceanic spreading.

The Podvodnikov Basin has a highly stretched continental crust. The key evidence is the presence of half-grabens and SDR-like units, typical of continental crustal extension.

Additional data are required to better understand the crustal structure of the Arctic Ocean. Examples of crustal structural modelling using seismic data were presented in a number of publications (e.g., Jokat and Ickrath, 2015; Chian et al., 2016; Oakey and Saltus, 2016; Evangelatos et al., 2017; Kashubin et al., 2018; Lebedeva-Ivanova et al., 2019; Poselov et al., 2019; Savin, 2020). A new generation of such models could integrate data on the geological evolution and basin structure and architecture with constraints from geophysical observations of the crust and lithosphere.

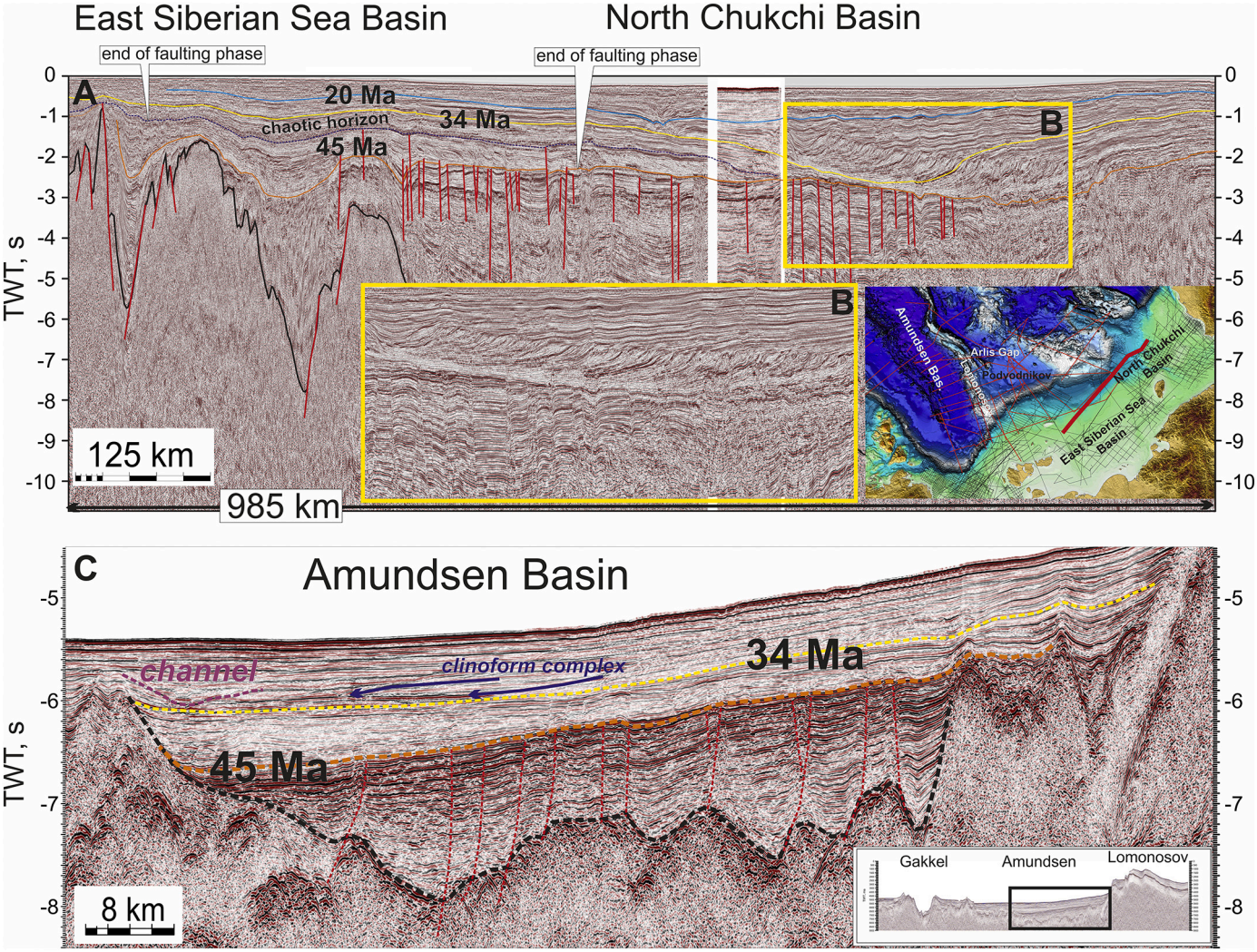

Fig. 62. A. Interpretation of composite seismic profile for the East Siberian Sea and the Chukchi Sea Shelf (lines ION 12-1440 – Arc 14-01 – ION 11-1400). B. Enlarged section of seismic profile without interpretation. C. Interpretation of fragment of seismic profile ARC 14-05 for the Amundsen Basin (see Fig. 25 for location). Two profiles show observed faulting with an age close to 45 Ma.

5.3. *Proposed model of the Arctic Ocean history*

Many reconstructions of the formation history of the Arctic Ocean presently exist (e.g., Alvey et al., 2008; Amato et al., 2015; Grantz et al., 2011; Grantz and Hart, 2012; Hutchinson et al., 2017; Lawver et al., 2015; Mosher et al., 2012; Shephard et al., 2013). It is clear that models of different authors differ significantly (Paper-1, Nikishin et al., 2021a). We propose as a hypothesis that the Arctic Ocean probably was formed during four phases with different kinematics. The key tectonostratigraphic phases are: 133-125 Ma, 125-80 Ma, 80-56 Ma, and 56-0 Ma.

The boundaries of the first phase correspond to two regional unconformities observed on the Alaskan Arctic Shelf: 133 Ma – the Lower Cretaceous Unconformity (LCU) and 125 Ma – the Brookian Unconformity (BU) (Sherwood et al., 2002). According to our model, the LCU corresponds to the onset of opening of the Canada Basin, and the BU to the end of formation of the Canada Basin. The duration of Canada Basin formation is approximately 8 Ma. Such a rapid formation time is typical of back-arc basins of the type observed in the Sea of Japan and the South China Sea (see Ziegler and Cloetingh, 2004 for a review). Their widths have similar values (about 600-700 km) as to what is observed in the Arctic region.

The timing of the cessation of Canada Basin formation probably coincides with the onset of the large-scale collapse of the Verkhoyansk-Chukotka Orogen and onset of continental rifting in the East Siberian Sea and in the Russian part of the Chukchi Sea (Miller and Verzhbitsky, 2009; Nikishin et al., 2014, 2017). A major rearrangement of lithospheric plate kinematics occurred at ca. 125 Ma. The collapse of the Verkhoyansk-Chukotka Orogen and onset of the impact of the HALIP superplume corresponded to this rearrangement. A similar situation occurred approximately at the Permian/Triassic boundary in West Siberia where plume magmatism (e.g. the Siberian Platform, Taimyr) and large-scale rifting took place simultaneously in different places (e.g., Nikishin et al., 2002). In the Arctic, these processes led to formation of the deep-water rifted Podvodnikov and the Toll-Mendeleev-Nautilus basins and the volcanic edifice of the Alpha-Mendeleev Rise on continental crust strongly thinned by rifting. These processes lasted approximately till 80 Ma.

80 Ma is the approximate time of the end of subduction-related volcanism in the Okhotsk-Chukotka volcanic belt (Fig. 2) (Akinin, 2012). After that, formation of the Koryakia-West Kamchatka

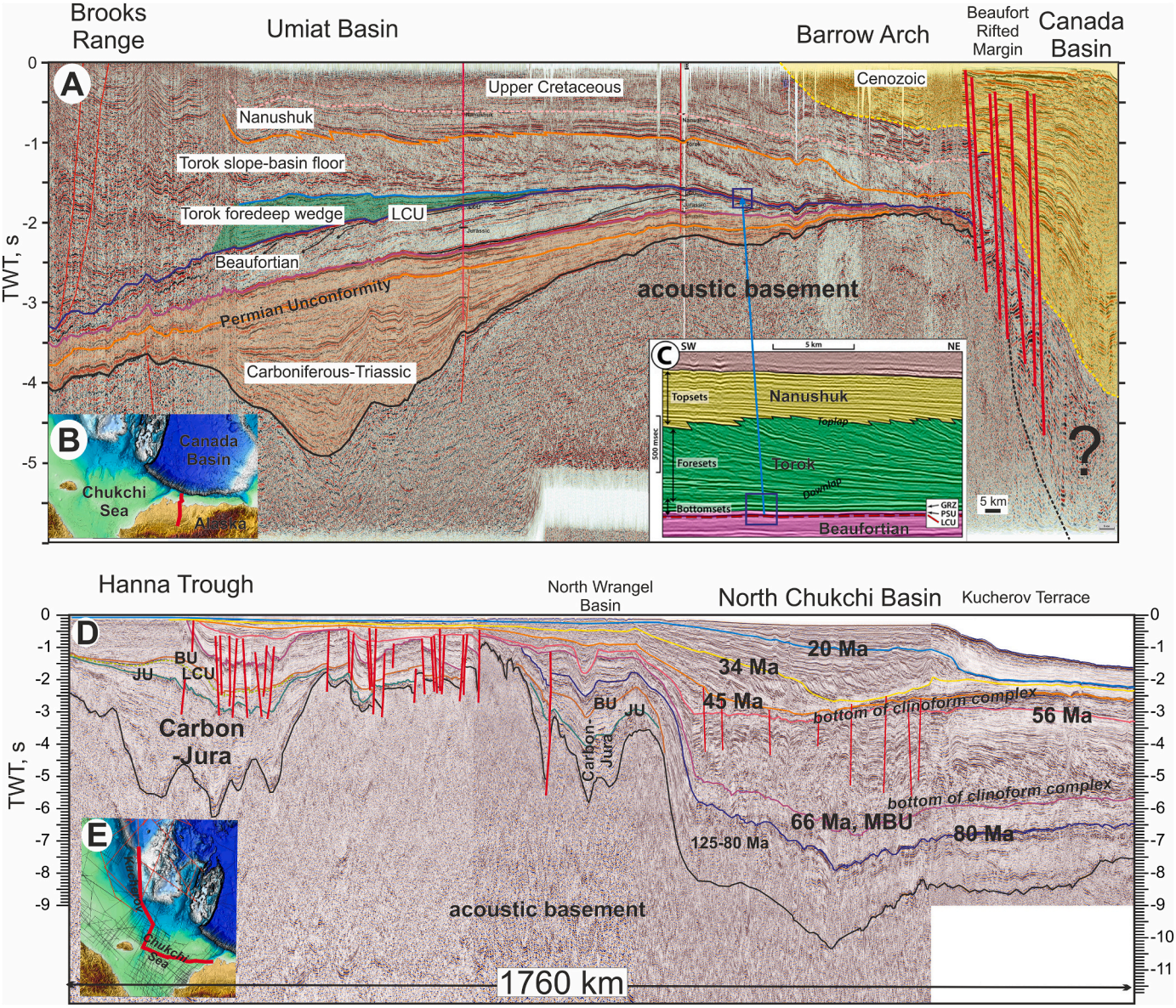

Fig. 63. A. Composite seismic profile for the Arctic Alaska Basin (lines usgs-r-8, usgs-6-74, usgs-6D-74, usgs-4-74, usgs-GM-5S, usgs-GM-5D, usgs-GM-4D, usgs_HW81-24, usgs_HW81-11, usgs_WB-558, and usgs-71GSG-G-88). Seismic data from U.S. Geological Survey. Data of Houseknecht (2019a, 2019b) were used for interpretation. B. Location of the profile. C. Detail of seismic image with approximate position on line A (Houseknecht, 2019b). LCU – Lower Cretaceous Unconformity, PSU – Pebble Shale Unit, GRZ – Gamma-Ray Zone; condensed sections are between LCU and GRZ. D. Composite seismic profile for the North Chukchi Basin (Fig. 10). E. Location of the profile.

accretional orogen began (Soloviev, 2008; Akinin, 2012) whose formation ended at ca. 50-45 Ma (Soloviev, 2008). The end of subduction-related volcanism in the Okhotsk-Chukotka volcanic belt may correspond to the time of significant plate kinematic rearrangement and end of Alpha-Mendeleev Rise formation.

During the 80 Ma-66 (56) Ma time interval, large-scale slip fault deformation possibly occurred and resulted in the formation of the West Makarov and other rift basins. These slip fault deformations probably controlled the plate kinematics in the Atlantic and Pacific Regions.

From 56 Ma (or earlier) onward the formation history of the Arctic Ocean was associated with opening of the Atlantic Ocean and the Eurasia Basin was formed.

6. Conclusions

In this study, a new seismic stratigraphic framework is proposed for much of the Arctic Ocean. We identified and traced extensively a number of boundaries with ages of 100 Ma, 80 Ma, 66 Ma, 56 Ma, 34 Ma and 20 Ma. The new seismic stratigraphic framework led to a new model for the geological history of the Arctic Ocean (it should be noted, however, that we specifically did not include the Canada Basin).

On the shelves of the Laptev, East Siberian and Chukchi Seas, large-scale continental rifting took place in the Aptian-Albian. The Podvodnikov Basin and probably the Toll Basin started to form not earlier than the Aptian; the rifting processes were completed by ca. 100-90 Ma.

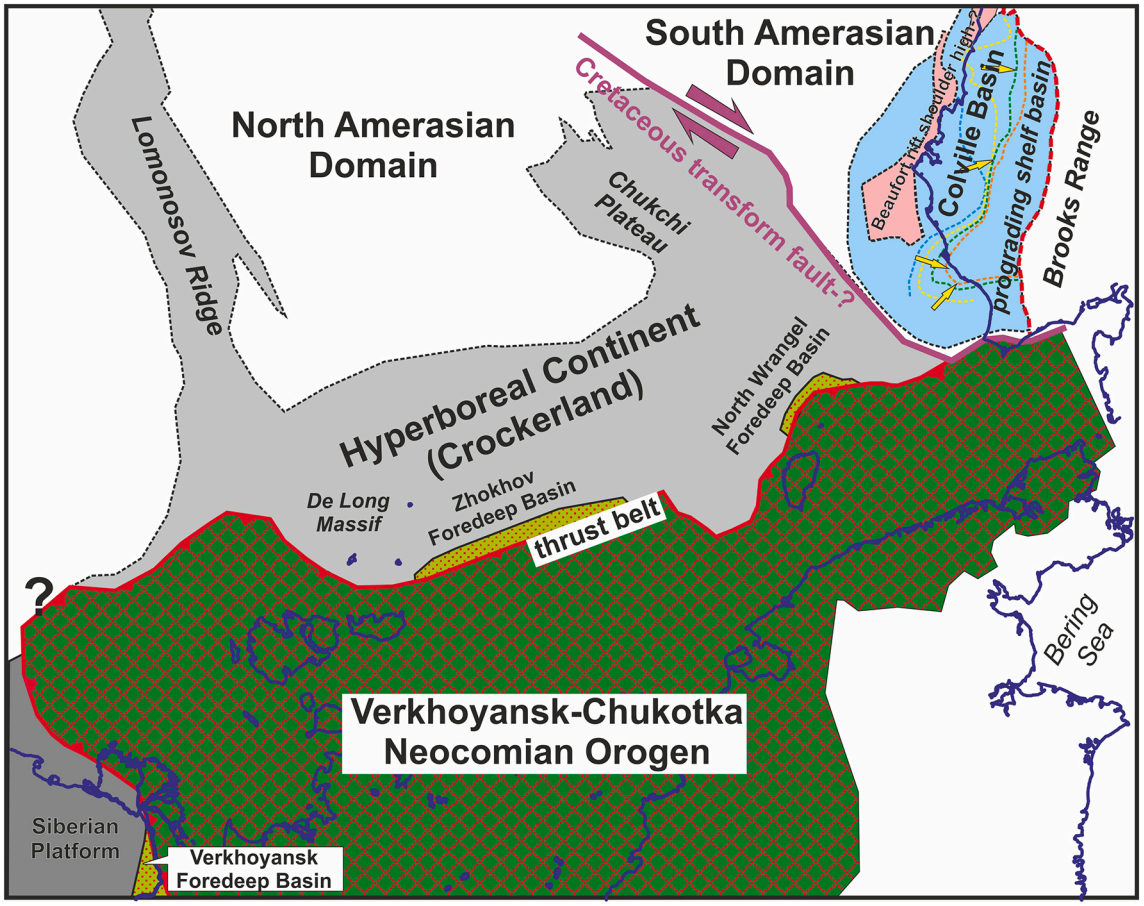

Fig. 64. Types of Late Jurassic to Neocomian seismic sequences and some paleogeographic elements on a modern geographic basis. Data for the Alaska region are from Houseknecht (2019a, 2019b).

We propose the existence of a new Aptian igneous province north of Wrangel Island. The Alpha-Mendeleev Igneous Province was surrounded on all sides (except the area of the Canada Basin) by Early Cretaceous igneous provinces. An approximately simultaneous onset of magmatism at 130-125 Ma is likely to have occurred within a vast area. Analysis of seismic data shows that the Arlis Gap Buried High is a continuation of the structure underlying the Mendeleev Rise. Our data also show that most of the Makarov Basin basement constitutes a continuation of the Alpha Ridge structure. Summing up these data, it appears that the Alpha-Mendeleev Igneous Province started to form at the eastern margin of the Lomonosov Ridge. That is, the Alpha-Mendeleev Igneous Province started to form at ca. 125 Ma as a volcanic rifted continental margin. The Arctic superplume HALIP probably did not result in the opening of a new ocean. No data are available to conclusively prove that a large-scale formation of oceanic crust was taking place in the Late Cretaceous in the Alpha-Mendeleev Rise area. The problem of structure and origin of the Alpha-Mendeleev Rise will require further analysis. A key novel finding is the presence of SDR-like units in the Mendeleev Rise and Podvodnikov and Toll basins.

The time interval of about 80-66 (56) Ma is characteristic of strike-slip fault tectonics. The West Makarov Basin was formed in this time likely as a pull-apart basin. During the Late Cretaceous-Paleocene (ca. 80-56 Ma), continental rifting widely manifested itself in the western part of the Laptev Sea and on the western slope of the Lomonosov Ridge. This rifting preceded the opening of the Eurasia Basin. In the western part of the Laptev Sea, an igneous province was identified using seismic data. The possible age of volcanism is ca. 56 Ma. This magmatism preceded the opening of the Eurasia Basin.

The 45-34 Ma (or 45-20 Ma) time interval constitutes a period of large-scale vertical intraplate movements in the Arctic Ocean. At that time, relative highs commonly experienced uplift, while relative lows experienced subsidence. Synchronously with vertical movements, activation of normal faulting took place on the Lomonosov Ridge and Mendeleev Rise. The present-day bathymetry of the Arctic Ocean was formed at this time with processes of vertical movement and normal faulting continuing up until the present time. The transition from normal spreading to ultra-slow spreading on the Gakkel Ridge happened at 45 Ma. Synchronously with this event, intraplate vertical movements started and a phase of super-regional, low-amplitude normal faulting took place. Normal faults of this age are detected in widespread regions ranging from the Amundsen Basin up to the shelves of the East Siberian and Chukchi Seas.

Climatic events are recorded in the sedimentary cover of the Arctic Ocean. During the 56-45 Ma time interval, as constrained by analysis of seismic facies, a marked period of global warming occurred in the Arctic region. An abrupt cooling that began at 45 Ma was caused by a sharp

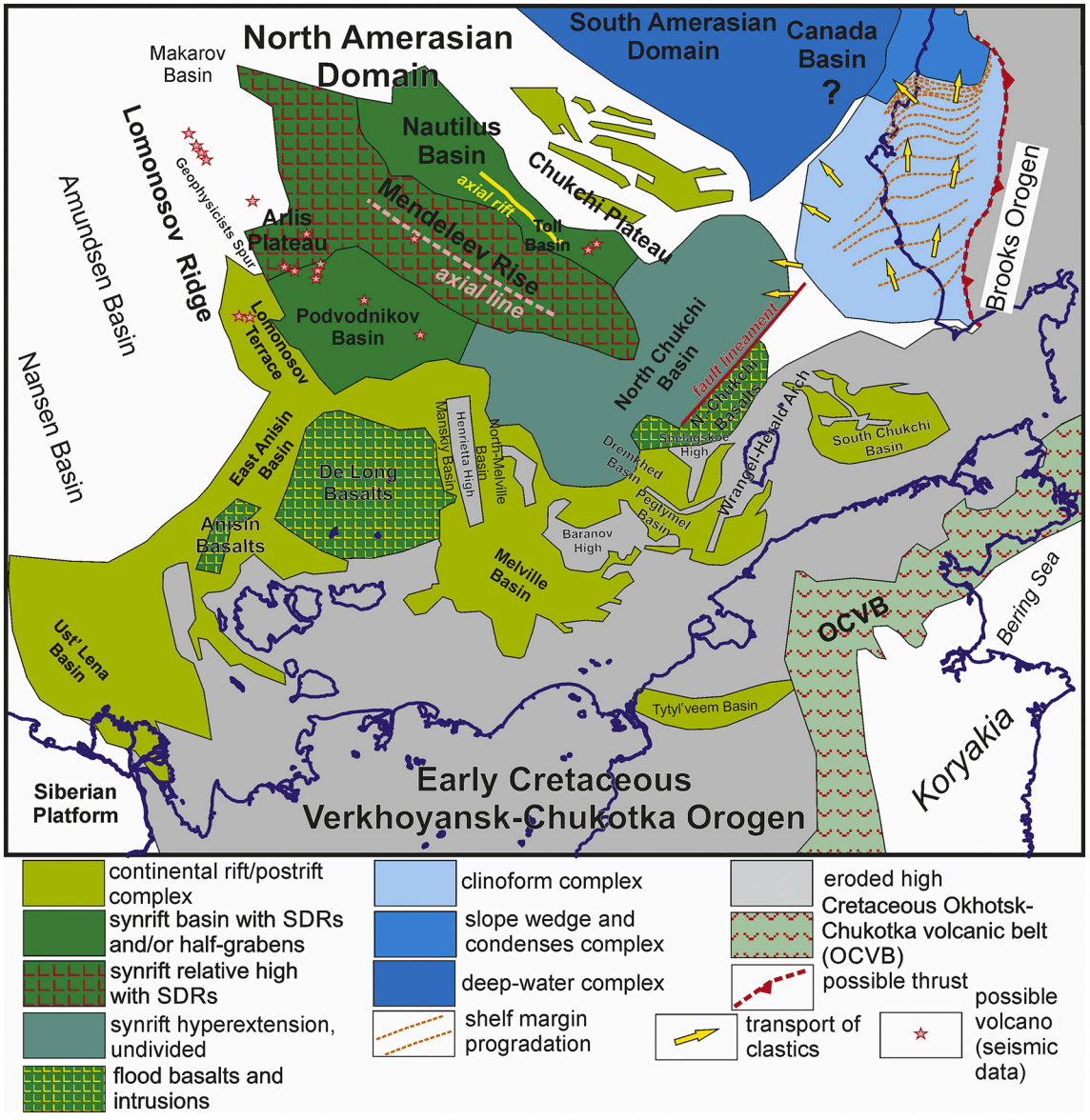

Fig. 65. Types of the Aptian-Albian seismic sequences and some paleogeographic elements on a modern geographic basis. Data for the Alaska region are from Houseknecht (2019a, 2019b).

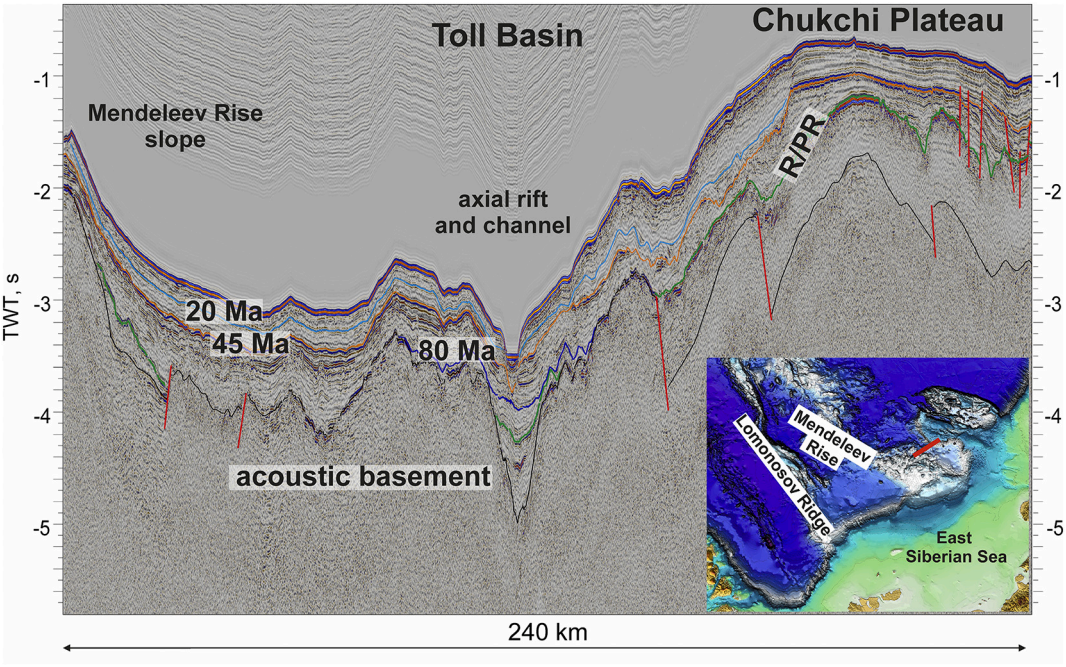

Fig. 66. Interpretation of western part of seismic profile ARC12_19. Location of the profile is shown on the map. The Toll Basin is located between Mendeleev Rise and Chukchi Plateau. The basin is characterized by axial V-shape paleorift of the Cretaceous age. The rift strikes along the basin (Fig. 65). Mendeleev Rise and Chukchi Plateau have systems of half-grabens along slopes of the Toll Basin. R/PR – rift/postrift boundary.

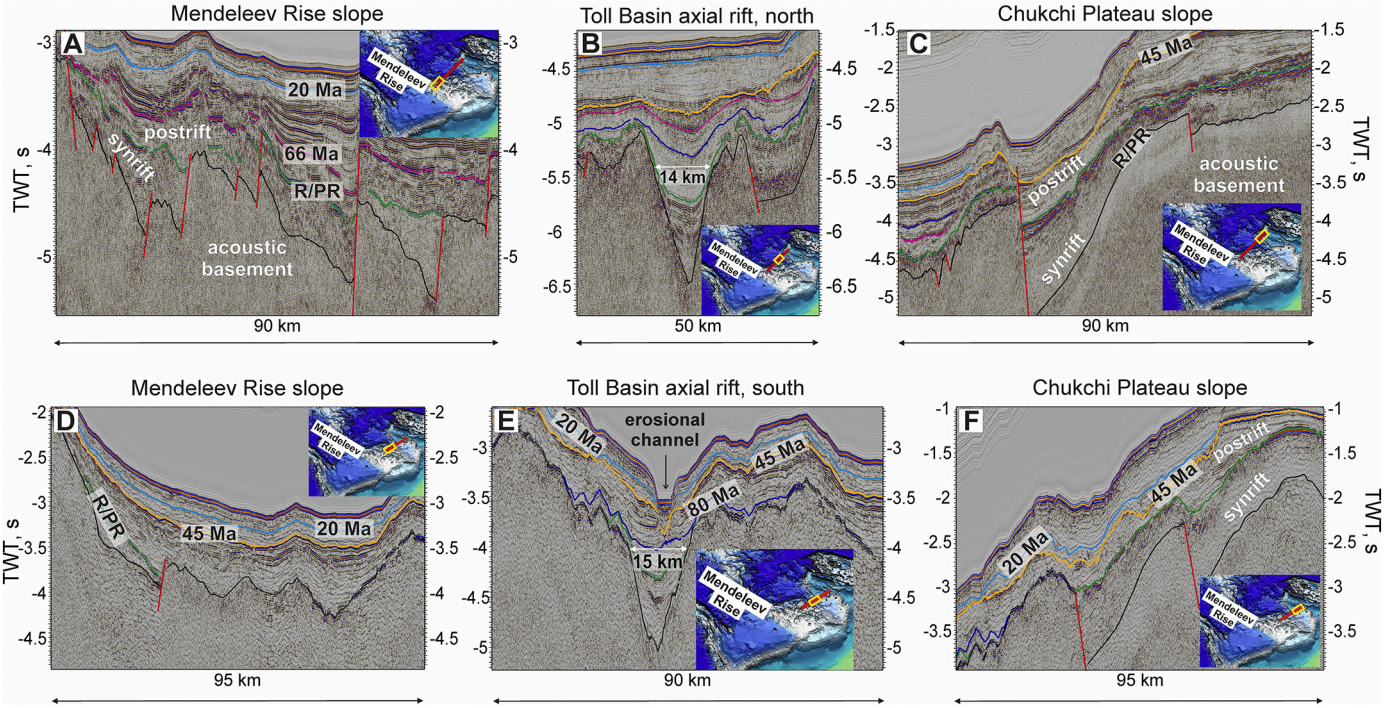

Fig. 67. Interpretation of seismic data for the Toll Basin Axial Rift region. A, B, C. Fragments of seismic profile ARC12_04 from Mendeleev Rise toward Chukchi Plateau. D, E, F. Fragments of seismic profile ARC12_19 from Mendeleev Rise toward Chukchi Plateau (Fig. 66). The profiles are parallel to each other. Slopes of Mendeleev Rise and Chukchi Plateau have similar and symmetric horst and half-graben structure. Axial zone of the Toll Basin is characterized by buried Cretaceous trough-like rift with V-shape. Width of this rift is close to 14-15 km. This trough could be explained as a failed start of lithospheric separation.

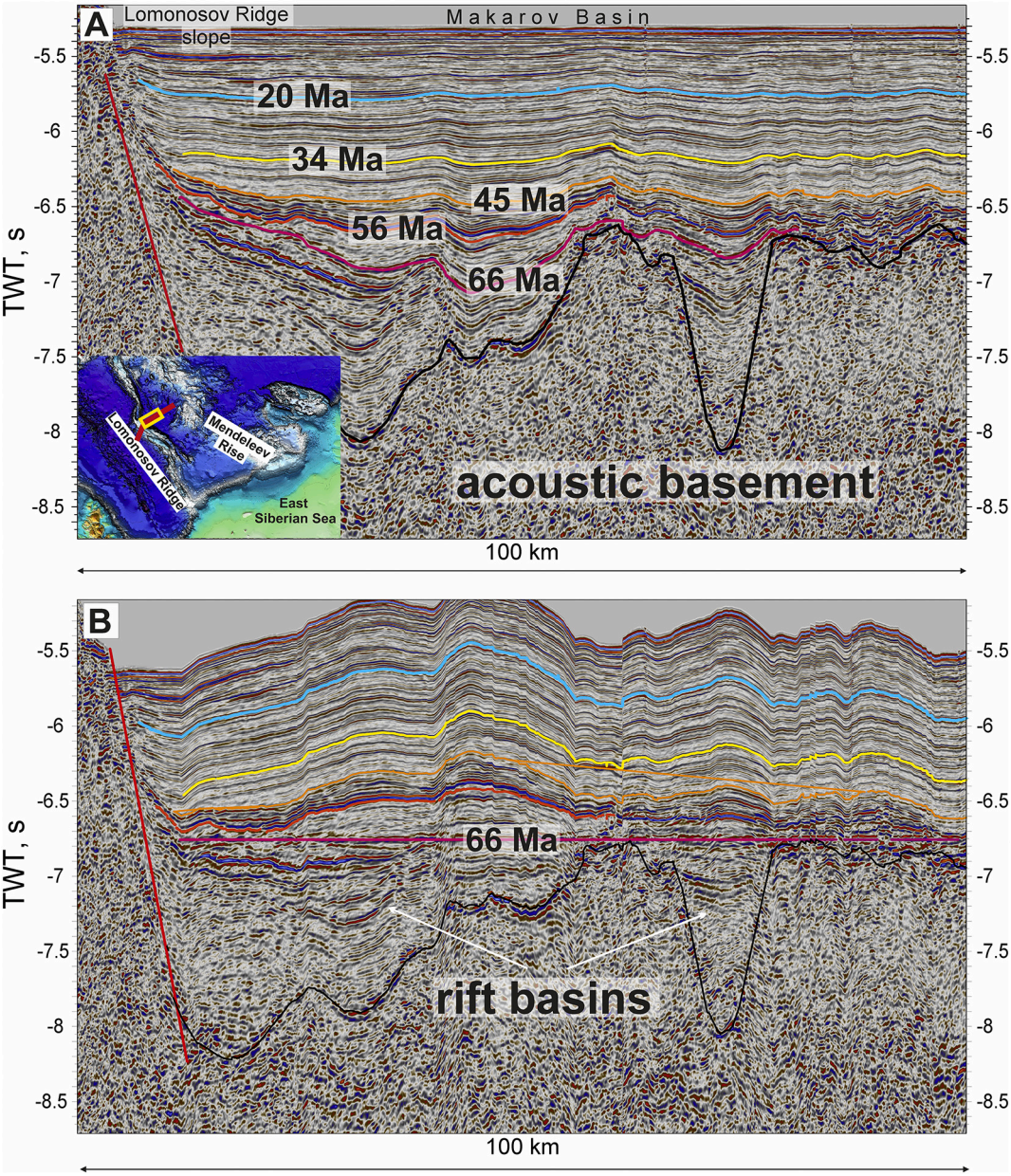

Fig. 68. A. Interpretation of fragment of profile ARC_14-07 shown in Fig. 5. The profile crosses the Makarov Basin and the Lomonosov Ridge slope. This profile is nearly orthogonal to the profile on Fig. 28. V-shape trough is observed in the central part of the Makarov Basin. This trough, a rift basin, is possibly the same as shown in Fig. 28. Another rift basin is located between the Lomonosov Ridge and Makarov Basin. B. Profile flattened on the 66 Ma horizon. We assume a pre-66 Ma age of rifting.

change in paleogeography that occurred in response to an acceleration of uplift around the ocean.

Declaration of Competing Interest

We have no conflict of interest.

Acknowledgements

The authors are grateful to the Ministry of Natural Resources and Ecology of Russia for the opportunity to publish this paper. Discussions with C. Gaina, E. Miller, V. Pease, W. Jokat, D. Hutchinson, J.I. Faleide, S. Drachev, R. Stephenson, D. Franke, A. Escalona, I. Norton, N. Lebedeva-Ivanova, E. Lundin, A. Doré, E. Weigelt, D. Mosher, and D. Zastrozhnov stimulated our work. We are thankful to many Russian geologists from different scientific organizations with whom we conducted numerous discussions: L.I. Lobkovsky, V.A. Vernikovsky, S.D. Sokolov, S.G. Skolotnev, A.K. Khudoley, A.V. Prokopiev, O.V. Petrov, E. V. Shipilov, A.V. Stoupakova, E.A. Gusev, P.V. Rekant, V.A. Poselov, S. N. Kashubin, V.V. Akinin, A.S. Alekseev, G.N. Aleksandrova, A.B. Herman, V.A. Savin, and others. In the course of studying the Arctic, we had the opportunity to conduct scientific discussions with geologists from different companies: Rosneft, Total, ExxonMobil, Statoil, BP, Gazprom Neft, Gazprom. We thank companies MAGE, DMNG and ION-GXT for the use of their seismic data. E. Bulgakova, A. Popova, M. Skaryatin, A. Fedechkina, I. Mazaeva, O. Makhova, S. Zaytseva, N. Kulyukina, and D. Igtisamov (Rosneft) provided constructive feedback for our seismic data interpretation. The work of AMN, SIF, KFS, and NNZ was supported by RFBR grants (18-05-70011 and 18-05-00495). We thank François Roure and anonymous reviewers for generous, detailed, and constructive

criticism. We express many thanks to Tim Horscroft and Gillian Foulger as editors for this paper.

Appendix A. Supplementary data

Supplementary data (mainly regional seismic profiles without interpretation) are presented in: https://yadi.sk/d/yZ1N6crs_eFbeA. Supplementary data to this article can be found online at https://doi.org/10.1016/j.earscirev.2021.103581.

References

Abdelmalak, M.M., Meyer, R., Planke, S., Faleide, J.I., Gernigon, L., Frieling, J., Sluijs, A., Reichart, G.-J., Zastrozhnov, D., Theissen-Krah, S., Said, A., Myklebust, R., 2016. Pre-breakup magmatism on the Vøring Margin: Insight from new sub-basalt imaging and results from Ocean Drilling Program Hole 642E. Tectonophysics 675, 258–274. https://doi.org/10.1016/j.tecto.2016.02.037.

Akhmet'ev, M.A., Zaporozhets, N.I., Yakovleva, A.I., Aleksandrova, G.N., Beniamovsky, V.N., Oreshkina, T.V., Gnibidenko, Z.N., Dolya, Z.A., 2010. Comparative analysis of marine paleogene sections and biota from West Siberia and the Arctic Region. Stratigr. Geol. Correl. 18, 635–659. https://doi.org/10.1134/S0869593810060043.

Akinin, V.V., 2012. Late Mesozoic and Cenozoic magmatism and lower crust modifications in the northern framing of Pacific. IGEM RAS, Moscow.

Aleksandrova, G.N., 2016. Geological evolution of Chauna depression (North-Eastern Russia) during Paleogene and Neogene. 1. Paleogene. (in Russian). Bull. Moscow Soc. Nat. Geol. Ser. 91, 148–164 (in Russian).

Alvey, A., Gaina, C., Kusznir, N.J., Torsvik, T.H., 2008. Integrated crustal thickness mapping and plate reconstructions for the high Arctic. Earth Planet. Sci. Lett. 274, 310–321. https://doi.org/10.1016/j.epsl.2008.07.036.

Amato, J.M., Toro, J., Akinin, V.V., Hampton, B.A., Salnikov, A.S., Tuchkova, M.I., 2015. Tectonic evolution of the Mesozoic South Anyui suture zone, eastern Russia: A critical component of paleogeographic reconstructions of the Arctic region. Geosphere 11, 1530–1564. https://doi.org/10.1130/GES01165.1.

Backman, J., Moran, K., 2009. Expanding the cenozoic paleoceanographic record in the central arctic ocean: IODP expedition 302 synthesis. Open Geosci. 1 https://doi.org/10.2478/v10085-009-0015-6.

Backman, J., Jakobsson, M., Frank, M., Sangiorgi, F., Brinkhuis, H., Stickley, C., O'Regan, M., Løvlie, R., Pälike, H., Spofforth, D., Gattacecca, J., Moran, K., King, J., Heil, C., 2008. Age model and core-seismic integration for the Cenozoic Arctic Coring Expedition sediments from the Lomonosov Ridge. Paleoceanography 23. https://doi.org/10.1029/2007PA001476.

Bird, K.J., Houseknecht, D.W., Pitman, J.K., 2017. Geology and assessment of undiscovered oil and gas resources of the Hope Basin Province, 2008. In: Moore, T. E., Gautier, D.L. (Eds.), The 2008 Circum-Arctic Resource Appraisal. U.S. Geological Survey Professional Paper 1824, Reston, Virginia, pp. 1–9. https://doi.org/10.3133/pp1824D.

Brinkhuis, H., Schouten, S., Collinson, M.E., Sluijs, A., Damsté, J.S.S., Dickens, G.R., Huber, M., Cronin, T.M., Onodera, J., Takahashi, K., Bujak, J.P., Stein, R., van der Burgh, J., Eldrett, J.S., Harding, I.C., Lotter, A.F., Sangiorgi, F., van Cittert, H.K., de Leeuw, J.W., Matthiessen, J., Backman, J., Moran, K., 2006. Episodic fresh surface waters in the Eocene Arctic Ocean. Nature 441, 606–609. https://doi.org/10.1038/nature04692.

Brumley, K., 2014. Geologic history of the Chukchi Borderland, Arctic Ocean. A dissertation submitted to the department of geology and environmental sciences and the committee on graduate studies of Stanford university in partial fulfillment of the requirements for the degree of Doctor of philosophy. http://purl.stanford.edu/hz857zk1405.

Brumley, K., Miller, E.L., Konstantinou, A., Grove, M., Meisling, K.E., Mayer, L.A., 2015. First bedrock samples dredged from submarine outcrops in the Chukchi Borderland, Arctic Ocean. Geosphere 11, 76–92. https://doi.org/10.1130/GES01044.1.

Bruvoll, V., Kristoffersen, Y., Coakley, B.J., Hopper, J.R., 2010. Hemipelagic deposits on the Mendeleev and northwestern Alpha submarine Ridges in the Arctic Ocean: acoustic stratigraphy, depositional environment and an inter-ridge correlation calibrated by the ACEX results. Mar. Geophys. Res. 31, 149–171. https://doi.org/10.1007/s11001-010-9094-9.

Bruvoll, V., Kristoffersen, Y., Coakley, B.J., Hopper, J.R., Planke, S., Kandilarov, A., 2012. The nature of the acoustic basement on Mendeleev and northwestern Alpha ridges, Arctic Ocean. Tectonophysics 514–517, 123–145. https://doi.org/10.1016/j.tecto.2011.10.015.

Butsenko, V.V., Poselov, V.A., Zholondz, S.M., Smirnov, O.E., 2019. Seismic attributes of the Podvodnikov Basin basement. Dokl. Earth Sci. 488, 1182–1185. https://doi.org/10.1134/S1028334X19100015.

Chernykh, A.A., Krylov, A.A., 2011. Sedimentogenesis in the Amundsen Basin from geophysical data and drilling results on the Lomonosov Ridge. Dokl. Earth Sci. 440, 1372–1376. https://doi.org/10.1134/S1028334X11100011.

Chian, D., Jackson, H.R., Hutchinson, D.R., Shimeld, J.W., Oakey, G.N., Lebedeva-Ivanova, N., Li, Q., Saltus, R.W., Mosher, D.C., 2016. Distribution of crustal types in Canada Basin, Arctic Ocean. Tectonophysics 691, 8–30. https://doi.org/10.1016/j.tecto.2016.01.038.

Coakley, B., Brumley, K., Lebedeva-Ivanova, N., Mosher, D., 2016. Exploring the geology of the central Arctic Ocean; understanding the basin features in place and time. J. Geol. Soc. Lond. 173, 967–987. https://doi.org/10.1144/jgs2016-082.

Corfu, F., Polteau, S., Planke, S., Faleide, J.I., Svensen, H., Zayoncheck, A., Stolbov, N., 2013. U–Pb geochronology of Cretaceous magmatism on Svalbard and Franz Josef Land, Barents Sea Large Igneous Province. Geol. Mag. 150, 1127–1135. https://doi.org/10.1017/S0016756813000162.

Craddock, W.H., Houseknecht, D.W., 2016. Cretaceous–Cenozoic burial and exhumation history of the Chukchi shelf, offshore Arctic Alaska. Am. Assoc. Pet. Geol. Bull. 100, 63–100. https://doi.org/10.1306/09291515010.

Cramer, B.S., Toggweiler, J.R., Wright, J.D., Katz, M.E., Miller, K.G., 2009. Ocean overturning since the Late Cretaceous: inferences from a new benthic foraminiferal isotope compilation. Paleoceanography 24. https://doi.org/10.1029/2008PA001683.

Dick, H.J.B., Lin, J., Schouten, H., 2003. An ultraslow-spreading class of ocean ridge. Nature 426, 405–412. https://doi.org/10.1038/nature02128.

Dobretsov, N.L., Vernikovsky, V.A., Karyakin, Y.V., Korago, E.A., Simonov, V.A., 2013. Mesozoic–Cenozoic volcanism and geodynamic events in the Central and Eastern Arctic. Russ. Geol. Geophys. 54, 874–887. https://doi.org/10.1016/j.rgg.2013.07.008.

Døssing, A., Jackson, H.R., Matzka, J., Einarsson, I., Rasmussen, T.M., Olesen, A.V., Brozena, J.M., 2013. On the origin of the Amerasia Basin and the High Arctic Large Igneous Province—Results of new aeromagnetic data. Earth Planet. Sci. Lett. 363, 219–230. https://doi.org/10.1016/j.epsl.2012.12.013.

Dove, D., Coakley, B., Hopper, J., Kristoffersen, Y., Team, H.G., 2010. Bathymetry, controlled source seismic and gravity observations of the Mendeleev ridge; implications for ridge structure, origin, and regional tectonics. Geophys. J. Int. 183, 481–502. https://doi.org/10.1111/j.1365-246X.2010.04746.x.

Drachev, S., Saunders, A., 2006. The Early Cretaceous Arctic LIP: its geodynamic setting and implications for Canada Basin opening. In: Scott, R.A., Thurston, D.K. (Eds.), Proceedings of the Fourth International Conference on Arctic Margins. US Department of the Interior MMS, Dartmouth, Nova Scotia, Canada, pp. 216–223.

Drachev, S.S., 2016. Fold belts and sedimentary basins of the Eurasian Arctic. Arktos 2, 21. https://doi.org/10.1007/s41063-015-0014-8.

Drachev, S.S., Malyshev, N.A., Nikishin, A.M., 2010. Tectonic history and petroleum geology of the Russian Arctic Shelves: an overview. Geol. Soc. Lond. Pet. Geol. Conf. Ser. 7, 591–619. https://doi.org/10.1144/0070591.

Drachev, S.S., Mazur, S., Campbell, S., Green, C., Tishchenko, A., 2018. Crustal architecture of the East Siberian Arctic Shelf and adjacent Arctic Ocean constrained by seismic data and gravity modeling results. J. Geodyn. 119, 123–148. https://doi.org/10.1016/j.jog.2018.03.005.

Ehlers, B.-M., Jokat, W., 2013. Paleo-bathymetry of the northern North Atlantic and consequences for the opening of the Fram Strait. Mar. Geophys. Res. 34, 25–43. https://doi.org/10.1007/s11001-013-9165-9.

Embry, A., Beauchamp, B., 2008. Chapter 13, Sverdrup Basin. In: Sedimentary Basins of the World, pp. 451–471. https://doi.org/10.1016/S1874-5997(08)00013-0.

Embry, A., Dixon, J., 1994. The age of the Amerasia Basin. In: Fujita, K., Thurston, D.K. (Eds.), Proceedings of the 1992 International Conference on Arctic Margins. U.S. Dept. of the Interior Minerals Management Service, OCS Study, Anchorage, pp. 289–294.

Embry, A.F., 1990. Geological and geophysical evidence in support of the hypothesis of anticlockwise rotation of northern Alaska. Mar. Geol. 93, 317–329. https://doi.org/10.1016/0025-3227(90)90090-7.

Embry, A.F., Osadetz, K.G., 1989. Stratigraphy and tectonic significance of Cretaceous volcanism in the Queen Elizabeth Islands. Canad. Arctic Archipelago: Reply. Can. J. Earth Sci. 26, 2740–2741. https://doi.org/10.1139/e89-236.

Evangelatos, J., Mosher, D.C., 2016. Seismic stratigraphy, structure and morphology of Makarov Basin and surrounding regions: tectonic implications. Mar. Geol. 374, 1–13. https://doi.org/10.1016/j.margeo.2016.01.013.

Evangelatos, J., Funck, T., Mosher, D.C., 2017. The sedimentary and crustal velocity structure of Makarov Basin and adjacent Alpha Ridge. Tectonophysics 696–697, 99–114. https://doi.org/10.1016/j.tecto.2016.12.026.

Evenchick, C.A., Davis, W.J., Bédard, J.H., Hayward, N., Friedman, R.M., 2015. Evidence for protracted High Arctic large igneous province magmatism in the central Sverdrup Basin from stratigraphy, geochronology, and paleodepths of saucer-shaped sills. Geol. Soc. Am. Bull. 127, 1366–1390. https://doi.org/10.1130/B31190.1.

Foulger, G.R., Doré, T., Emeleus, C.H., Franke, D., Geoffroy, L., Gernigon, L., Hey, R., Holdsworth, R.E., Hole, M., Höskuldsson, Á., Julian, B., Kusznir, N., Martinez, F., McCaffrey, K.J.W., Natland, J.H., Peace, A., Petersen, K., Schiffer, C., Stephenson, R., Stoker, M., 2020. A continental Greenland-Iceland-Faroe Ridge. Earth-Sci. Rev. 102926 https://doi.org/10.1016/j.earscirev.2019.102926.

Franke, D., 2013. Rifting, lithosphere breakup and volcanism: Comparison of magma-poor and volcanic rifted margins. Mar. Pet. Geol. 43, 63–87. https://doi.org/10.1016/j.marpetgeo.2012.11.003.

Funck, T., Jackson, H.R., Shimeld, J., 2011. The crustal structure of the Alpha Ridge at the transition to the Canadian Polar Margin: Results from a seismic refraction experiment. J. Geophys. Res. 116, B12101 https://doi.org/10.1029/2011JB008411.

Gaina, C., Werner, S.C., Saltus, R., Maus, S., 2011. Chapter 3 Circum-Arctic mapping project: new magnetic and gravity anomaly maps of the Arctic. Geol. Soc. Lond. Mem. 35, 39–48. https://doi.org/10.1144/M35.3.

Gaina, C., Medvedev, S., Torsvik, T.H., Koulakov, I., Werner, S.C., 2014. 4D Arctic: A glimpse into the structure and evolution of the arctic in the light of new geophysical maps, plate tectonics and tomographic models. Surv. Geophys. 35, 1095–1122. https://doi.org/10.1007/s10712-013-9254-y.

Gaina, C., Nasuti, A., Kimbell, G.S., Blischke, A., 2017. Break-up and seafloor spreading domains in the NE Atlantic. Geol. Soc. Lond. Spec. Publ. 447, 393–417. https://doi.org/10.1144/SP447.12.

Galloway, J.M., Tullius, D.N., Evenchick, C.A., Swindles, G.T., Hadlari, T., Embry, A., 2015. Early Cretaceous vegetation and climate change at high latitude: Palynological evidence from Isachsen Formation, Arctic Canada. Cretac. Res. 56, 399–420. https://doi.org/10.1016/j.cretres.2015.04.002.

Geoffroy, L., 2005. Volcanic passive margins. Compt. Rendus Geosci. 337, 1395–1408. https://doi.org/10.1016/j.crte.2005.10.006.

Glebovsky, V.Y., Kaminsky, V.D., Minakov, A.N., Merkur'ev, S.A., Childers, V.A., Brozena, J.M., 2006. Formation of the Eurasia Basin in the Arctic Ocean as inferred from geohistorical analysis of the anomalous magnetic field. Geotectonics 40, 263–281. https://doi.org/10.1134/S0016852106040029.

Glebovsky, V.Y., Astafurova, E.G., Chernykh, A.A., Korneva, M.A., Kaminsky, V.D., Poselov, V.A., 2013. Thickness of the Earth's crust in the deep Arctic Ocean: Results of a 3D gravity modeling. Russ. Geol. Geophys. 54, 247–262. https://doi.org/10.1016/j.rgg.2013.02.001.

Gradstein, F.M., Ogg, J.G., Schmitz, M.D., Ogg, G.M. (Eds.), 2012. The Geologic Time Scale. Elsevier. https://doi.org/10.1016/C2011-1-08249-8.

Grantz, A., Hart, P.E., 2012. Petroleum prospectivity of the Canada Basin, Arctic Ocean. Mar. Pet. Geol. 30, 126–143. https://doi.org/10.1016/j.marpetgeo.2011.11.001.

Grantz, A., Scott, R.A., Drachev, S.S., Moore, T.E., Valin, Z.C., 2011. Chapter 2 Sedimentary successions of the Arctic Region (58–64° to 90°N) that may be prospective for hydrocarbons. Geol. Soc. Lond. Mem. 35, 17–37. https://doi.org/10.1144/M35.2.

Hadlari, T., Midwinter, D., Galloway, J.M., Dewing, K., Durbano, A.M., 2016. Mesozoic rift to post-rift tectonostratigraphy of the Sverdrup Basin, Canadian Arctic. Mar. Pet. Geol. 76, 148–158. https://doi.org/10.1016/j.marpetgeo.2016.05.008.

Harding, I.C., Charles, A.J., Marshall, J.E.A., Pälike, H., Roberts, A.P., Wilson, P.A., Jarvis, E., Thorne, R., Morris, E., Moremon, R., Pearce, R.B., Akbari, S., 2011. Sea-level and salinity fluctuations during the Paleocene–Eocene thermal maximum in Arctic Spitsbergen. Earth Planet. Sci. Lett. 303, 97–107. https://doi.org/10.1016/j.epsl.2010.12.043.

Harrison, J.C., Brent, T.A., 2005. Basins and fold belts of Prince Patrick Island and adjacent area. Can. Arctic Islands. https://doi.org/10.4095/220345.

Harrison, J.C., St-Onge, M.R., Petrov, O.V., Strelnikov, S.I., Lopatin, B.G., Wilson, F.H., Tella, S., Paul, D., Lynds, T., Shokalsky, S.P., Hults, C.K., Bergman, S., Jepsen, H.F., Solli, A., 2011. Geological map of the Arctic; Geological Survey of Canada, Map 2159A, scale 1:5 000 000.

Hegewald, A., Jokat, W., 2013. Tectonic and sedimentary structures in the northern Chukchi region, Arctic Ocean. J. Geophys. Res. Solid Earth 118, 3285–3296. https://doi.org/10.1002/jgrb.50282.

Helwig, J., Kumar, N., Emmet, P., Dinkelman, M.G., 2011. Chapter 35 Regional seismic interpretation of crustal framework, Canadian Arctic passive margin, Beaufort Sea, with comments on petroleum potential. Geol. Soc. Lond. Mem. 35, 527–543. https://doi.org/10.1144/M35.35.

Herman, A.B., Spicer, R.A., 1996. Palaeobotanical evidence for a warm Cretaceous Arctic Ocean. Nature 380, 330–333. https://doi.org/10.1038/380330a0.

Herman, A.B., Spicer, R.A., Spicer, T.E.V., 2016. Environmental constraints on terrestrial vertebrate behaviour and reproduction in the high Arctic of the Late Cretaceous. Palaeogeogr. Palaeoclimatol. Palaeoecol. 441, 317–338. https://doi.org/10.1016/j.palaeo.2015.09.041.

Herrle, J.O., Schröder-Adams, C.J., Davis, W., Pugh, A.T., Galloway, J.M., Fath, J., 2015. Mid-cretaceous high arctic stratigraphy, climate, and oceanic anoxic events. Geology 43, 403–406. https://doi.org/10.1130/G36439.1.

Homza, T.X., Bergman, S.C., 2019. A Geologic Interpretation of the Chukchi Sea Petroleum Province: Offshore Alaska, USA. The American Association of Petroleum Geologists. https://doi.org/10.1306/AAPG119.

Houseknecht, D.W., 2019a. Evolution of the Arctic Alaska Sedimentary Basin. In: The Sedimentary Basins of the United States and Canada. Elsevier, pp. 719–745. https://doi.org/10.1016/B978-0-444-63895-3.00018-8.

Houseknecht, D.W., 2019b. Petroleum systems framework of significant new oil discoveries in a giant Cretaceous (Aptian–Cenomanian) clinothem in Arctic Alaska. Am. Assoc. Pet. Geol. Bull. 103, 619–652. https://doi.org/10.1306/08151817281.

Houseknecht, D.W., Bird, K.J., 2011. Chapter 34 Geology and petroleum potential of the rifted margins of the Canada Basin. Geol. Soc. Lond. Mem. 35, 509–526. https://doi.org/10.1144/M35.34.

Houseknecht, D.W., Wartes, M.A., 2013. Clinoform deposition across a boundary between orogenic front and foredeep - an example from the Lower Cretaceous in Arctic Alaska. Terra Nova 25, 206–211. https://doi.org/10.1111/ter.12024.

Houseknecht, D.W., Craddock, W.H., Lease, R.O., 2016. Upper Cretaceous and Lower Jurassic strata in shallow cores on the Chukchi Shelf, Arctic Alaska. In: USGS Prof. Pap. 1814, p. 37. https://doi.org/10.3133/pp1814C.

Huber, B.T., MacLeod, K.G., Watkins, D.K., Coffin, M.F., 2018. The rise and fall of the Cretaceous Hot Greenhouse climate. Glob. Planet. Chang. 167, 1–23. https://doi.org/10.1016/j.gloplacha.2018.04.004.

Hutchinson, D.R., Jackson, H.R., Houseknecht, D.W., Li, Q., Shimeld, J.W., Mosher, D.C., Chian, D., Saltus, R.W., Oakey, G.N., 2017. Significance of Northeast-trending features in Canada Basin, Arctic Ocean. Geochem. Geophys. Geosyst. 18, 4156–4178. https://doi.org/10.1002/2017GC007099.

Ilhan, I., Coakley, B.J., 2018. Meso–Cenozoic evolution of the southwestern Chukchi Borderland, Arctic Ocean. Mar. Pet. Geol. 95, 100–109. https://doi.org/10.1016/j.marpetgeo.2018.04.014.

Jakobsson, M., Backman, J., Rudels, B., Nycander, J., Frank, M., Mayer, L., Jokat, W., Sangiorgi, F., O'Regan, M., Brinkhuis, H., King, J., Moran, K., 2007. The early Miocene onset of a ventilated circulation regime in the Arctic Ocean. Nature 447, 986–990. https://doi.org/10.1038/nature05924.

Jakobsson, M., Mayer, L., Coakley, B., Dowdeswell, J.A., Forbes, S., Fridman, B., Hodnesdal, H., Noormets, R., Pedersen, R., Rebesco, M., Schenke, H.W., Zarayskaya, Y., Accettella, D., Armstrong, A., Anderson, R.M., Bienhoff, P., Camerlenghi, A., Church, I., Edwards, M., Gardner, J.V., Hall, J.K., Hell, B., Hestvik, O., Kristoffersen, Y., Marcussen, C., Mohammad, R., Mosher, D., Nghiem, S. V., Pedrosa, M.T., Travaglini, P.G., Weatherall, P., 2012. The International Bathymetric chart of the Arctic Ocean (IBCAO) Version 3.0. Geophys. Res. Lett. 39 https://doi.org/10.1029/2012GL052219.

Jakobsson, M., Mayer, L.A., Bringensparr, C., et al., 2020. The International Bathymetric Chart of the Arctic Ocean Version 4.0. Sci Data 7, 176. https://doi.org/10.1038/s41597-020-0520-9.

Jenkyns, H.C., Forster, A., Schouten, S., Sinninghe Damsté, J.S., 2004. High temperatures in the Late Cretaceous Arctic Ocean. Nature 432, 888–892. https://doi.org/10.1038/nature03143.

Jokat, W., 2003. Seismic investigations along the western sector of Alpha Ridge, Central Arctic Ocean. Geophys. J. Int. 152, 185–201. https://doi.org/10.1046/j.1365-246X.2003.01839.x.

Jokat, W., 2005. The sedimentary structure of the Lomonosov Ridge between 88°N and 80°N. Geophys. J. Int. 163, 698–726. https://doi.org/10.1111/j.1365-246X.2005.02786.x.

Jokat, W., Ickrath, M., 2015. Structure of ridges and basins off East Siberia along 81°N, Arctic Ocean. Mar. Pet. Geol. 64, 222–232. https://doi.org/10.1016/j.marpetgeo.2015.02.047.

Jokat, W., Ickrath, M., O'Connor, J., 2013. Seismic transect across the Lomonosov and Mendeleev Ridges: Constraints on the geological evolution of the Amerasia Basin, Arctic Ocean. Geophys. Res. Lett. 40, 5047–5051. https://doi.org/10.1002/grl.50975.

Kashubin, S.N., Pavlenkova, N.I., Petrov, O.V., Mil'shteyn, E.D., Shokalsky, S.P., Erinchek, Y.M., 2013. Earth crust types of the Circum-Polar Arctics. Reg. Geol. I Metallog. 55, 5–20 (in Russian).

Kashubin, S.N., Petrov, O.V., Artemieva, I.M., Morozov, A.F., Vyatkina, D.V., Golysheva, Y.S., Kashubina, T.V., Milshtein, E.D., Rybalka, A.V., Erinchek, Y.M., Sakulina, T.S., Krupnova, N.A., Shulgin, A.A., 2018. Crustal structure of the Mendeleev Rise and the Chukchi Plateau (Arctic Ocean) along the Russian wide-angle and multichannel seismic reflection experiment "Arctic-2012". J. Geodyn. 119, 107–122. https://doi.org/10.1016/j.jog.2018.03.006.

Knudsen, C., Hopper, J.R., Bierman, P.R., Bjerager, M., Funck, T., Green, P.F., Ineson, J. R., Japsen, P., Marcussen, C., Sherlock, S.C., Thomsen, T.B., 2018. Samples from the Lomonosov Ridge place new constraints on the geological evolution of the Arctic Ocean. Geol. Soc. Lond. Spec. Publ. 460, 397–418. https://doi.org/10.1144/SP460.17.

Kos'ko, M.K., Trufanov, G.V., 2002. Middle Cretaceous to Eopleistocene sequences on the New Siberian Islands: an approach to interpret offshore seismic. Mar. Pet. Geol. 19, 901–919.

Kos'ko, M.K., Cecile, M.P., Harrison, J.C., Ganelin, V.G., Khandoshko, N.V., Lopatin, B. G., 1993. Geology of Wrangel Island, between Chukchi and East Siberian seas, northeastern Russia. Geol. Surv. Canada Bull. 461, 101.

Kos'ko, M.K., Sobolev, N.N., Korago, E.A., Proskurnin, V.F., Stolbov, N.M., 2013. Geology of Novosibirskian Islands – a basis for interpretation of geophysical data on the Eastern Arctic shelf of Russia. Neftegazov. Geol. Teor. I Prakt. 8. https://doi.org/10.17353/2070-5379/17_2013.

Kumar, N., Granath, J.W., Emmet, P.A., Helwig, J.A., Dinkelman, M.G., 2011. Chapter 33 Stratigraphic and tectonic framework of the US Chukchi Shelf: exploration insights from a new regional deep-seismic reflection survey. Geol. Soc. Lond. Mem. 35, 501–508. https://doi.org/10.1144/M35.33.

Kuzmichev, A.B., 2009. Where does the South Anyui suture go in the New Siberian islands and Laptev Sea? Implications for the Amerasia basin origin. Tectonophysics 463, 86–108. https://doi.org/10.1016/j.tecto.2008.09.017.

Kuzmichev, A.B., Aleksandrova, G.N., Herman, A.B., 2009. Aptian-Albian coaliferous sediments of Kotel'nyi Island (New Siberian Islands): new data on the section structure and ignimbrite volcanism. Stratigr. Geol. Correl. 17, 519–543. https://doi.org/10.1134/S0869593809050050.

Kuzmichev, A.B., Aleksandrova, G.N., Herman, A.B., Danukalova, M.K., Simakova, A.N., 2013. Paleogene-Neogene sediments of Bel'kov Island (New Siberian Islands): characteristics of sedimentary cover in the eastern Laptev shelf. Stratigr. Geol. Correl. 21, 421–444. https://doi.org/10.1134/S0869593813040059.

Langinen, A.E., Lebedeva-Ivanova, N.N., Gee, D.G., Zamansky, Y.Y., 2009. Correlations between the Lomonosov Ridge, Marvin Spur and adjacent basins of the Arctic Ocean based on seismic data. Tectonophysics 472, 309–322. https://doi.org/10.1016/j.tecto.2008.05.029.

Laverov, N.P., Lobkovsky, L.I., Kononov, M.V., Dobretsov, N.L., Vernikovsky, V.A., Sokolov, S.D., Shipilov, E.V., 2013. A geodynamic model of the evolution of the Arctic basin and adjacent territories in the Mesozoic and Cenozoic and the outer limit of the Russian Continental Shelf. Geotectonics 47, 1–30. https://doi.org/10.1134/S0016852113010044.

Lawver, L., Norton, I., Garagan, L., 2015. The bigger picture: A need for the whole earth plate tectonic setting when reconstructing Greenland. In: 3P Arctic. The Polar Petroleum Potential. Conference & Exibition. Abstract Book. Stavanger, p. 61.

Lebedeva-Ivanova, N., Gaina, C., Minakov, A., Kashubin, S., 2019. ArcCRUST: arctic crustal thickness from 3-D gravity inversion. Geochem. Geophys. Geosyst. https://doi.org/10.1029/2018GC008098, 2018GC008098.

Lebedeva-Ivanova, N.N., Gee, D.G., Sergeyev, M.B., 2011. Chapter 26 Crustal structure of the East Siberian continental margin, Podvodnikov and Makarov basins, based on

refraction seismic data (TransArctic 1989–1991). Geol. Soc. Lond. Mem. 35, 395–411. https://doi.org/10.1144/M35.26.
Lobkovsky, L.I., 2016. Deformable plate tectonics and regional geodynamic model of the Arctic region and Northeastern Asia. Russ. Geol. Geophys. 57, 371–386. https://doi.org/10.1016/j.rgg.2016.03.002.
Mathieu, L., van Wyk de Vries, B., Holohan, E.P., Troll, V.R., 2008. Dykes, cups, saucers and sills: analogue experiments on magma intrusion into brittle rocks. Earth Planet. Sci. Lett. 271, 1–13. https://doi.org/10.1016/j.epsl.2008.02.020.
Miller, E.L., Verzhbitsky, V.E., 2009. Structural studies near Pevek, Russia: implications for formation of the East Siberian Shelf and Makarov Basin of the Arctic Ocean. Stephan Mueller Spec. Publ. Ser. 4, 223–241. https://doi.org/10.5194/smsps-4-223-2009.
Miller, E.L., Soloviev, A., Kuzmichev, A., Gehrels, G.E., Toro, J., Tuchkova, M., 2008. Jura-Cretaceous foreland basin deposits of the Russian Arctic: Separated by birth of Makarov Basin?, in. Nor. J. Geol. 201–226.
Miller, E.L., Gehrels, G.E., Pease, V., Sokolov, S., 2010. Paleozoic and Mesozoic stratigraphy and U–Pb detrital zircon geochronology of Wrangel Island, Russia: constraints on paleogeography and paleocontinental reconstructions of the Arctic. Am. Assoc. Pet. Geol. Bull. 94, 665–692.
Miller, E.L., Akinin, V.V., Dumitru, T.A., Gottlieb, E.S., Grove, M., Meisling, K., Seward, G., 2018a. Deformational history and thermochronology of Wrangel Island, East Siberian Shelf and coastal Chukotka, Arctic Russia. Geol. Soc. Lond. Spec. Publ. 460, 207–238. https://doi.org/10.1144/SP460.7.
Miller, E.L., Meisling, K.E., Akinin, V.V., Brumley, K., Coakley, B.J., Gottlieb, E.S., Hoiland, C.W., O'Brien, T.M., Soboleva, A., Toro, J., 2018b. Circum-Arctic Lithosphere Evolution (CALE) Transect C: displacement of the Arctic Alaska–Chukotka microplate towards the Pacific during opening of the Amerasia Basin of the Arctic. Geol. Soc. Lond. Spec. Publ. 460, 57–120. https://doi.org/10.1144/SP460.9.
Minakov, A., Yarushina, V., Faleide, J.I., Krupnova, N., Sakoulina, T., Dergunov, N., Glebovsky, V., 2018. Dyke emplacement and crustal structure within a continental large igneous province, northern Barents Sea. Geol. Soc. Lond. Spec. Publ. 460, 371–395. https://doi.org/10.1144/SP460.4.
Moran, K., Backman, J., Brinkhuis, H., Clemens, S.C., Cronin, T., Dickens, G.R., Eynaud, F., Gattacceca, J., Jakobsson, M., Jordan, R.W., Kaminski, M., King, J., Koc, N., Krylov, A., Martinez, N., Matthiessen, J., McInroy, D., Moore, T.C., Onodera, J., O'Regan, M., Pälike, H., Rea, B., Rio, D., Sakamoto, T., Smith, D.C., Stein, R., St John, K., Suto, I., Suzuki, N., Takahashi, K., Watanabe, M., Yamamoto, M., Farrell, J., Frank, M., Kubik, P., Jokat, W., Kristoffersen, Y., 2006. The Cenozoic palaeoenvironment of the Arctic Ocean. Nature 441, 601–605. https://doi.org/10.1038/nature04800.
Morozov, A.F., Petrov, O.V., S.P. S, Kashubin, S.N., Kremenetsky, A.A., Shkatov, M.Y., Kaminsky, V.D., Gusev, E.A., Grikurov, G.E., Rekant, P.V., Shevchenko, S.S., Sergeev, S.A., Shatov, V.V., 2013. New geological data substantiating continental nature of region of Central-Arctic rises. Reg. Geol. I Metallog. 55, 34–55.
Mosher, D.C., Shimeld, J., Hutchinson, D., Chian, D., Lebedova-Ivanova, N., Jackson, R., 2012. Canada Basin revealed. In: Society of Petroleum Engineers - Arctic Technology Conference 2012, pp. 805–815.
Mukasa, S.B., Andronikov, A., Brumley, K., Mayer, L.A., Armstrong, A., 2020. Basalts from the Chukchi Borderland: 40Ar/39Ar Ages and Geochemistry of submarine intraplate lavas dredged from the western Arctic Ocean. Am. Geophys. Union. https://doi.org/10.1029/2019JB017604.
Nikishin, A.M., Ziegler, P., Abbott, D., Brunet, M.-F., Cloetingh, S., 2002. Permo–Triassic intraplate magmatism and rifting in Eurasia: implications for mantle plumes and mantle dynamics. Tectonophysics 351, 3–39. https://doi.org/10.1016/S0040-1951(02)00123-3.
Nikishin, A.M., Petrov, E.I., Malyshev, N.A., 2014. Geological Structure and History of the Arctic Ocean. EAGE Publications bv. https://doi.org/10.3997/9789462821880.
Nikishin, A.M., Petrov, E.I., Malyshev, N.A., Ershova, V.P., 2017. Rift systems of the Russian Eastern Arctic shelf and Arctic deep water basins: link between geological history and geodynamics. Geodyn. Tectonophys. 8, 11–43. https://doi.org/10.5800/GT-2017-8-1-0231.
Nikishin, A.M., Gaina, C., Petrov, E.I., Malyshev, N.A., Freiman, S.I., 2018. Eurasia Basin and Gakkel Ridge, Arctic Ocean: Crustal asymmetry, ultra-slow spreading and continental rifting revealed by new seismic data. Tectonophysics 746, 64–82. https://doi.org/10.1016/j.tecto.2017.09.006.
Nikishin, A.M., Startseva, K.F., Verzhbitsky, V.E., Cloetingh, S., Malyshev, N.A., Petrov, E.I., Posamentier, H., Freiman, S.I., Lineva, M.D., Zhukov, N.N., 2019. Sedimentary Basins of the East Siberian Sea and the Chukchi Sea and the adjacent area of the Amerasia Basin: Seismic stratigraphy and stages of geological history. Geotectonics 53, 635–657. https://doi.org/10.1134/S0016852119060104.
Nikishin, A.M., Petrov, E.I., Cloetingh, S., Korniychuk, A.V., Morozov, A.F., Petrov, O.V., Poselov, V.A., Beziazykov, A.V., Skolotnev, S.G., Malyshev, N.A., Verzhbitsky, V.E., Posamentier, H.W., Freiman, S.I., Rodina, E.A., Startseva, K.F., Zhukov, N.N., 2021a. Arctic ocean mega project: Paper 1 - Data collection. Earth-Sci. Rev. https://doi.org/10.1016/j.earscirev.2021.103559.
Nikishin, A.V., Petrov, E.I., Cloetingh, S., Freiman, S.I., Malyshev, N.A., Morozov, A.F., Posamentier, H.W., Verzhbitsky, V.E., Zhukov, N.N., Startseva, 2021b. Arctic Ocean Mega-project: Paper 3 – Mesozoic to Cenozoic geological evolution. Earth Sci. Rev. https://doi.org/10.1016/j.earscirev.2019.103034.
O'Brien, C.L., Robinson, S.A., Pancost, R.D., Sinninghe Damsté, J.S., Schouten, S., Lunt, D.J., Alsenz, H., Bornemann, A., Bottini, C., Brassell, S.C., Farnsworth, A., Forster, A., Huber, B.T., Inglis, G.N., Jenkyns, H.C., Linnert, C., Littler, K., Markwick, P., McAnena, A., Mutterlose, J., Naafs, B.D.A., Püttmann, W., Sluijs, A., van Helmond, N.A.G.M., Vellekoop, J., Wagner, T., Wrobel, N.E., 2017. Cretaceous sea-surface temperature evolution: constraints from TEX 86 and planktonic foraminiferal oxygen isotopes. Earth-Sci. Rev. 172, 224–247. https://doi.org/10.1016/j.earscirev.2017.07.012.
O'Regan, M., Moran, K., Baxter, C.D.P., Cartwright, J., Vogt, C., Kölling, M., 2010. Towards ground truthing exploration in the central Arctic Ocean: a Cenozoic compaction history from the Lomonosov Ridge. Basin Res. 22, 215–235. https://doi.org/10.1111/j.1365-2117.2009.00403.x.
O'Sullivan, P.B., Murphy, J.M., Blythe, A.E., 1997. Late Mesozoic and Cenozoic thermotectonic evolution of the central Brooks Range and adjacent North Slope foreland basin, Alaska: Including fission track results from the Trans-Alaska Crustal Transect (TACT). J. Geophys. Res. Solid Earth 102, 20821–20845. https://doi.org/10.1029/96JB03411.
Oakey, G.N., Saltus, R.W., 2016. Geophysical analysis of the Alpha–Mendeleev ridge complex: characterization of the high arctic large Igneous Province. Tectonophysics 691, 65–84. https://doi.org/10.1016/j.tecto.2016.08.005.
Ogg, J.G., Ogg, G.M., Gradstein, F.M., 2016. A Concise Geologic TimeScale. Elsevier.
Omosanya, K.O., Johansen, S.E., Abrahamson, P., 2016. Magmatic activity during the breakup of Greenland-Eurasia and fluid-flow in Stappen High, SW Barents Sea. Mar. Pet. Geol. 76, 397–411. https://doi.org/10.1016/j.marpetgeo.2016.05.017.
Parfenov, L.M., Kuzmin, M.I. (Eds.), 2001. Tectonics, Geodynamics and Metallogeny of the Territory of the Sakha Republic (Yakutia). MAIK "Nauka/Interperiodika," Moscow.
Pease, V., Drachev, S., Stephenson, R., Zhang, X., 2014. Arctic lithosphere — A review. Tectonophysics 628, 1–25. https://doi.org/10.1016/j.tecto.2014.05.033.
Peters, K., Schenk, O., Bird, K., 2011. Timing of petroleum system events controls accumulations on the North Slope, Alaska. In: AAPG Memoir.
Petrov, O., Morozov, A., Shokalsky, S., Kashubin, S., Artemieva, I.M., Sobolev, N., Petrov, E., Ernst, R.E., Sergeev, S., Smelror, M., 2016. Crustal structure and tectonic model of the Arctic region. Earth-Sci. Rev. 154, 29–71. https://doi.org/10.1016/j.earscirev.2015.11.013.
Petrov, O.V., 2017. Tectonic map of the Arctic. VSEGEI Publishing House, St. Petersburg.
Piskarev, A., Poselov, V., Kaminsky, V. (Eds.), 2019. Geologic Structures of the Arctic Basin. Springer International Publishing, Cham. https://doi.org/10.1007/978-3-319-77742-9.
Polteau, S., Hendriks, B.W.H., Planke, S., Ganerød, M., Corfu, F., Faleide, J.I., Midtkandal, I., Svensen, H.S., Myklebust, R., 2016. The early cretaceous barents Sea Sill Complex: distribution, 40Ar/39Ar geochronology, and implications for carbon gas formation. Palaeogeogr. Palaeoclimatol. Palaeoecol. 441, 83–95. https://doi.org/10.1016/j.palaeo.2015.07.007.
Popova, A.B., Makhova, O.S., Malyshev, N.A., Verzhbitskiy, V.E., Obmetko, V.V., Borodulin, A.A., 2018. Construction of an integrated seismic-geological model of the East Siberian Sea shelf. Neft. Khozyaystvo - Oil Ind. 30–34. https://doi.org/10.24887/0028-2448-2018-4-30-34.
Poselov, V.A., Avetisov, G.P., Butsenko, V.V., Zholondz, S.M., Kaminsky, V.D., Pavlov, S.P., 2012. The Lomonosov Ridge as a natural extension of the Eurasian continental margin into the Arctic Basin. Russ. Geol. Geophys. 53, 1276–1290. https://doi.org/10.1016/j.rgg.2012.10.002.
Poselov, V.A., Verba, V.V., Zholondz, S.M., Butsenko, V.V., 2019. The rises of the Amerasia basin, arctic ocean, and possible equivalents in the Atlantic ocean. Океанология 59, 810–825. https://doi.org/10.31857/S0030-1574595810-825.
Prokopiev, A.V., Ershova, V.B., Anfinson, O., Stockli, D., Powell, J., Khudoley, A.K., Vasiliev, D.A., Sobolev, N.N., Petrov, E.O., 2018. Tectonics of the New Siberian Islands archipelago: Structural styles and low-temperature thermochronology. J. Geodyn. 121, 155–184. https://doi.org/10.1016/j.jog.2018.09.001.
Pugh, A.T., Schröder-Adams, C.J., Carter, E.S., Herrle, J.O., Galloway, J., Haggart, J.W., Andrews, J.L., Hatsukano, K., 2014. Cenomanian to Santonian radiolarian biostratigraphy, carbon isotope stratigraphy and paleoenvironments of the Sverdrup Basin, Ellef Ringnes Island, Nunavut, Canada. Palaeogeogr. Palaeoclimatol. Palaeoecol. 413, 101–122. https://doi.org/10.1016/j.palaeo.2014.06.010.
Puscharovsky, Y.M., 1960. Some general problems of the Artic tectonics. Reports Acad. Sci. USSR 9, 15–28 (in Russian).
Rekant, P., Sobolev, N., Portnov, A., Belyatsky, B., Dipre, G., Pakhalko, A., Kaban'kov, V., Andreeva, I., 2019. Basement segmentation and tectonic structure of the Lomonosov Ridge, arctic Ocean: insights from bedrock geochronology. J. Geodyn. 128, 38–54. https://doi.org/10.1016/j.jog.2019.05.001.
Rekant, P.V., Gusev, E.A., 2012. Seismic geologic structure model for the sedimentary cover of the Laptev Sea part of the Lomonosov Ridge and adjacent parts of the Amundsen Plain and Podvodnikov Basin. Russ. Geol. Geophys. 53, 1150–1162. https://doi.org/10.1016/j.rgg.2012.09.003.
Rekant, P.V., Petrov, O.V., Kashubin, S.N., Rybalka, A.V., Shokalsky, S.P., Petrov, E.O., Vinokurov, I.Y., Gusev, E.A., 2015. Geological history of sedimentary cover of deep-water part of the Arctic Basin according to seismic data. Reg. Geol. I Metallog. 55, 34–55 (in Russian).
Rogov, M.A., Ershova, V.B., Shchepetova, E.V., Zakharov, V.A., Pokrovsky, B.G., Khudoley, A.K., 2017. Earliest cretaceous (late Berriasian) glendonites from Northeast Siberia revise the timing of initiation of transient early cretaceous cooling in the high latitudes. Cretac. Res. 71, 102–112. https://doi.org/10.1016/j.cretres.2016.11.011.
Saltus, R.W., Miller, E.L., Gaina, C., Brown, P.J., 2011. Chapter 4 Regional magnetic domains of the Circum-Arctic: a framework for geodynamic interpretation. Geol. Soc. Lond. Mem. 35, 49–60. https://doi.org/10.1144/M35.4.
Savin, V.A., 2020. Earth crust structure of sedimentary basins of the Laptev and East Siberian seas based on geophysical modelling. In: VNIIOkeangeologia, p. 128. PhD Thesis. (in Russian). http://www.ipgg.sbras.ru/ru/education/commettee/savin2019.

Schröder-Adams, C., 2014. The Cretaceous Polar and Western Interior seas: paleoenvironmental history and paleoceanographic linkages. Sediment. Geol. 301, 26–40. https://doi.org/10.1016/j.sedgeo.2013.12.003.

Schröder-Adams, C.J., Herrle, J.O., Embry, A.F., Haggart, J.W., Galloway, J.M., Pugh, A. T., Harwood, D.M., 2014. Aptian to Santonian foraminiferal biostratigraphy and paleoenvironmental change in the Sverdrup Basin as revealed at Glacier Fiord, Axel Heiberg Island, Canadian Arctic Archipelago. Palaeogeogr. Palaeoclimatol. Palaeoecol. 413, 81–100. https://doi.org/10.1016/j.palaeo.2014.03.010.

Sekretov, S.B., 2001. Northwestern margin of the East Siberian Sea, Russian Arctic: seismic stratigraphy, structure of the sedimentary cover and some remarks on the tectonic history. Tectonophysics 339, 353–371. https://doi.org/10.1016/S0040-1951(01)00108-1.

Shephard, G.E., Müller, R.D., Seton, M., 2013. The tectonic evolution of the Arctic since Pangea breakup: Integrating constraints from surface geology and geophysics with mantle structure. Earth-Sci. Rev. 124, 148–183. https://doi.org/10.1016/j.earscirev.2013.05.012.

Sherwood, K.W., Johnson, P.P., Craig, J.D., Zerwick, S.A., Lothamer, R.T., Thurston, D. K., Hurlbert, S.B., 2002. Structure and stratigraphy of the Hanna Trough, U.S. Chukchi Shelf, Alaska. In: Miller, E.L., Grantz, A., Klemperer, S.L. (Eds.), Special Paper 360: Tectonic Evolution of the Bering Shelf-Chukchi Sea-Artic Margin and Adjacent Landmasses. Geological Society of America, Boulder. Colorado, pp. 39–66. https://doi.org/10.1130/0-8137-2360-4.39.

Shipilov, E.V., 2016. Basaltic magmatism and strike-slip tectonics in the Arctic margin of Eurasia: evidence for the early stage of geodynamic evolution of the Amerasia Basin. Russ. Geol. Geophys. 57, 1668–1687. https://doi.org/10.1016/j.rgg.2016.04.007.

Skaryatin, M.V., Batalova, A.A., Vorgacheva, E.Y., Bulgakova, E.A., Zaytseva, S.A., Igtisamov, D.V., Moiseeva, R.K., Verzhbitskiy, V.E., Malyshev, N.A., Obmetko, V.V., Borodulin, A.A., 2020. Salt tectonics and petroleum prospectivity of the Russian Chukchi Sea. Neft. khozyaystvo - Oil Ind. 2, 12–17. https://doi.org/10.24887/0028-2448-2020-2-12-17.

Skolotnev, S., Aleksandrova, G., Isakova, T., Tolmacheva, T., Kurilenko, A., Raevskaya, E., Rozhnov, S., Petrov, E., Korniychuk, A., 2019. Fossils from seabed bedrocks: Implications for the nature of the acoustic basement of the Mendeleev Rise (Arctic Ocean). Mar. Geol. 407, 148–163. https://doi.org/10.1016/j.margeo.2018.11.002.

Skolotnev, S.G., Fedonkin, M.A., Korniychuk, A.V., 2017. New data on the geological structure of the southwestern Mendeleev Rise. Arctic Ocean. Dokl. Earth Sci. 476, 1001–1006. https://doi.org/10.1134/S1028334X17090173.

Sokolov, S.D., Bondarenko, G.Y., Morozov, O.L., Shekhovtsov, V.A., Glotov, S.P., Ganelin, A.V., Kravchenko-Berezhnoy, I.R., 2002. South Anyui suture, northeast Arctic Russia: Facts and problems. In: Miller, E.L., Grantz, A., Klemperer, S. (Eds.), Special Paper 360: Tectonic Evolution of the Bering Shelf-Chukchi Sea-Artic Margin and Adjacent Landmasses. Geological Society of America, Boulder. Colorado, pp. 209–224. https://doi.org/10.1130/0-8137-2360-4.209.

Sokolov, S.D., Tuchkova, M.I., Moiseev, A.V., Verzhbitsky, V.E., Malyshev, N.A., Gushchina, M.Yu., 2017. Tectonic Zoning of Wrangel Island, Arctic Region. Geotectonics, 2017 51 (1), 3–16. https://doi.org/10.1134/S0016852117010083.

Soloviev, A.V., 2008. Investigation of the Tectonic Processes of the Convergent Setting of Lithosphere Plates: Fission-Track Dating and Structural Analysis. Nauka, Moscow.

Stein, R., 2008. Arctic Ocean Sediments: Processes, Proxies, and Paleoenvironment, 1st ed. Elsevier Science.

Stein, R., Jokat, W., Niessen, F., Weigelt, E., 2015. Exploring the long-term Cenozoic Arctic Ocean climate history: a challenge within the International Ocean Discovery Program (IODP). Arktos 1, 3. https://doi.org/10.1007/s41063-015-0012-x.

Thórarinsson, S.B., Söderlund, U., Døssing, A., Holm, P.M., Ernst, R.E., Tegner, C., 2015. Rift magmatism on the Eurasia basin margin: U–Pb baddeleyite ages of alkaline dyke swarms in North Greenland. J. Geol. Soc. Lond. 172, 721–726. https://doi.org/10.1144/jgs2015-049.

Toro, J., Miller, E.L., Prokopiev, A.V., Zhang, X., Veselovskiy, R., 2016. Mesozoic orogens of the Arctic from Novaya Zemlya to Alaska. J. Geol. Soc. Lond. 173, 989–1006. https://doi.org/10.1144/jgs2016-083.

Vernikovsky, V.A., Dobretsov, N.L., Metelkin, D.V., Matushkin, N.Y., Koulakov, I.Y., 2013. Concerning tectonics and the tectonic evolution of the Arctic. Russ. Geol. Geophys. 54, 838–858. https://doi.org/10.1016/j.rgg.2013.07.006.

Vernikovsky, V.A., Morozov, A.F., Petrov, O.V., Travin, A.V., Kashubin, S.N., Shokal'sky, S.P., Shevchenko, S.S., Petrov, E.O., 2014. New data on the age of dolerites and basalts of Mendeleev Rise (Arctic Ocean). Dokl. Earth Sci. 454, 97–101. https://doi.org/10.1134/S1028334X1402007X.

Verzhbitsky, V.E., Sokolov, S.D., Tuchkova, M.I., Frantzen, E.M., Little, A., Lobkovsky, L. I., 2012. The South Chukchi Sedimentary Basin (Chukchi Sea, Russian Arctic), in: Tectonics and Sedimentation. American Association of Petroleum Geologists, Tulsa, Oklahoma, pp. 267–290. https://doi.org/10.1306/13351557M1003534.

Verzhbitsky, V.E., Sokolov, S.D., Tuchkova, M.I., 2015. Present-day structure and stages of tectonic evolution of Wrangel Island, Russian eastern Arctic Region. Geotectonics 49, 165–192. https://doi.org/10.1134/S001685211503005X.

Weigelt, E., Jokat, W., Franke, D., 2014. Seismostratigraphy of the Siberian Sector of the Arctic Ocean and adjacent Laptev Sea Shelf. J. Geophys. Res. Solid Earth 119, 5275–5289. https://doi.org/10.1002/2013JB010727.

Weigelt, E., Jokat, W., Eisermann, H., 2020. Deposition history and paleo-current activity on the southeastern Lomonosov Ridge and its Eurasian flank based on seismic data. Geochem. Geophys. Geosyst. 21, e2020GC009133 https://doi.org/10.1029/2020GC009133.

West, C.K., Greenwood, D.R., Basinger, J.F., 2015. Was the Arctic Eocene 'rainforest' monsoonal? Estimates of seasonal precipitation from early Eocene megafloras from Ellesmere Island. Nunavut. Earth Planet. Sci. Lett. 427, 18–30. https://doi.org/10.1016/j.epsl.2015.06.036.

Wilkinson, C.M., Ganerød, M., Hendriks, B.W.H., Eide, E.A., 2017. Compilation and appraisal of geochronological data from the North Atlantic Igneous Province (NAIP). Geol. Soc. Lond. Spec. Publ. 447, 69–103. https://doi.org/10.1144/SP447.10.

Yang, L., Ren, J., McIntosh, K., Pang, X., Lei, C., Zhao, Y., 2018. The structure and evolution of deepwater basins in the distal margin of the northern South China Sea and their implications for the formation of the continental margin. Mar. Pet. Geol. 92, 234–254. https://doi.org/10.1016/j.marpetgeo.2018.02.032.

Zakharov, Y.D., Shigeta, Y., Popov, A.M., Velivetskaya, T.A., Afanasyeva, T.B., 2011. Cretaceous climatic oscillations in the Bering area (Alaska and Koryak Upland): Isotopic and palaeontological evidence. Sediment. Geol. 235, 122–131. https://doi.org/10.1016/j.sedgeo.2010.03.012.

Ziegler, P.A., 1988. Evolution of the Arctic-North Atlantic and the Western Tethys. Am. Assoc. Pet. Geol. Mem. 43, 1–198.

Ziegler, P.A., Cloetingh, S., 2004. Dynamic processes controlling evolution of rifted basins. Earth-Sci. Rev. 64, 1–50. https://doi.org/10.1016/S0012-8252(03)00041-2.